

**LASER INDUCED THERMAL LENS AND
NEAR INFRARED ABSORPTION STUDIES OF
CH OVERTONES IN SOME ORGANIC COMPOUNDS**

ABDUL RASHEED T. M.

**THESIS SUBMITTED
IN PARTIAL FULFILMENT OF THE REQUIREMENTS
FOR THE DEGREE OF
DOCTOR OF PHILOSOPHY**

**LASER DIVISION
DEPARTMENT OF PHYSICS
COCHIN UNIVERSITY OF SCIENCE AND TECHNOLOGY**

1987

DEDICATED TO

THE MEMORY OF MY FATHER WHO CARED FOR EDUCATION

AND

MY MOTHER WHO ALWAYS PRAYS FOR ME

DECLARATION

Certified that the work presented in this thesis is based on the original work done by me under the guidance of Dr.V.P.Narayanan Nampoori, Reader, Department of Physics, Cochin University of Science and Technology, and has not been included in any other thesis submitted previously for the award of any degree.


Cochin-682 022
September 16, 1987


T.M.Abdul Rasheed

CERTIFICATE

Certified that the work presented in this thesis is based on the bona fide work done by Mr.T.M.Abdul Rasheed, Research Student, under my guidance in the Department of Physics, Cochin University of Science and Technology and has not been included in any other thesis submitted previously for the award of any degree.

Cochin-682 022
September 16, 1987


V.P.Narayanan Nampoori
Reader of Physics
(Supervising Teacher)

ACKNOWLEDGEMENTS

I am deeply indebted to Dr.V.P.Narayanan Nampoori, Reader, Department of Physics, Cochin University of Science and Technology, Cochin for his constant guidance and supervision throughout the course of this work.

I express my deep sense of gratitude to Prof. K.Sathianandan for his interest in my work and for the timely helps he has extended to me throughout the course of the present work.

I am grateful to all members of the faculty, library, laboratory and non-teaching staff of the Department of Physics for their co-operation during the period of the work.

I am extremely grateful to Mr.K.P.B.Moosad and Mr.Thomas Baby, research scholars of the laser division for the valuable helps extended to me during the course of this work.

I owe a lot to my colleagues and friends in the laser division, thin films division and other laboratories for their good wishes and encouragements rendered during the period of this work.

I take this opportunity to acknowledge the assistance given by the staff of USIC of Cochin University in the fabrication works.

Special thanks are due to Mr.K.P.Sasidharan for the neat typing of the manuscript.

Finally, I thank DST (Govt. of India) and DAE (Govt. of India) for providing research fellowships during the period of research.

T.M.Abdul Rasheed.

PREFACE

Vibrational overtone spectroscopy of X-H (X=C,N,O) containing molecules is an area of recent interest. The spectroscopic studies of higher vibrational levels yield valuable informations, regarding, the molecular structure, intra- and inter-molecular interactions, radiationless transitions, intra-molecular vibrational relaxations, multiphoton excitations and chemical reactivities, which cannot be obtained by other spectroscopic methods.

This thesis presents the results of experimental investigations on the overtone spectra of some organic compounds in the liquid phase for the characterization of CH bonds. The spectra in the fifth overtone region ($\Delta V=6$) are recorded using a dual beam thermal lens setup and the lower overtones ($\Delta V=2-5$) are recorded spectrophotometrically.

The thesis is presented in six chapters. The first chapter presents a review of the area of vibrational overtone spectroscopy of X-H containing molecules. It contains the description of the local mode model with application to benzene, the refinements that have been made by various workers

in the local mode model including the theory of coupled local mode oscillators with applications to different molecular systems and an outline of the different investigations appeared on the intensity aspects of overtone transitions. On the application side, the important areas of characterization of CH bonds in organic compounds, intra-molecular vibrational relaxation and overtone photochemistry are briefly reviewed.

The second chapter presents a brief outline of the formation, characteristics and the techniques of thermal lens effect with emphasis on applications in measuring weak absorptions. The various other applications of thermal lens techniques in Physics and Chemistry are also briefly discussed.

The third chapter contains the description of our dual beam thermal lens setup used for recording the fifth overtone spectra. It contains the details of the experimental configuration, the components of the apparatus and the various experimental considerations that are to be carefully executed for the successful recording of the overtone spectra. A brief description of the spectrophotometric measurements of the lower overtones is also given towards the end of the chapter.

The fourth chapter contains the details of the present investigations on the overtone spectra of some aromatic molecules, namely, acetophenone, benzaldehyde, styrene and polystyrene.

The physical mechanism of the change in aryl CH force constant (and bond length) upon substitution on the benzene ring is proposed and discussed in detail. The presence of nonequivalent methyl CH bonds in acetophenone is established for the first time and the possible factors influencing the local mode parameters of the methyl CH bonds are discussed. The overtone spectra of styrene and polystyrene are compared to those of benzene leading to the prediction of a small change in the aryl CH bond length in polystyrene with respect to benzene. The work on polystyrene presents the first thermal lens overtone spectrum of a solid and that of a polymer.

The fifth chapter contains the details of the present investigations on the overtone spectra of some aliphatic compounds, namely, trichloroethylene, 1,2 dichloro- and dibromoethanes, and 2-butanone. Trichloroethylene belongs to the class of olefinic compounds which are interesting candidates for overtone photochemistry. Moreover, this molecule contains only a single isolated CH bond and hence can be a potential candidate for mode selective rupture of the CH bond. The fifth overtone data of trichloroethylene obtained here is used to predict the change in CH bond length with respect to ethylene. The electron withdrawing property of chlorine atoms is shown to be the main reason for the increase of CH bond strength. The Fermi resonance observed in the $\Delta V=3$ region is analyzed and the interaction

matrix element is calculated. The low frequency vibration involved in the Fermi interaction is shown to be CH deformation rather than C=C stretch or C=C stretch + CH deformation. The overtone spectra of 1,2 dichloro- and dibromoethanes in the $\Delta V=2-5$ regions show pure local mode overtones, local-local combinations and local-normal combinations. The pure local mode overtones and local-local combinations are interpreted using a coupled C_{2v} local mode Hamiltonian. The possible assignments of the local-normal combinations are also given. The analysis of the overtone spectrum of 2-butanone has shown that the methyl group away from the carbonyl maintains C_{3v} symmetry and that adjacent to the carbonyl contains nonequivalent CH bonds. A C_{3v} coupled local mode Hamiltonian is used to predict the pure local mode overtones and the local-local combinations, and this analysis has shown that the main peaks observed in the spectrum correspond to this methyl group.

The sixth chapter presents the summary and conclusions of the present overtone spectroscopic studies.

Part of the investigations presented in the thesis has been published/accepted for publication in the form of the following papers:

- (1) Overtone Spectra of 1,2 Dichloro- and Dibromo-Ethanes in the Near Infrared Region

T.M.Abdul Rasheed, V.P.N.Nampoori and K.Sathianandan,
Chemical Physics (Netherlands) 108, 349 (1986).

- (2) Near Infrared Spectrum of 2-Butanone--A Local Mode Analysis
T.M.Abdul Rasheed, V.P.N.Nampoori and K.Sathianandan,
Spectrochimica Acta (UK) 1987, in press.
- (3) CH Overtones in Acetophenone and Benzaldehyde--Aryl and
Methyl Local Modes
T.M.Abdul Rasheed, K.P.B.Moosad, V.P.N.Nampoori and
K.Sathianandan, Journal of Physical Chemistry (USA) 1987,
in press.
- (4) CH Local Mode Excitations and Fermi Resonance in Trichloro-
ethylene
T.M.Abdul Rasheed, K.P.B.Moosad, V.P.N.Nampoori and
K.Sathianandan, Spectrochimica Acta (UK) 1987, in press.
- (5) Fifth CH Overtone Spectrum of Trichloroethylene Detected
by Laser Induced Thermal Lens Effect
T.M.Abdul Rasheed, K.P.B.Moosad, Thomas Baby, V.P.N.
Nampoori and K.Sathianandan, Proceedings of the Fourth
Quantum Electronics Symposium held during Dec.29, 1986-
Jan.1, 1987 at Cochin University of Science & Technology,
conducted by DAE, Government of India, pp.98-99.
- (6) Fifth Overtone Spectra of Aromatic CH in Chloro and Bromo
Benzenes Detected by Dual Beam CW Thermal Lens Effect
T.M.Abdul Rasheed, K.P.B.Moosad, Thomas Baby, V.P.N.
Nampoori and K.Sathianandan, Laser Applications in Spectro-
scopy and Optics (LASO'87) 5-10 Jan.1987, IIT Madras, Paper-13.

CONTENTS

	<u>Page</u>
PREFACE ..	i
CHAPTER 1 VIBRATIONAL OVERTONE EXCITATIONS OF POLYATOMIC MOLECULES IN THE GROUND ELECTRONIC STATE ..	1
1.10 Introduction ..	1
1.20 Theoretical Description of Higher Excited.. Vibrational Levels--the Local Mode Model	2
1.21 Outline of the Quantum Mechanical Local .. Mode Model	7
1.22 Refinements in the Local Mode Model ..	13
1.23 Intensity Aspects in Overtone Spectra ..	20
1.30 Applications of Overtone Spectroscopy ..	24
1.31 Characterization of CH bonds in Organic .. Compounds	24
1.32 Intramolecular Vibrational Relaxation .. (IVR)	32
1.33 Overtone Photochemistry ..	38
CHAPTER 2 LASER INDUCED THERMAL LENS EFFECT-- THEORY AND APPLICATIONS ..	52
2.10 Introduction ..	52
2.20 Orders of Magnitude of Photothermal .. Effects	54
2.30 Thermal Effects on Refractive Index ..	57
2.40 The Photothermal Lens ..	58
2.41 Focal Length of the Thermal Lens ..	60
2.42 Time Development of Focal Length-- Gordon's Equation ..	63

	<u>Page</u>
2.50 The Extracavity Method of Hu and Whinnery..	66
2.60 The Dual Beam Thermal Lens Technique ..	73
2.70 Thermal Lens Produced by Pulsed Lasers ..	78
2.80 Applications of Thermal Lens Effect ..	79
2.81 Absorption Spectroscopy ..	79
2.82 Analytical Applications ..	79
2.83 Energy Transfer Studies in Gas Media ..	80
2.84 Bulk Thermal Properties ..	81
2.85 Measurements of Absolute Quantum Yields ..	81
2.86 Chemical Reactions ..	82
CHAPTER 3 EXPERIMENTAL TECHNIQUES ..	89
3.10 Introduction ..	89
3.20 Thermal Lens Experimental Configuration ..	89
3.21 The Pump Source--Ring Dye Laser ..	93
3.22 The Chopper ..	95
3.23 The Probe Source ..	95
3.24 The Detector Assembly ..	96
3.25 The Lock-in Amplifier ..	96
3.26 The Ratiometer and the Recorder ..	97
3.27 The Wavemeter ..	97
3.30 Experimental Considerations ..	98
3.40 Measurement of Lower Overtones ..	106
CHAPTER 4 ANALYSIS OF CH OVERTONE SPECTRA OF SOME ..	108
AROMATIC COMPOUNDS	
4.10 Introduction ..	108
4.11 Aryl CH Overtones in Substituted Benzenes..	108
4.12 Nonequivalent Methyl CH Overtones in ..	111
Anisotropic Environments	
4.20 Experimental ..	115

	<u>Page</u>
4.30 Results and Discussion ..	116
4.31 Aryl CH Overtones in Acetophenone and Benzaldehyde ..	116
4.32 The Proposed Mechanism of the Change in Aryl CH Bond Length ..	125
4.33 Nonequivalent Methyl CH Bonds in Acetophenone ..	131
4.34 Aryl CH Overtones in Styrene and Poly- styrene ..	136
CHAPTER 5 ANALYSIS OF CH OVERTONE SPECTRA OF SOME ALIPHATIC COMPOUNDS ..	148
5.10 Introduction ..	148
5.20 Experimental ..	153
5.30 Results and Discussion ..	154
5.31 Overtone Spectrum of Trichloroethylene ..	154
5.31a Pure CH Overtones ..	154
5.31b Fermi Resonance in the $\Delta V=3$ Region ..	165
5.32 Overtone Spectra of 1,2 Dichloro- and Dibromo-Ethanes ..	169
5.32a Pure CH Local Mode Overtones and Local- Local Combinations ..	169
5.32b Local-Normal Combinations ..	184
5.33 Overtone Spectrum of 2-Butanone ..	187
CHAPTER 6 SUMMARY AND CONCLUSIONS ..	201

Chapter 1

VIBRATIONAL OVERTONE EXCITATION OF POLYATOMIC MOLECULES IN THE GROUND ELECTRONIC STATE

1.10 Introduction

In recent years, the attention of many molecular spectroscopists all over the world have turned to the study of the different aspects of higher excited vibrational levels of the ground electronic state of polyatomic molecules containing X-H (X = C,N,O) oscillators¹⁻⁴. The major reasons for this interest are the following: First, it is recognized in the study of radiationless electronic transitions that higher excited levels of hydrogen atom based vibrations play a key role in accepting the excited electronic energy⁵⁻⁹. Second, the normal mode model, which is found successful in describing the fundamental vibrations of molecules, fails to provide a satisfactory description of the anharmonic overtones. It is found that the introduction of normal mode anharmonic coupling terms into the normal mode model results in the prediction of complicated spectral patterns, contrary to experimental observations¹⁰⁻¹². Third, an understanding of higher excited vibrational states is essential in the development of

the theory of multiphoton photochemistry as well as bond selective chemistry, which are active areas of current research¹³⁻¹⁷. The possibility of bond specific excitation will depend upon the nature of the initially prepared state, the channels and time scales of relaxation of the excitation energy etc. The spectroscopic studies of higher overtone states are concerned with excitation of bonds to a significant fraction of their bond dissociation energies, and this can provide a link between chemical reactivity and spectroscopic properties. Finally, the development of laser based experimental techniques, such as photoacoustic and thermal lens techniques, made it possible to measure very weak ($\alpha = 10^{-3} - 10^{-7} \text{ cm}^{-1}$) optical transitions due to overtone excitation both conveniently and accurately.

1.20 Theoretical Description of Higher Excited Vibrational Levels--The Local Mode Model

Considerable interest has been focused on the success of the local mode (LM) model for describing higher excited vibrational levels^{10,12}. This model was introduced by Henry and Siebrand in their attempt to model radiationless electronic transitions in polyatomic molecules⁵. They found that the Franck-Condon factors for $T_1 \rightsquigarrow S_0$ and $S_1 \rightsquigarrow S_0$ transitions are governed by the anharmonicity of the CH stretching modes.

They also found semiquantitative agreement between the anharmonicity parameter in the Franck-Condon factors and the known anharmonicity of the CH molecule. This led the authors to find the relation between the CH anharmonicity constant in the CH molecule and that in a hydrocarbon molecule. The local mode model is the outcome of these investigations.

The concept of local modes is complementary to that of normal modes. Normal modes arise from the analysis of vibrational motions for infinitesimal amplitudes, where the molecule is considered as $3N-6(5)$ uncoupled harmonic oscillators^{18,19}. This description is a good model in understanding the fundamental and, to some extent the lower overtone spectra of polyatomic molecules^{18,19}. However it cannot be valid under every conditions. Continued pumping of energy into the vibrational modes of a molecule leads to dissociation which is a nonharmonic behaviour. Also, physical intuition suggests that the molecule may follow low energy pathways leading to dissociation which are unlikely to be along the normal coordinates. As an example, if one continuously pump energy into the totally symmetric vibrational mode of benzene, the dissociation along this coordinate requires the simultaneous rupture of all the six CH bonds. This is a prohibitively high energy process. The breaking of one or two CH bonds is more likely. The coordinate corresponding to

rupture of one or two CH bonds involves the coupling of several normal modes. One can make the above arguments more explicit by considering the anharmonicities and dissociation energies. For diatomic molecules there is a clearcut relation between anharmonicity constant X and dissociation energy D . For example, if Morse potential is assumed $X = \frac{-\omega^2}{4D}$. However, in the case of a polyatomic molecule the relation between normal mode anharmonicity constants X_{KL} , bond dissociation energies D_i and the normal mode dissociation energies D_k is not obvious. For those normal modes in which vibrational energy is evenly distributed among a number of equivalent chemical bonds, the dissociation energy D_k refers to the sum of all bond energies D_i ; $D_k = \sum_i D_i$. This implies a large value of D_k and hence a small value of the diagonal normal mode anharmonicity constant X_{KK} . As mentioned earlier, the physically important dissociation is the rupture of a single chemical bond. The vibration associated with this rupture is not a normal mode but it is termed as a local mode. Its dissociation energy is much smaller than the normal mode dissociation energy; $D_i \ll D_k$ so that the corresponding anharmonicity constant X_{ii} will be much larger than X_{KK} . In other words for high vibrational quantum levels, the vibrational energy becomes increasingly more diagonal in a local mode representation than in a normal mode representation, that is, the molecule will oscillate in a pattern closer to a local mode rather than a normal mode.

Henry and coworkers used these local mode ideas to obtain normal mode anharmonicity constants and thus describe the overtone spectra of molecules like NH_3 , C_6H_6 , CH_2Cl_2 etc. in terms of the components of normal mode anharmonicity constants. From these studies they concluded that higher vibrational levels of X-H (X = C,N,O) containing molecules cannot be described in terms of a set of symmetry allowed normal mode components but instead by a relatively small number of most anharmonic motions namely, localized excitations of bond modes¹⁰.

A quantum mechanical description of the one dimensional (single bond based) appearance of CH overtone spectra with particular application to benzene has been given by Swofford et al in their study of the fifth overtone spectra of benzene and its deuterated analogues using thermal lens technique¹². The theory given by Swofford et al forms the basis of the local mode treatment of any molecule and hence it is briefly outlined below.

If one uses conventional normal mode description, the number of symmetry allowed states increases dramatically with quantum number¹⁸. The total number of vibrational levels increases much more rapidly with the quantum number. This is given by Bose statistics by which there are $\binom{V+N-1}{V}$ ways of distributing V quanta over N sites. Thus there are 462 CH

based levels for benzene at $V = 6$. Of these, 150 states are allowed. These are the 75 doubly degenerate states of E_1 symmetry. However experimental observations show no evidence for this great variety of CH based excitations. Only a single broad peak is observed in the aryl CH $\Delta V = 6$ region for benzene, deuterated benzenes and substituted benzenes. This clearly demonstrates the success of the local mode model of uncoupled anharmonic oscillators localized on individual CH bonds.

The empirical evidence of one dimensional anharmonic oscillator in the overtone spectrum of benzene has been known from as early as 1928 when Ellis²⁰ fitted the observed overtone bands to the equation

$$\Delta E_{V,0} = AV + BV^2 \quad (1.1)$$

where A and B are constants and V is the overtone level.

A plot of $\frac{\Delta E}{V}$ versus V for the observed bands from $V = 1$ to 8^{12} yielded $A = 3095 \text{ cm}^{-1}$ and $B = -58.4 \text{ cm}^{-1}$. The above empirical equation of Ellis follows directly from the theory of one dimensional anharmonic oscillator¹⁸ the energy levels of which are given by perturbation theory as

$$\Delta E_{V,0} = -\frac{1}{2}(X_1 + \frac{1}{2}X_2) + (V + \frac{1}{2})X_1 + (V + \frac{1}{2})^2 X_2 \quad (1.2)$$

where X_1 is the mechanical frequency and X_2 is the anharmonicity. The empirical constants A and B in eqn.(1.1) are related to these through $X_1 = (A-B)$ and $X_2 = B$. (X_1 and X_2 are related to conventional spectroscopic parameters through $X_1 = \omega_e$ and $X_2 = -\omega_e x_e$).

1.21 Outline of Quantum Mechanical Local Mode Model¹²

In seeking one dimensional simplicity, Swofford et al assumed that the molecular Hamiltonian can be separated into those of two independent subspaces. The $(3N-6)$ dimensional molecular space is divided into a subspace of dimension s having coordinate $R_1 \dots R_s$ within which H is partitionable to one dimensional Hamiltonians and the remaining space $s' = (3N-6-s)$ where no partitioning is possible.

Thus

$$H = \sum_{j=1}^s H_j + H_{s'} \quad (1.3)$$

with
$$H_j = \frac{1}{2} g_{jj} p_j^2 + V_j(R_j); j=1 \dots s \quad (1.4)$$

$H_{s'}$ is the Hamiltonian for the unpartitionable subspace s' . p_j are now conjugate to R_j . The g_{jj} ($j=1 \dots s$) are the diagonal elements of the g matrix for the s coordinate system. For separability, not only the s dimensional block in g be diagonal

but the variation of $|g|$ with respect to $R_1 \dots R_s$ must be negligible. (When the set $\{R_j\}$ constitutes the $3N-6$ normal coordinates with $s' = 0$ and V_j is taken quadratic in R_j the eqn. (1.4) describes the ordinary normal mode problem).

Once the Hamiltonian is partitioned, one can write the k^{th} molecular eigenstate $|\psi_k\rangle$ to be characterised by a set of quantum numbers $V_j(k)$ ($j=1 \dots s, s'$) each belonging to a subspace

$$H|\psi_k\rangle = E_k|\psi_k\rangle \quad (1.5)$$

with
$$|\psi_k\rangle = \prod_j |\phi_{V_j(k)}\rangle \quad (j=1 \dots s, s') \quad (1.6)$$

and
$$H_j|\phi_{V_j(k)}\rangle = E_{V_j(k)}|\phi_{V_j(k)}\rangle \quad (1.7)$$

The energy of the k^{th} eigenstate is given by

$$E_k = \sum_j E_{V_j(k)} \quad (1.8)$$

Any operator \hat{O} which can be partitioned in the same subspaces such that

$$\hat{O} = \sum_j \hat{O}_j(R_j), \quad (1.9)$$

$\langle \psi_k | \hat{O} | \psi_l \rangle \neq 0$ is possible only when $v_j(k) = v_j(l)$ for all j but one. Thus if the electric dipole moment is separable in the same subspace as the Hamiltonian, then those electric dipole transitions, which couple the ground state (all $v_j = 0$) into excited states containing excitations ($v_j \neq 0$) in more than one coordinate of the partitioned space are forbidden.

Considering the benzene problem, the coordinates suitable for partition are the six CH stretching valence coordinates $\Delta r_1 \dots \Delta r_6$. Swofford and coworkers logically justified the neglect of, the contributions of the g matrix cross terms and the dependence of $|g|$ on Δr_i in the kinetic energy term, and the interactions between the CH subset s and the s' subspace of the remaining 24 valence coordinates in the potential energy term. They concluded that the higher terms in the bond centered potential are more important than the interaction potential terms.

There are $\frac{(V+5)!}{V!5!} = 462$ CH stretching states in benzene at the $V = 6$ quantum level. A state at V is specified by the number of quanta at each CH site i.e., by $(v_1 \dots v_6)$, subject to the constraint that $\sum_j v_j = V$. Thus $V = 6$ yields eleven classes $(6,0,0,0,0,0), (5,1,0,0,0,0) \dots (1,1,1,1,1,1)$. In $(6,0,0,0,0,0)$ all the six quanta are in a single CH site. This class is six-fold degenerate. In $(5,1,0,0,0,0)$ five quanta are in one CH site and one in any of the remaining five

sites. This class is thirty-fold degenerate. For (1,1,1,1,1,1) there is one quantum at each CH site and there is no degeneracy for this class. The primitive state vectors are products of the form

$$|v_1\rangle|v_2\rangle|v_3\rangle|v_4\rangle|v_5\rangle|v_6\rangle|v_{s'}\rangle$$

Assuming $v_{s'} = 0$ the product functions in each class can be symmetrized to form bases for irreducible representations of the D_{6h} point group. The irreducible representations are A_{1g} , A_{2g} , B_{1u} , B_{2u} and E_{1u} of which electric dipole transitions occur from ground A_{1g} to excited E_{1u} levels only. The most anharmonic (6,0,0,0,0,0) has the lowest energy and the most harmonic (1,1,1,1,1,1) state has the highest energy. The formally allowed E_{1u} levels span over a wide spectral range¹² and one must expect a richly detailed absorption band. However, electric dipole operator belongs to the class of operators like \hat{O} discussed earlier so that it couples states which differ in quantum number v_j in only one j . Thus light incident on an unexcited (0,0,0,0,0,0) state leads to excited states in only one local mode at a time (0... v_j ...) ($j=1\dots 6; s'$) (As far as CH excitations are concerned $s' = 0$). Thus for any v there is only one class which can be dipole coupled to the ground state. This is the ($v,0,0,0,0,0$) class, which is six fold degenerate. Thus the local mode model predicts a unique single state

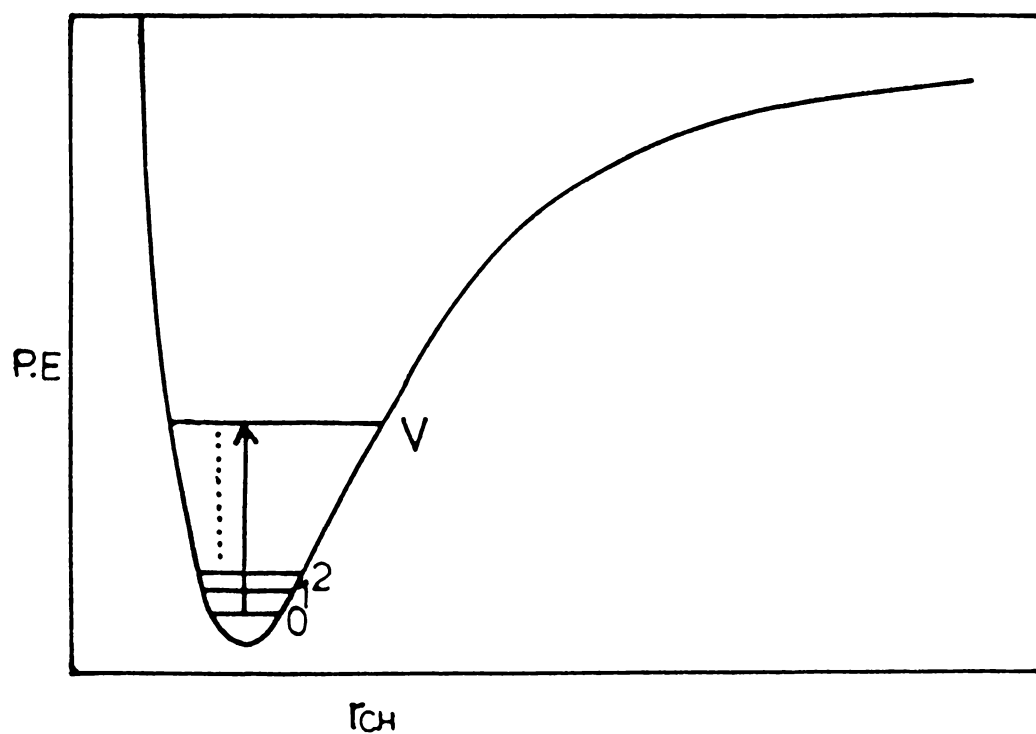


Fig.1.1 Schematic of overtone absorption in the ground electronic state. r_{CH} represents the local coordinate. The intensity of the transitions rapidly decrease for higher and higher values of V . The transition energy obeys the anharmonic relation $\Delta E = AV + BV^2$.

excitation at all V . The spectroscopic energies of these single state excitations are given by eqn.(1.1). The experimental observations are thus in agreement with the predictions of the local mode model. Fig.1.1 shows the schematic of the $0 \rightarrow V$ overtone transition.

The success of the local mode model has again been demonstrated by comparing the $\Delta V = 6$ absorption spectra of benzene and benzene d_5 . No significant difference in band shape or peak energy are observed for the two molecules in contrast to the predictions of the strongly coupled normal mode model. On the other hand, the similarity in the observed spectra is predicted by the local mode model.

The local mode model has been used widely for interpreting the overtone spectra of a wide variety of molecules¹⁰. It is found that in addition to pure overtones, additional weak features are found in many overtone spectra. These are combination bands arising from excitation of more than one local mode (local-local combinations) or excitation of low frequency vibrations of the molecule along with a pure local mode (local-normal combinations). The appearance of these combination bands in overtone spectra implies the presence of nonzero couplings between local modes and between local and normal modes. However, the magnitudes of these couplings are found to be much smaller than the diagonal local mode

anharmonicity values. This allows the local mode description to be used as a good zero order picture to start with in the calculations of higher vibrational spectra. Henry and co-workers¹⁰ have stated the following empirical rules related to overtone spectra: (1) Local mode overtones involving high frequency oscillators are most intense but fall off rapidly in intensity with increasing vibrational quantum number. (2) Local-local and local-normal combinations occur generally with much less intensity than pure local mode overtones. (3) Combination bands fall off more quickly in intensity than do the pure overtones with increase in quantum number.

1.22 Refinements in Local Mode Model

Refinements in the local mode model through inclusion of the terms neglected in the zero order local mode model have been suggested by many workers. Sage and Jortner^{2,21-23} used Morse oscillator function to model the CH bond potential and included the Wilson G matrix cross terms involving CH bending and stretching vibrations in the Hamiltonian. Wallace²⁴⁻²⁶ used Morse oscillator potential to model the CH bond potential and included potential energy cross terms of the type $F_{ij}Q_iQ_j$ in the Hamiltonian. Halonen²⁷ calculated the CH and CD overtone spectra in benzene and deuterobenzene using a model in which anharmonic local mode oscillators are coupled through kinetic energy (Wilson G matrix cross terms) to the C-C framework.

A number of papers have appeared on the energetics of overtone transitions in molecules containing coupled oscillator systems, that is, groups in which a common X atom contains more than one hydrogen atom. When more than one hydrogen atom share a common X atom, coupling between the oscillators produce symmetry effects in the spectra. The effects of symmetry in the local mode picture is briefly discussed by Swofford et al¹². Gelbart et al²⁸ pointed out that symmetry adaptation is completely compatible with energy localization. Moller and Mortensen²⁹ have analyzed the states of water molecule using the so-called local mode picture, and have shown that the symmetry effects arising from the equivalence of the two CH bonds are important. The local mode picture uses the local mode model as the starting point and considers the interaction between the equivalent local modes, and can thus be used to interpret the entire spectra atleast down to first overtone level. Henry et al used the local mode picture and symmetry effects to analyze the overtone spectra of water³⁰ dihalomethanes³¹ and recently those of deuterated dihalomethanes³². The spectra of all these molecules display splittings between symmetric and antisymmetric combinations of local mode states arising from the coupling of the two equivalent CH/CD oscillators in these compounds. A C_{2v} model Hamiltonian containing inter-oscillator coupling terms is shown to predict the full overtone spectra of these compounds. We have studied the overtone spectra

of 1,2 dihaloethanes in the near infrared region³³ where also the symmetry effects are observed. We have shown that the model Hamiltonian used for dihalomethanes can be used to interpret the overtone spectra of 1,2 dihaloethanes (Chapter 5). Henry and coworkers analyzed the overtone spectra of ammonia³⁰ and neopentane^{34,35} using a C_{3v} model Hamiltonian which is an extension of the C_{2v} Hamiltonian used for dihalomethanes. The observed splittings of the A and E components of the overtone spectra are well predicted by this Hamiltonian. We have used the C_{3v} local mode Hamiltonian to analyze the overtone spectrum of 2-butanone³⁶. We have shown that the CH_3 group away from the carbonyl maintains C_{3v} symmetry whereas that adjacent to the carbonyl is affected by the anisotropic environments of lone pair and π electron effects and loses C_{3v} symmetry (Chapter 5). Halonen and Child have given a local mode theory of C_{3v} molecules like CH_3D , CHD_3 , SiH_3D and $SiHD_3$ ³⁷ and that of O_h molecules like SF_6 , WF_6 and UF_6 ³⁸. These authors also used coupled local mode Hamiltonians for calculating the spectra.

The general form of the coupled local mode Hamiltonian used for an XH_n system is³¹⁻³⁸

$$\begin{aligned}
 H = & \sum_i V_i + \omega x \sum_i (V_i + V_i^2) \\
 & + \frac{\epsilon}{2} \sum_{i=1}^n \sum_{j=1}^n \gamma (a_i^+ - a_i)(a_j^+ - a_j) \\
 & + \frac{\epsilon}{2} \sum_{i=1}^n \sum_{j=1}^n \phi (a_i + a_i)(a_j + a_j)
 \end{aligned} \tag{1.10}$$

Here the first two terms represent the unperturbed local mode energy and the last two terms represent the harmonic coupling between the local modes. ω and ω_x are respectively the mechanical frequency (X_1) and anharmonicity ($-X_2$) of the XH bonds, V_i and V_j are the quantum numbers for the i^{th} and j^{th} X-H bond respectively. The parameter γ characterizes the kinetic energy coupling between the different XH oscillators and ϕ the corresponding potential energy coupling. These coupling parameters are related to Wilson G and F matrix elements respectively.

$$\gamma = -\frac{1}{2} \frac{G_{ij}}{G_{ii}} \quad (1.11a)$$

$$\phi = -\frac{1}{2} \frac{F_{ij}}{F_{ii}} \quad (1.11b)$$

The operators a^+ and a are related to the normalized momentum and coordinate variables through

$$p = (a^+ - a) \quad (1.12a)$$

$$q = (a^+ + a), \quad (1.12b)$$

and have the usual raising and lowering properties in the harmonic oscillator limit³⁹

Table 1.1

C_{2v} Hamiltonian matrices for a system of two coupled
CH oscillators (All matrix elements are in units of ω)

$$\begin{array}{l}
 |11\rangle \\
 |20\rangle_+
 \end{array}
 \begin{bmatrix}
 2-4x & -2(\gamma-\emptyset) \\
 -2(\gamma-\emptyset) & 2-6x
 \end{bmatrix}
 \quad
 |21\rangle_- : (2-6x)$$

$$\begin{array}{l}
 |21\rangle_- \\
 |30\rangle_-
 \end{array}
 \begin{bmatrix}
 3-8x+2(\gamma-\emptyset) & -\sqrt{3}(\gamma-\emptyset) \\
 -\sqrt{3}(\gamma-\emptyset) & 3-12x
 \end{bmatrix}
 \quad
 \begin{array}{l}
 |21\rangle_+ \\
 |30\rangle_+
 \end{array}
 \begin{bmatrix}
 3-8x-2(\gamma-\emptyset) & -\sqrt{3}(\gamma-\emptyset) \\
 -\sqrt{3}(\gamma-\emptyset) & 3-12x
 \end{bmatrix}$$

$$\begin{array}{l}
 |31\rangle_- \\
 |40\rangle_-
 \end{array}
 \begin{bmatrix}
 4-14x & -2(\gamma-\emptyset) \\
 -2(\gamma-\emptyset) & 4-20x
 \end{bmatrix}
 \quad
 \begin{array}{l}
 |22\rangle \\
 |31\rangle_+ \\
 |40\rangle_+
 \end{array}
 \begin{bmatrix}
 4-12x & -\sqrt{12}(\gamma-\emptyset) & 0 \\
 -\sqrt{12}(\gamma-\emptyset) & 4-14x & -2(\gamma-\emptyset) \\
 0 & -2(\gamma-\emptyset) & 4-20x
 \end{bmatrix}$$

$$\begin{array}{l}
 |32\rangle_- \\
 |41\rangle_- \\
 |50\rangle_-
 \end{array}
 \begin{bmatrix}
 5-18x+3(\gamma-\emptyset) & -\sqrt{8}(\gamma-\emptyset) & 0 \\
 -\sqrt{8}(\gamma-\emptyset) & 5-22x & -\sqrt{5}(\gamma-\emptyset) \\
 0 & -\sqrt{5}(\gamma-\emptyset) & 5-30x
 \end{bmatrix}$$

$$\begin{array}{l}
 |32\rangle_+ \\
 |41\rangle_+ \\
 |50\rangle_+
 \end{array}
 \begin{bmatrix}
 5-18x-3(\gamma-\emptyset) & -\sqrt{8}(\gamma-\emptyset) & 0 \\
 -\sqrt{8}(\gamma-\emptyset) & 5-22x & -\sqrt{5}(\gamma-\emptyset) \\
 0 & -\sqrt{5}(\gamma-\emptyset) & 5-30x
 \end{bmatrix}$$

$$\begin{aligned}\langle v + 1 | a^+ | v \rangle &= (v + 1)^{\frac{1}{2}} \\ \langle v - 1 | a | v \rangle &= v^{\frac{1}{2}}\end{aligned}\tag{1.13}$$

These properties are shown to be valid to a good approximation even for Morse oscillators³¹. This is called ladder approximation. Since manifolds corresponding to different values of the total quantum number ($\sum_i v_i$) are well separated in energy, inter-manifold couplings are neglected. With these two approximations the Hamiltonian matrix elements are calculated for the symmetrized basis sets relevant to the problem. Tables 1.1 and 1.2 shows the Hamiltonian matrices for XH_2 and XH_3 groups^{31,34}. The details of the calculation of overtone spectra using these Hamiltonian matrices are given in Chapter 5 where our work on 1,2 dihaloethanes and 2-butanone are presented.

It is seen that the effective inter-oscillator coupling strength decreases with increasing level of excitation and for $\Delta v_{\text{X-H}} \gg 3$, the spectra are dominated by transitions to states whose components have all the excitation energy localized on one of the equivalent XH oscillators. The symmetry labels are no longer required for these higher states where symmetrized local mode overtone states are quasi-degenerate. This behaviour is clearly indicated in the observed overtone spectra of many compounds³⁰⁻³⁸ and local mode-normal mode correlation diagrams given by some workers^{37,38}.

1.23 Intensity Aspects in Overtone Spectra

Although the local mode model has been used extensively to explain X-H stretching overtone spectra of a wide variety of molecules, relatively very little attention has been directed to the problem of overtone intensities. In a molecule with a set of equivalent X-H oscillators, the intensities of the X-H overtone peaks depend on (1) the functional dependence of the dipole moment of the electronic ground state on the local coordinates, (2) the matrix elements of the powers of the coordinates between the Morse oscillator wave functions, and (3) the mixing of pure local mode states among themselves or with other normal modes.

Two problems in the intensity aspects are found to be of particular interest—the fall off in intensity of local mode overtones and the relative intensities of local-local combinations and pure local mode overtones for a given V manifold. Burberry and Albracht⁴⁰ investigated the fall off in intensity of the local mode transitions with increasing quantum number V . They used linear and diagonal quadratic terms in the electric dipole moment function with the two expansion coefficient taken to be empirically determined parameters.

This method involves the difficulty that, even if the off-diagonal terms are neglected, the term involving v^{th} power of the coordinate in the dipole moment function may be needed to explain the intensity of the $0 \rightarrow v$ transition⁴¹. Wallace and Wu²⁶ used only the linear term in the electric dipole moment operator to interpret the fall off in overtone intensity of dihalomethanes. Schek et al⁴² attempted to account for the intensities of CH stretching overtones in crystalline naphthalene in terms of a dipole moment function of the form $\mu(R) = kR \exp(-R/R^*)$ where R^* was chosen empirically to give the best fit in the spectra. In another study, Burberry and Albrecht⁴³ have attempted to account for the observed local mode combination intensities in tetramethylsilane and benzene. In one calculation, it is assumed that the intensity arises solely from an off-diagonal quadratic term in the dipole moment operator, the coefficient of which is treated as an empirical parameter. The matrix elements of the dipole moment are evaluated using single oscillator wave functions which are obtained by diagonalizing a quartic potential in a harmonic oscillator basis. In the second calculation, the electric dipole moment function is assumed to be separable in local coordinates, and the combination intensities are assumed to arise solely from mixing of the zeroth order local mode states by terms upto quadratic levels in both potential and kinetic energies. The authors concluded

from the comparative study of the two cases that the second source, namely mixing of zero order local mode states, is more important than off-diagonal terms in dipole moment function. Stannard et al⁴⁴ have carried out a detailed calculation of overtone intensities in water molecule. The result of their studies indicated that the most important source of overtone and combination intensity arises from diagonal and off-diagonal terms higher than linear in the electric dipole moment operator, i.e., intensity borrowing due to off-diagonal terms in the local coordinate vibrational Hamiltonian is relatively unimportant. Tamagaka et al⁴⁵ have fitted the observed overtone intensities in a series of molecules with first and second order terms in a one dimensional or two dimensional dipole moment function.

Henry and coworkers have recently given a theoretical description of the overtone intensities in dihalomethanes⁴⁶ where the functional dependence of dipole moment on local coordinates is determined from CNDO calculations and numerical differentiation techniques. Morse oscillator wave functions are used to describe the vibrational states within a symmetrized local mode description, and the evaluate the matrix elements over powers of local coordinates. Vibrational mixing of symmetrized Morse oscillator product states is determined from a harmonic coupling model. The theory predicts that

vibrational mixing is the more important source of intensity for combination bands than off-diagonal terms in the local co-ordinate expansion of the electric dipole moment. For pure overtones significant contribution in intensity arise from terms of first, second and third derivatives of dipole expansion.

An entirely different approach to the problem of origin of overtone intensities has been suggested recently by Medvedev⁴⁷. This author used the quasi-classical Landau-Lifshitz formula to overtone transitions. The transition probabilities are expressed in terms of the repulsive branch of molecular potential which is characterized by a constant β describing its rapid rise in the region of strong interatomic repulsion. This work shows that for a $0 \rightarrow V$ transition with $V > 1$, the repulsive branch of the molecular potential contributes to the transition matrix element whereas the attractive branch of the potential contributes for $V = 1$ transition. Lewerentz and Quack⁴⁸ who use the Mecke function in their study of the isolated CH overtone intensities in chloroform and bromoform disagrees with the arguments of Medvedev and point out that the range of internuclear distance corresponding to the repulsive branch of the molecular potential contributes less than 1% to the total matrix element $\langle v | \mu | 0 \rangle$.

Also the band strengths are shown to be determined by the shape of the dipole function, contrary to the arguments of Medvedev.

A number of other workers have also studied the intensity aspects in overtone spectra of molecules containing X-H oscillators. However a general theory of overtone intensities has not been developed so far.

1.30 Applications of X-H Overtone Spectroscopy

1.31 Characterization of CH Bonds in Organic Compounds

The most widely known application of overtone spectroscopy is the characterization of CH bonds in organic compounds. Considerable use has been made of CH overtone absorption as a sensitive probe of structural information in polyatomic molecules. The infrared spectral study of vibrational fundamentals has been accepted as a well established technique for obtaining important structural information about molecules. But the spectra of strongly coupled fundamentals of the CH stretching vibrations become difficult to understand in terms of the influence of environment on a particular CH oscillator. In the fundamental IR spectroscopy, the details of the individual CH bonds are obtained by studying the partially deuterated analogues of a molecule, where

all the CH sites except that under observation are deuterated. This yields the so called isolated CH stretching frequency which will be free from spectral complications from other degenerate and nearly degenerate modes, and reveals the factors influencing individual CH bonds. McKean and his coworkers have applied this technique to obtain structural details of a number of organic molecules belonging to different classes⁴⁹.

There are additional advantages in using overtone absorption spectroscopy for characterizing individual CH bonds in a molecule. First is the practical reason that one can avoid dependence on deuterated samples which are often not readily available and also difficult to prepare. The overtone bands are quite well resolved even for very similar oscillators. A shift of $\sim 10 \text{ cm}^{-1}$ in the CH fundamental region causes a shift of $\sim 70 \text{ cm}^{-1}$ in the fifth overtone region⁵⁰. Third, the CH stretching parameters obtained from fitting a number of sequential overtones for each local mode oscillator promise higher precision than single measurements in the infrared. Even with partial deuteration the isolated CH fundamentals may be perturbed by Fermi resonance with overtone of CH deformation mode⁴⁹. Finally, the overtone spectra also give the anharmonicity values of local mode oscillators which determine the shape of the oscillator

potential, whereas IR studies yield only the frequencies of isolated CH bonds.

In the light of the success of the local mode model for describing the overtone vibrations, it is seen that overtone studies can provide important new information on molecular structural aspects. The local mode parameters X_1 and X_2 are characteristic of the particular CH oscillator and thus give rise to distinct absorption peaks corresponding to the distinct nonequivalent CH oscillators in the molecule. The nonequivalence of CH oscillators can arise from different origins. As is well known alkyl and aryl CH bonds are nonequivalent due to the difference in states of carbon hybridization. In an alkane there exist primary, secondary and tertiary CH bonds which are nonequivalent. Cycloalkanes contain axial and equatorial CH bonds which interconvert to each other rapidly⁵¹. Nonequivalence of CH bonds can also arise from conformational origin, inter and intra molecular environmental origins etc.

Alkyl and aryl CH bonds in toluene and xylenes display distinguishable peaks in their overtone spectra⁵²⁻⁵⁴ as do the primary, secondary and tertiary CH bonds in alkanes^{50,55}. Perry and Zewail have observed the resolved contributions of α and β CH bonds in the overtone spectrum of naphthalene⁵⁶. In

later investigations it has been found that the local mode parameters are dependent not only on the type of CH oscillator but also on the environment. The local mode anharmonicity of CH_3 oscillators in 3-methyl pentane decreases markedly on passing from liquid to solid state⁵⁷. This decrease has been attributed to viscosity dependence of the CH local mode potential through the creation of a viscosity dependent barrier to dissociation in the solid phase. This renders the CH vibrations more harmonic in the solid phase resulting in a reduction of the anharmonicity value. A similar effect has been observed for the CH_3 local oscillators in several methyl substituted butanes⁵⁸ and pentanes⁵⁹. Here, intramolecular steric crowding of the methyl groups provides a barrier to large amplitude vibrational motions. As a result the local mode anharmonicity decreases regularly as the steric hindrance increase due to increased methyl substitution. We have studied the aryl CH overtone spectra of liquid styrene and solid polystyrene in the near infrared and visible regions. However no appreciable difference in anharmonicity values is observed between the two cases. We have concluded that even if there is a change in anharmonicity due to change of phase this would have been compensated by a difference in steric environments between the two molecules. However a comparison with the benzene overtone peak positions yields the result that the aryl CH bonds in polystyrene are slightly longer than in benzene whereas those in styrene are of almost equal length to those of benzene (Chapter 4).

Much work has been carried out on the effect of substituent atoms or groups on CH oscillators of molecules which are reflected by shifts in the overtone transition energy and local mode parameters. Studies on halomethanes^{60,61} have revealed the importance of the mass, electronegativity, and steric influences of the halogens in determining the local mode parameters of the CH bonds in these compounds. Our work on the overtone spectrum of trichloroethylene⁶² has shown that the CH bond length in this compound is considerably smaller than that in ethylene (Chapter 5). Extensive studies on the aryl CH overtones of substituted benzenes have been carried out by several workers⁶³⁻⁶⁵. The general result of these studies is that an electron withdrawing group or atom when substituted in the benzene ring causes an increase in the mechanical frequency of the ring CH bonds, while an electron donating group causes a decrease in the mechanical frequency. We have studied the overtone spectra of some substituted benzenes and have proposed the physical mechanism of the change in aryl CH bond force constant (and hence mechanical frequency) upon substitution on the ring⁶⁶. An extensive discussion on the earlier works on substituted benzenes is given in Chapter 4 where our work in this area is presented.

Conformationally nonequivalent CH bonds have been detected and characterized by overtone spectroscopy in many molecules. Subtle environmental differences occurring in

such cases is detected through the actual resolution of the contributions of the inequivalent CH bonds to the overtone spectrum. In the overtone spectrum of hexamethyl benzene two components have been observed with an intensity ratio of 2:1⁶⁷. In this molecule the restricted methyl group rotation results in a geared or cog-wheel like arrangement of methyl groups around the benzene ring. The result of such an arrangement is the existence of two types of conformationally inequivalent CH bonds in the methyl groups which give rise to the two components observed in the overtone spectrum. Similarly the overtone spectra of toluene and xylenes⁵⁴ clearly indicates the presence of inequivalent CH bonds in the methyl groups. Two peaks are observed in the methyl regions of the spectrum of o-xylene and three peaks in the methyl regions of the spectra of toluene, m-xylene and p-xylene. The two peaks in the o-xylene spectrum are shown to arise from the two types of inequivalent CH bonds in the methyl groups. In the case of toluene, m-xylene and p-xylene the highest frequency peak is associated with the in-plane methyl CH, the lowest frequency peak with the two out-of-plane methyl CH bonds, and the central peak is assigned to transitions originating from rotational levels above the rotational barrier. A recent study of the spectra of trimethyl benzenes⁶⁸ also show the presence of inequivalent methyl CH bonds similar to those in toluene and xylenes. CH overtone spectroscopic studies in penta and

tetra haloethanes in the liquid and gas-phase⁶⁹ have revealed the existence of considerable intermolecular interactions in penta haloethanes and the contributions of the gauche and trans conformers of tetra haloethanes. From the deconvolution of the overtone bands the gauche - trans energy difference has been evaluated.

The study of overtone spectra of cycloalkanes and cycloalkenes has helped in correlating overtone band structures to molecular conformational properties. In cyclohexane two resolved bands are observed at each overtone level corresponding to axial and equatorial CH oscillators^{70,71}. It is seen that neither the inter conversion rate of the cyclohexane chair configuration nor even the considerably faster pseudo-rotation in cyclopentane⁷⁰ is sufficiently rapid to motionally average in overtone absorption the nonequivalent CH sites in these molecules. This is in contrast to the situation in NMR where the nonequivalence is averaged out due to the slower 'shutter speed' of r.f. absorption compared to the near infrared and visible overtone absorption⁷⁰.

Recent studies on nonequivalent CH oscillators include those on molecules containing methyl groups subjected to anisotropic environments created by nonbonding electron pairs (lone pairs) on an adjacent hetero atom (O, S, N) or by π electrons of an adjacent double bond^{72,73}. In all such

molecules two distinct bands at each quantum level are observed as the overtones of the nonequivalent methyl CH bonds. Thus, methanol, acetaldehyde, acetone, and several other compounds contain such nonequivalent methyl CH oscillators. The effect is explained as the interaction of the electron lone pair with the CH bonds situated trans to the lone pair (lone pair trans effect) or as the interaction of out-of the molecular plane CH bonds with the π cloud (π cloud effect)^{72,73}. A different mechanism appears to operate in the case of $C=O$ containing molecules where a simple trans effect cannot explain the relative strength of the two types of methyl CH bonds⁷³. Our work on acetophenone⁶⁶ has shown for the first time that the methyl group in this molecule contains two types of CH bonds. The mechanical frequency of the in-plane CH bond in this molecule is much larger than that in acetaldehyde and acetone. Quantum mechanical resonance between different valence bond structures seem to play a key role in this behaviour. The out-of-plane CH bonds show decreased mechanical frequency with respect to acetone and acetaldehyde. This is attributed to the large $C=O$ bond length in acetophenone which results in decreased π interaction. More discussion on inequivalent methyl CH bonds arising from anisotropic environments is given in Chapters 4 and 5 where our studies on acetophenone and 2-butanone are presented.

It thus follows that CH overtone absorption spectroscopy will be of continued interest as a sensitive probe of structural information in polyatomic molecules.

1.32 Intramolecular Vibrational Redistribution (IVR)

Understanding intramolecular vibrational energy transfer in large polyatomic molecules is one of the most important challenges in chemical reaction dynamics and is of crucial importance in assessing the possibilities of mode selective chemistry¹³⁻¹⁷.

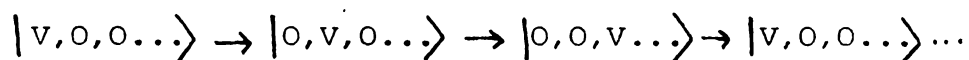
Overtone studies in room temperature gas-phase^{35,74-77} and low temperature gas and solid-phase^{56,78,79} have revealed that intramolecular vibrational relaxation (IVR) occur in a variety of hydrocarbons on a surprisingly fast time scale. These studies are based primarily on the observation of Lorentzian line shapes for high overtone spectra under the above mentioned 'collision free' conditions and indicate that energy flows out of an excited vibrational local mode in time scales as small as 50 femtoseconds.

The most extensively studied species is naturally benzene and its deuterated analogues, both experimentally^{74,75,79} and theoretically⁸⁰⁻⁸⁴. Local mode line shapes have also been investigated in neopentane and its deuterated analogues³⁵ the

tetramethyl compounds of Si, Ge, and Sn⁷⁷, deuterated methanes⁸⁵, tetramethyl dioxetane⁷⁸, durene⁸⁶ and naphthalene^{56,87,88}. Intramolecular vibrational dynamics in compounds containing isolated CH bonds have been analyzed using tridiagonal Fermi resonance Hamiltonian obtained spectroscopically^{89,90}. It is generally agreed that the local mode line shapes for relatively large molecules are determined by intramolecular processes, but there is much disagreement over the identity of the kind of coupling mechanism causing IVR. There are two general types of possible intramolecular line broadening mechanisms. One is life time broadening (uncertainty principle) due to the decay of the excited state population. Several coupling schemes have been proposed to account for the decay of the initially prepared state⁸⁰⁻⁸⁴. The second type of broadening mechanism is dephasing in which line broadening occurs due to the modulation of the overtone transition frequency by other vibrational modes of the molecule^{91,92}. No population decay occurs for pure dephasing. Both the mechanisms, dephasing and life time broadening have been applied to benzene to interpret the line width data. However there are two general arguments against the significant contribution of dephasing to overtone line widths. The first objection is that dephasing predicts a general increase in overtone line widths with increase of the vibrational quantum

number V . However experimental observations show that this need not be true⁷⁵⁻⁷⁷. Secondly, dephasing predicts that the line widths should be very sensitive to temperature and should become very narrow at low temperatures, due to the depopulation of the lower frequency modes. However, recent experiments have shown that overtone line widths are insensitive to changes in temperature down to very low temperatures. The $\Delta v_{CH} = 5$ overtone spectrum of tetramethyl dioxetane obtained in a seeded supersonic expansion is found to be essentially same as the room temperature photoacoustically detected gas-phase spectrum⁷⁸. The low temperature (1.8K) overtone spectrum of crystalline benzene⁷⁹ has line widths similar to those measured in the gas-phase at room temperature^{74,75}.

Another process, in which no population decay of excited state occurs, but can cause line broadening has also been suggested⁹³. This process can be represented as



where the V vibrational quanta hop among the equivalent CH sites. This process can be important in small molecules like water but will be a very slow process in large molecules like benzene, neopentane, tetramethyl dioxetane etc.

These arguments and observations have led the scientists to the conclusion that in almost all cases the major contribution of overtone line widths in gas-phase as well as in low temperature (molecular beam or crystal) arise from homogeneous broadening due to the decay of excited state population. The decay of excited state occurs due to coupling of this state with other vibrational motions. Several such coupling routes have been proposed. Bray and Berry⁷⁴, Reddy, Heller and Berry⁷⁵ and Heller and Mukamel⁸⁰ considered a local-local coupling scheme in which local mode overtone states are initially coupled to local-local combinations states. The major couplings are considered to be the combination states with only one vibrational quantum has been redistributed. i.e., $|v,0,0\dots\rangle \rightarrow |v-1,1,0\dots\rangle$. Stannard and Gelbart⁸¹ quantum dynamically modelled the overtone decay of benzene assuming that the coupling between CH oscillators to be primarily responsible for the broad overtone line shapes. They observed no decay of the initially prepared state. Sage and Jortner⁸² considered a coupling model in which overtone states are resonantly coupled to the full density of ring modes. However the specific interactions responsible for the population decay are not identified in this work. Sibert et al⁸³ presented calculations in which kinetic energy coupling to the CCH in plane wag was found to play a key role in the relaxation of the overtone states and obtained good agreement with experimental results. Based on the initial work of

Sibert et al which identified the physical coupling responsible for the overtone decay, Buch et al⁹⁴ provided model calculations for the line widths of overtone transitions in benzene and deuterated benzenes for different overtone levels. They assumed a Bixon - Jortner type line shape function. The matrix elements are calculated based on the original suggestion of Sibert et al⁸³ as due to the Coriolis type 2:1 kinetic energy interaction between CH stretch and nearly degenerate overtone of CCH wag. The calculation of the density of effectively coupled states is carried out using a statistical wave function approximation⁹⁵. The behaviour of CH and CD overtone line widths (oscillatory behaviour with quantum number and isotope effects) in benzene, deuterated benzenes and pentafluorobenzene predicted by the theory showed good agreement with experimental results. The authors concluded that the overtone line widths are not determined by the overall density of states but depends on the density of effectively coupled states only. This result is contrary to the Sage-Jortner model⁸². Almost simultaneously to the work of Buch et al, Sibert et al gave detailed quantum mechanical and classical mechanical⁸⁴ calculations of CH and CD overtones in benzene and deuterated benzenes. The authors analytically calculated the matrix elements of the 2:1 Fermi interaction between CH stretch and CCH in-plane wag which in turn are coupled to C-C stretches C-C-C in-plane bends etc. Only kinetic

energy couplings are considered in these calculations since the potential couplings turn out to be very small⁸⁴. The results obtained are in good qualitative agreement with experimental findings. The authors have given a detailed discussion of the state preparation in experiments like those of Reddy et al and have also given several suggestions for future experiments.

As benzene is the 'hydrogen atom' of aromatic molecules, one can identify neopentane to have the same position among large aliphatic compounds. Like in benzene, all the CH bonds in neopentane are equivalent. However unlike in benzene each carbon atom in neopentane is bonded to three hydrogen atoms. In a recent work, Henry and coworkers³⁵ successfully explained the behaviour of gas phase overtone line widths of neopentane using the scheme of Sibert et al. In neopentane the CH stretching overtone states are coupled to combinations involving CH deformation modes.

The mechanism of overtone relaxation as the coupling of CH overtone states to combinations involving overtones of CH deformation is also considered in the theoretical studies of Hutchinson et al⁹⁶ and high resolution spectroscopic experimental studies of Quack et al^{89,90}. Hutchinson et al modelled both classically and quantum mechanically the CH overtone relaxation in HC_n chains ($n = 4-8$). The analysis

has shown that ultra fast (50-100 fs) irreversible vibrational energy transfer due to sequential nonlinear resonance occurs in even small hydrocarbons. Later classical studies by Sumpter and Thomson⁹⁷ in model four atom systems also showed agreement with the predictions of Hutchinson et al. Quack and coworkers used tridiagonal stretch-bend Fermi resonance Hamiltonian obtained from high resolution gas-phase spectra to solve time dependent Schrodinger equation. These studies also revealed subpicosecond relaxation of vibrational energy out of the excited CH overtone states. The Fermi type kinetic energy interaction between CH stretch and CH deformation motions thus seems to be a universal coupling mechanism in many organic molecules, eventhough certain olefinic compounds indicate coupling of CH stretch overtone with combination involving C=C stretch⁹⁸. However, our work on liquid trichloroethylene⁶² indicates overtone coupling with CH deformation motion rather than C=C stretching motion (Chapter 5).

1.33 Overtone Photochemistry

The observation of single photon excitations of X-H bonds in polyatomic molecules sparked an interest in local mode specific chemistry during the past ten years. This is due to the fact that the local mode excitation can prepare molecules with well-defined internal energy combined with the possibility that the initial vibrational energy

distribution may be nonrandom. Berry and Reddy used steady state photolysis and Stern-Volmer analysis to measure the unimolecular rate coefficient as a function of energy, for the isomerization of methyl isocyanide and allyl isocyanide⁹⁹. Crim and coworkers employed time resolved techniques to measure unimolecular rate constant for decomposition of tetramethyl dioxetane and t-butyl hydroperoxide¹⁰⁰. Zare and coworkers have also studied t-butyl hydroperoxide using steady state photolysis¹⁰¹. Jasinski and coworkers measured the overtone induced unimolecular reaction rate constants for the isomerization of cyclobutene as a function of energy and overtone transition by studying the pressure dependence of photo-isomerization rate constant¹⁰². These authors also studied the overtone induced isomerization of 2-methyl cyclopentadiene and 1-cyclopropyl cyclobutene¹⁰³. The results of most of these studies are in reasonable agreement with statistical unimolecular rate theories such as RRKM theory¹⁰⁴, which assumes that energy randomization is rapid and complete prior to unimolecular reactions. Two exceptions have been noted. Zare and coworkers¹⁰¹ present evidence that a small fraction of t-butyl hydroperoxide molecules activated by the CH stretching overtone decompose prior to complete energy randomization. Berry and Reddy⁹⁹ note that allyl isocyanide exhibits small discrepancies from the predicted (by RRKM theory) monotonic increase of rate constant with energy. They

have attributed these discrepancies to a dependence of the rate coefficient on the particular type of CH overtone transition excited. They have thus suggested that overtone excitation of allyl isocyanide produces a nonrandom initial energy distribution which persists and affects the observed reaction rate on a microsecond time scale. However, the recently developed Master equation formalism by Miller and Chandler¹⁰⁵ which considers RRKM model along with collision effects has been used to explain the observations of Zare et al as well as those of Berry and Reddy. This shows that the assumption of nonstatistical initial energy distribution need not be true.

Perry and Zewail¹⁰⁶ reported the results of picosecond measurements of $\Delta v_{\text{CH}} = 5$ local mode transitions of hydrogen peroxide where a picosecond pulse prepares the OH stretch overtone and a second pulse delayed in time monitors the population of OH radicals produced following the overtone excitation ($\text{HO-OH} \rightarrow 2\text{OH}$). These authors concluded that the energy distribution time from OH stretch to OO reaction coordinate is $< 60\text{ps}$. Crim and coworkers carried out the overtone spectroscopic measurements of predissociative states of hydrogen peroxide in a low pressure room temperature sample by exciting the OH stretching overtone transition with a dye laser and detecting the OH fragments using laser induced

fluorescence¹⁰⁰. In their later studies, these measurements are carried out in a supersonic jet¹⁰⁷. The vibrational overtone transitions in the predissociative state revealed homogeneous, lifetime broadened structure with predissociative life time ~ 3.5 ps. The measurement is also consistent with the time resolved experiment of Perry and Zewail mentioned earlier. A large number of other overtone photochemistry studies that have been carried out are given in a recent review¹⁰⁸.

A number of theoretical works have also been appeared on the topic of local mode bond specific excitations. Xie Bo-Min and coworkers recently reported a theoretical analysis of how bond selective chemical reactions can be promoted using frequency modulated lasers¹⁰⁹. Those authors concluded that with the rapid progress in fast pulse techniques and modulation techniques bond selective reactions initiated by local mode excitations can be achieved in practice. Bonds with large anharmonicity values are shown to have good selectivity. Holme and Hutchinson have recently presented a study of the dynamics of overtone excitation¹¹⁰. Eventhough a large number of papers, on the coupling and relaxation of an initially prepared local mode state have appeared in literature, no attention was given to the dynamics of overtone excitation process. This work thus forms the first of its kind. The authors have analysed quantum mechanically the process of

excitation and have shown that overtone excitation is a very slow process compared with IVR, slower by several orders of magnitude. The authors conclude that, localized excitations can be produced only by eigen state superposition. In a very recent paper¹¹¹ Hutchinson have given a detailed quantum mechanical study of state preparation, intramolecular energy transfer and unimolecular reaction induced by local mode overtone excitation. Photochemical yields are calculated for a range of frequencies and pulse widths of the laser.

The topics of IVR and overtone photochemistry are open for further theoretical and experimental research. Finer details of the interactions among the different molecular modes of vibration and the role and structure of quasi-continuum of vibrational levels¹¹² are to be known to design and interpret photochemistry experiments.

REFERENCES

1. B.R.Henry, in "Vibrational Spectra and Structure", J.R.Durig (Ed.), (Elsevier, New York, 1981), Vol.10, p.269 and refs. therein.
2. M.L.Sage and J.Jortner, in "Advances in Chemical Physics", 47, 293 (1981).
3. H.L.Fang and R.L.Swofford, in "Advances in Laser Spectroscopy", B.A.Garetz and J.R.Lombardi (Eds.), (Hayden, London, 1982), Vol.1, p.1 and refs.therein.
4. M.S.Child and L.Halonen, in "Advances in Chemical Physics", 57, 1 (1984) and refs.therein.
5. W.Siebrand, J.Chem.Phys.46, 440 (1967); *ibid.*, 47, 2411 (1967); W.Siebrand and D.F.Williams, *ibid.*, 49, 1860 (1968); B.R.Henry and W.Siebrand, *ibid.*, 49, 5369 (1968).
6. B.R.Henry and M.Kasha, Ann.Rev.Phys.Chem.19, 161 (1968).
7. J.Jortner, S.A.Rice and R.M.Hochstrasser, in "Advances in Photochemistry", A.A.Noyes, J.N.Pitts and G.Hammond (Eds.), (Wiley, New York, 1969), Vol.7, p.149.
8. J.B.Birks, "Photophysics of Aromatic Molecules", (Wiley, New York, 1970), Sec.5.9.
9. E.W.Schlag, S.Schneider and S.F.Fischer, Ann.Rev.Phys.Chem. 22, 465 (1971).

10. B.R.Henry, *Acc.Chem.Res.*10, 207 (1977); *Idem*, *J.Phys.Chem.*
80, 2160 (1976).
11. R.J.Heyward and B.R.Henry, *J.Mol.Spectrosc.*50, 58 (1974);
ibid., 57, 221 (1975); *Idem*, *Chem.Phys.*12, 387 (1976).
12. R.L.Swofford, M.E.Long and A.C.Albrecht, *J.Chem.Phys.*65, 179
(1976).
13. N.Bloembergen, *Opt.Commun.*15, 416 (1975).
14. R.V.Ambartzumian and V.S.Letokhov, *Acc.Chem.Res.*10, 61 (1977).
15. N.Bloembergen and E.Yablonovich, *Phys.Today*, 31, 23 (1978).
16. A.Ben-Shaul, Y.Haas, K.L.Kompa and R.D.Levine, "Lasers and
Chemical Change", (Springer Verlag, 1981), Chapter 5 and refs.
therein.
17. M.Quack, in "Advances in Chemical Physics", 50, 395 (1982),
and refs.therein.
18. E.B.Wilson, Jr, J.C.Decius and P.C.Gross, "Molecular Vibrations",
(Mc Graw Hill, New York, 1955).
19. G.Herzberg, "Infrared and Raman Spectra of Polyatomic Molecules",
(Van Nostrand, New York, 1945).
20. J.W.Ellis, *Trans.Faraday.Soc.*25, 888 (1929); *Idem*, *Phys.Rev.*
32, 906 (1928); *Idem*, *ibid.*, 33, 27 (1929).

21. M.L.Sage, Chem.Phys.35, 375 (1978).
22. M.L.Sage and J.Jortner, Chem.Phys.Lett.62, 451 (1979).
23. M.L.Sage, J.Phys.Chem.83, 1455 (1979).
24. R.Wallace, Chem.Phys.11, 189 (1975).
25. J.Bron and R.Wallace, Can.J.Chem.55, 2292 (1977).
26. R.Wallace and A.A.Wu, Chem.Phys.39, 221 (1979).
27. L.Halonen, Chem.Phys.Lett.87, 221 (1982).
28. W.M.Gelbart, P.R.Stannard and M.L.Elert, Int.J.Quantum.Chem.
14, 703 (1978).
29. H.S.Moller and O.S.Mortensen, Chem.Phys.Lett.66, 539 (1979).
30. I.A.Watson, B.R.Henry and I.G.Ross, Spectrochim.Acta.Part A,
37, 857 (1981).
31. O.S.Mortensen, B.R.Henry, and M.A.Mohammadi, J.Chem.Phys.
75, 4800 (1981).
32. M.K.Ahmed and B.R.Henry, J.Phys.Chem.90, 1081 (1986).
33. T.M.A.Rasheed, V.P.N.Nampoori and K.Sathianandan, Chem.Phys.
108, 349 (1986).
34. B.R.Henry, A.W.Tarr, O.S.Mortensen, W.F.Murphy and D.A.C.
Compton, J.Chem.Phys.79, 2583 (1983).

35. A.W.Tarr and B.R.Henry, *J.Chem.Phys.*84, 1355 (1986).
36. T.M.A.Rasheed, V.P.N.Nampoori and K.Sathianandan, *Spectrochim. Acta.*(1987), in press.
37. L.Halonen and M.S.Child, *J.Chem.Phys.*79, 4355 (1983).
38. L.Halonen and M.S.Child, *J.Chem.Phys.*79, 559 (1983).
39. Leonard I.Schiff, "Quantum Mechanics", 3rd Edn., (McGraw-Hill, 1968), p.182.
40. M.S.Burberry and A.C.Albrecht, *J.Chem.Phys.*70, 147 (1979).
41. J.L.Dunham, *Phys.Rev.*35, 1347 (1930).
42. I.Schek, J.Jortner and M.L.Sage, *Chem.Phys.Lett.*64, 209 (1979).
43. M.S.Burberry and A.C.Albrecht, *J.Chem.Phys.*71, 4631 (1979).
44. P.R.Stannard, M.L.Elert and W.M.Gelbart, *J.Chem.Phys.*74, 6050 (1981).
45. K.Tamagake, S.Hyodo and T.Fujiyama, *Bull.Chem.Soc.Jpn.*55, 1267 (1982); Idem, *ibid*, 55, 1272 (1982); Idem, *ibid.*, 55, 1277 (1982).
46. O.S.Mortensen, M.K.Ahmed, B.R.Henry and A.W.Tarr, *J.Chem.Phys.*82, 3903 (1985).
47. E.S.Medvedev, *J.Mol.Spectrosc.*114, 1 (1985); Idem, *Chem.Phys.*73, 243 (1982); Idem, *Chem.Phys.Lett.*120, 173 (1985); Idem, *Spectrosc.Lett.*18, 447 (1985).

48. M.Lewerenz and M.Quack, Chem.Phys.Lett.123, 197 (1986).
49. D.C.Mc Kean, Chem.Soc.Rev.7, 3, 399 (1978), and refs.therein.
50. J.S.Wong and C.B.Moore, J.Chem.Phys.77, 603 (1982).
51. J.D.Roberts and M.C.Caserio, "Basic Principles of Organic Chemistry", (Benjamin, New York, 1964).
52. M.S.Burberry, J.A.Morrel, A.C.Albrecht and R.L.Swofford, J.Chem.Phys.70, 5522 (1979).
53. R.J.Heyward and B.R.Henry, 12, 387 (1976).
54. K.M.Gough and B.R.Henry, J.Phys.Chem.88, 1298 (1984).
55. W.R.A.Greenlay and B.R.Henry, J.Chem.Phys.69, 82 (1978).
56. J.W.Perry and A.H.Zewail, J.Chem.Phys.70, 582 (1979).
57. W.R.A.Greenlay and B.R.Henry, Chem.Phys.Lett.53, 325 (1978).
58. B.R.Henry and R.J.D.Miller, Chem.Phys.Lett.60, 81 (1978).
59. B.R.Henry, M.A.Mohammadi and J.A.Thomson, J.Chem.Phys.
75, 3165 (1981).
60. B.R.Henry and I-Fu Hung, Chem.Phys.29, 465 (1978).
61. H.L.Fang and R.L.Swofford, J.Chem.Phys.72, 6382 (1980).
62. T.M.A.Rasheed, K.P.B.Moosad, V.P.N.Nampoori and K.Sathianandan, Spectrochim.Acta.(1987), in press.

63. Y.Mizugai and M.Katayama, *J.Am.Chem.Soc.*102, 6424 (1980);
Idem, *ibid.*, 103, 5061 (1981).
64. R.Nakagaki and I.Hanazaki, *Spectrochim.Acta.*40A, 57 (1984).
65. K.M.Gough and B.R.Henry, *J.Phys.Chem.*87, 3433 (1983).
66. T.M.A.Rasheed, K.P.B.Moosad, V.P.N.Nampoori and K.Sathianandan,
J.Phys.Chem. (1987), in press.
67. B.R.Henry and W.R.A.Greenlay, *J.Chem.Phys.*72, 5516 (1980).
68. M.K.Ahmed and B.R.Henry, *J.Phys.Chem.*90, 1737 (1986).
69. B.R.Henry and M.A.Mohammadi, *Chem.Phys.*55, 385 (1981).
70. B.R.Henry, I-Fu Hung, R.A.Mc Phail and H.L.Strauss,
*J.Am.Chem.Soc.*102, 515 (1980).
71. J.S.Wong, R.A.Mc Phail, C.B.Moore and H.L.Strauss, *J.Phys.Chem.*
86, 1478 (1982).
72. H.L.Fang and R.L.Swofford, *Appl.Opt.*21, 55 (1982).
73. H.L.Fang, D.M.Meister and R.L.Swofford, *J.Phys.Chem.*88, 405
(1984); Idem, *ibid.*, 88, 410 (1984).
74. R.G.Bray and M.J.Berry, *J.Chem.Phys.*71, 4909 (1979).
75. K.V.Reddy, D.F.Heller and M.J.Berry, *J.Chem.Phys.*76, 2814
(1982).

76. B.R.Henry and M.A.Mohammadi, Chem.Phys.Lett.75, 99 (1980).
77. B.R.Henry, M.A.Mohammadi, I.Hanazaki and R.Nakagaki,
J.Phys.Chem.87, 4827 (1983).
78. G.A.West, R.P.Mariella, J.A.Pete, W.B.Hammond and D.F.Heller,
J.Chem.Phys.75, 2006 (1981).
79. J.W.Perry and A.H.Zewail, J.Chem.Phys.80, 5333 (1984).
80. D.F.Heller and S.Mukamel, J.Chem.Phys.70, 463 (1979).
81. P.R.Stannard and W.M.Gelbart, J.Phys.Chem.85, 3592 (1981).
82. M.L.Sage and J.Jortner, Chem.Phys.Lett.62, 451 (1979).
83. E.L.Sibert III, W.P.Reinhardt and J.T.Hynes, Chem.Phys.Lett.
92, 455 (1982).
84. E.L.Sibert, W.P.Reinhardt and J.T.Hynes, J.Chem.Phys.
81, 1115 (1984); Idem, *ibid.*, 81, 1135 (1984).
85. J.W.Perry, D.J.Moll, A.Kuppermann and A.H.Zewail, J.Chem.Phys.
82, 1195 (1985).
86. J.W.Perry and A.H.Zewail, J.Phys.Chem.86, 5197 (1982).
87. J.W.Perry and A.H.Zewail, Chem.Phys.Lett.65, 31 (1979).
88. A.H.Zewail, W.M.Lambert, P.Felker, J.Perry and W.Warren,
J.Phys.Chem.86, 1184 (1982).

89. H.R.Dubal and M.Quack, *J.Chem.Phys.*81, 3779 (1984).
90. J.E.Baggot, M.C.Chuang, R.N.Zare, H.R.Dubal and M.Quack, *J.Chem.Phys.*82, 1186 (1985).
91. S.Mukamel, *J.Phys.Chem.*88, 832 (1984).
92. S.Mukamel and R.Islampour, *Chem.Phys.Lett.*108, 161 (1984).
93. R.T.Lawton and M.S.Child, *Mol.Phys.*40, 773 (1980).
94. V.Buch, R.B.Gerber and M.A.Ratner, *J.Chem.Phys.*81, 3393 (1984).
95. R.B.Gerber, V.Buch and M.A.Ratner, *Chem.Phys.Lett.*89, 171 (1982).
96. J.S.Hutchinson, W.P.Reinhardt and J.T.Hynes, *J.Chem.Phys.*79, 4247 (1983).
97. B.G.Sumpter and D.L.Thomson, *J.Chem.Phys.*82, 4557 (1985).
98. J.E.Baggot, H.J.Clase and I.M.Mills, *Spectrochim.Acta.*42A 2/3, 319 (1986).
99. K.V.Reddy and M.J.Berry, *Chem.Phys.Lett.*52, 111 (1977);
Idem, *ibid.*, 66, 223 (1979).
100. L.J.Bulter, T.M.Ticich, M.D.Likar and F.F.Crim, *J.Chem.Phys.*85, 2331 (1986); T.R.Rizzo, C.C.Hayden and F.F.Crim, *Faraday Discuss.Chem.Soc.*75, 223 (1983); Idem, *J.Chem.Phys.*81, 4501 (1984); H.R.Dubal and F.F.Crim, *ibid.*, 83, 3863 (1985); T.M.Ticich, T.R.Rizzo, H.R.Dubal and F.F.Crim, *ibid.*, 84, 1508 (1986).

101. D.W.Chandler, W.E.Ferneth and R.N.Zare, *J.Chem.Phys.*77, 4447 (1982).
102. J.M.Jasinski, J.K.Frisoli and C.B.Moore, *J.Chem.Phys.* 79, 1312 (1983).
103. J.M.Jasinski, J.K.Frisoli and C.B.Moore, *J.Phys.Chem.* 87, 2209 (1983); *Idem, ibid.*, 87, 3826 (1983).
104. P.J.Robinson and K.A.Holbrook, "Unimolecular Reactions", (Wiley Interscience, New York, 1972).
105. J.A.Miller and D.W.Chandler, *J.Chem.Phys.*85, 4502 (1986).
106. N.F.Scherer, F.E.Doany, A.H.Zewail and J.W.Perry, *J.Chem.Phys.* 84, 1932 (1986).
107. L.J.Buller, T.M.Ticich, M.D.Likar and F.F.Crim, *J.Chem.Phys.* 85, 2331 (1986).
108. F.F.Crim, *Ann.Rev.Phys.Chem.*35, 657 (1984).
109. Xie Bo-Min, Ding Jia-Qiang, and Wei Xie, *J.Chem.Phys.*84, 3819 (1986).
110. T.A.Holme and J.S.Hutchinson, *J.Chem.Phys.*84, 5455 (1986).
111. J.S.Hutchinson, *J.Chem.Phys.*85, 7087 (1986).
112. G.Hose and H.S.Taylor, *Chem.Phys.*84, 375 (1984) and refs.therein; Ref.16 Chapters 1,2 and 5.

LASER-INDUCED THERMAL LENS EFFECT--THEORY AND APPLICATIONS

2.10 Introduction

With the developments in the field of lasers, there has been a revival of interest in the thermal effects of electromagnetic radiations. This is because of the special properties which laser beams do possess and ordinary light beams do not possess. Lasers can provide highly directed, highly monochromatic radiations with high power densities. These properties opened the possibilities of extremely sensitive detection of the resultant heating of a sample. The measurement schemes, of the thermal effects of the incident radiation on a sample which monitor the residual energy content in the sample, are collectively referred to as photothermal techniques. The two main classes of these techniques that are currently in use are: (1) those based on the temperature variation of the refractive index which can be probed optically and (2) those based on pressure variations which can be probed acoustically. The first technique uses the formation and probing of the different types of optical elements resulting from the spatial variation of the refractive index due to the spatial temperature variations produced by the heating effect from one or more pump laser beams.

The most common optical element is the photothermal lens¹. It is the first photothermal element discovered and analysed in detail. The thermal lensing technique is widely used for measuring weak absorptivities ($10^{-3} - 10^{-6} \text{ cm}^{-1}$) and for recording the absorption spectra of weakly absorbing media (where the origin of the absorption may be one photon overtone transition in the ground electronic state or two photon electronic transition with very low fluorescence quantum yield). Besides the thermal lens, the other photothermal optical elements reported are the prism²⁻⁴, the interferometer⁵⁻¹², the transmission diffraction grating¹³ and the curved mirror¹⁴. The second method of probing photothermal effects uses photoacoustic (PA) effect, also called optoacoustic (OA) effect, which is the generation of acoustic waves due to the absorption of the incident modulated electromagnetic radiation. The effect was originally discovered by Alexander Graham Bell in 1880. With the availability of intense light sources like lasers and powerful lamps and highly sensitive acoustic detectors like microphones, hydrophones, and piezoelectric transducers, the PA technique has become an area of renewed interest. Many theoretical and experimental investigations on various physical phenomena including measurements of weak absorption, have been carried out in this active area. Many review articles have appeared on the PA technique and its applications¹⁵⁻¹⁷. Other sensitive methods for measuring thermal effects of electromagnetic radiations includes calorimetry¹⁸⁻²⁰, bulk physical measurements like extensometry²¹ etc.

The main experimental work carried out for the present thesis is the recording of the fifth CH overtone spectra of some organic compounds using a dual beam thermal lens setup. The formation, properties and the applications of the thermal lens technique with emphasis on the measurement of weak absorptions are briefly outlined in the following sections.

2.20 Orders of Magnitude of Photothermal Effects

The Lambert-Beer's law relates the power transmitted P_t (watts) after transverse through a thickness l (cm) of sample with absorptivity α (cm^{-1}) to the power incident P_i (watts) on the sample through

$$P_t = P_i e^{-\alpha l} \quad (2.1)$$

For a weakly absorbing sample ($\alpha \sim 10^{-3} \text{cm}^{-1}$) $e^{-\alpha l} \simeq (1 - \alpha l)$, so that the absorbed power

$$P_a \text{ (watts)} = (P_i - P_t) = \alpha P l \quad (2.2)$$

Considering an isolated cylindrical column of sample with radius $w = 0.1$ cm and length $l = 1$ cm illuminated by a laser of power $P = 10$ mW. The rate of energy delivery to the sample column is

$$\dot{Q}_{in} = \frac{\alpha P l}{J} = 2.39 \times 10^{-6} \text{ cal sec}^{-1} \quad (2.3)$$

Assuming complete dissipation of the incident energy as heat, the resulting rate of temperature rise in the sample is,

$$\dot{T} = \frac{\alpha P l}{J \pi w^2 l \rho C_p} = 2.1 \times 10^{-4} \text{K sec}^{-1} \quad (2.4)$$

where, $\pi w^2 l$ is the volume of the heated sample, ρ is its density, C_p is the specific heat at constant pressure and benzene is taken as an example ($\rho = 0.88 \text{ gm cm}^{-3}$, $C_p = 0.41 \text{ cal gm}^{-1} \text{K}^{-1}$). If the heated column is surrounded by the sample at ambient temperature, the rate of outward radial heat conduction is

$$\dot{Q}_{\text{out}} = k(2\pi w l) \frac{\Delta T}{b} \text{ cal. sec}^{-1} \quad (2.5)$$

where k is the thermal conductivity of the medium, ΔT is the difference in temperature between the illuminated and non-illuminated sample portions and b is the material thickness across which the temperature difference exists. In the steady state ($\dot{Q}_{\text{in}} = \dot{Q}_{\text{out}}$) the temperature gradient is

$$\frac{\Delta T}{b} = \frac{Q_{\text{in}}}{k(2\pi w l)} = 1.1 \times 10^{-2} \text{K cm}^{-1} \quad (2.6)$$

with $k = 3.41 \times 10^{-4} \text{ cal. sec}^{-1} \text{K}^{-1}$ for benzene.

If a Gaussian beam is used to illuminate the sample the major portion of the gradient is developed across the beam radius w .

Then the temperature difference between the illuminated and non-illuminated sample is

$$\Delta T = \left[\frac{\alpha P l}{J} / k 2 \pi w l \right] w = 1.1 \times 10^{-3} \text{K} \quad (2.7)$$

At the rate of temperature rise equation (2.4), the time required for reaching the steady state is,

$$\Delta t = \left[\frac{\alpha P l w}{J k 2 \pi w l} \right] / \left[\frac{\alpha P l}{J \pi w^2 l \rho C_p} \right] = \frac{1}{2} \frac{w^2 \rho C_p}{k} = 5.35 \text{ sec} \quad (2.8)$$

The calculations made above are not rigorous but they give the orders of magnitudes of the effects considered. The expression for Δt represents the fundamental response time of the photothermal effect. Since the response time is proportional to the area (w^2) of the illuminated portion, the response becomes fast for a focused beam. Rigorous analysis using heat conduction equation considers a parameter $t_c = \frac{w^2 \rho C_p}{4k}$ analogous to Δt above. The quantity $D = \frac{k}{\rho C_p}$ is known as the thermal diffusivity of the medium and it contains all the molecular parameters involved in heat conduction. Thus the response time is

$$t_c = \frac{w^2}{4D} \quad (2.9)$$

2.30 Thermal Effects on Refractive Index

As mentioned earlier, many photothermal effects are probed by its effects on the refractive index of the sample. By appropriate arrangement of sample illumination, one can create an index of refraction distribution in the medium which can then be probed optically. In principle, from the measurement of the index of refraction distribution and the thermal coefficient of the index of refraction, the temperature distribution can be calculated. Using the known thermal properties of the medium and the amount of heat deposited in the sample, the sample absorptivity can be estimated. On the other hand by studying the time development of the refractive index distribution the bulk thermal properties of the sample can be estimated.

In the regions of optical spectrum far away from the strong sample absorption features and at sample temperatures far away from phase transitions and critical points the refractive index is a well defined continuous function of temperature,

$$\frac{dn}{dT} = \left(\frac{\partial n}{\partial T}\right)_\rho + \left(\frac{\partial n}{\partial \rho}\right)\left(\frac{\partial \rho}{\partial T}\right) \quad (2.10)$$

In such a case the temperature variation of the refractive index is primarily determined by density changes (the second term) and the variation at constant density can be safely ignored. Since most media expand up on heating the value of $\frac{dn}{dT}$

is negative in most cases. For benzene $\frac{dn}{dT} = -3.9 \times 10^{-4} \text{K}^{-1}$. For the change of temperature of $1.1 \times 10^{-3} \text{K}$ deduced in the previous calculations, the change in refractive index is $\Delta n = \frac{dn}{dT} \Delta T = -4.3 \times 10^{-7}$. We see that the order of magnitude of change in refractive index is extremely small. A comparison, of this quantity with the dependences on refractive index on other variables, which one usually come across and make use of, is desirable. The spectral dependence of refractive index $\frac{dn}{d\lambda}$ of a conventional prism is $\sim 3 \times 10^{-5} \text{nm}^{-1}$ at 600 nm. A lens of focal length 1 metre has a refractive index curvature at its centre $\sim 7.5 \times 10^{-4} \text{cm}^{-1}$. Thus a laser beam of radius 0.1 cm incident on such a lens will experience an index change of $\sim 7.5 \times 10^{-5}$ across the beam radius. Finally, for a half wave optical path change to be introduced for $\lambda = 600 \text{ nm}$ on passing through a 1 cm sample, the change in refractive index should be $\sim 3 \times 10^{-5}$. This comparison shows that the measurement of small change in refractive index brought about by a change in temperature is not beyond possibility. This is clearly evidenced by the discovery and characterization of several photothermal optical elements mentioned in the earlier sections.

2.40 The Photothermal Lens

Thermal lens was first observed and described by Gordon and co-workers in 1964^{22,23}. The effect was observed accidentally when these workers attempted to enhance the

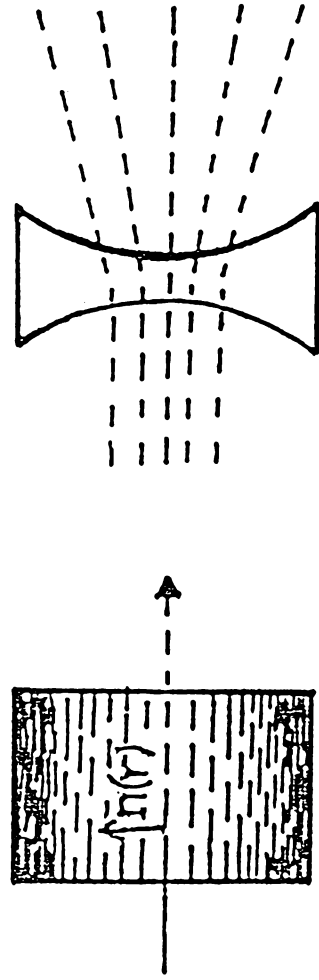
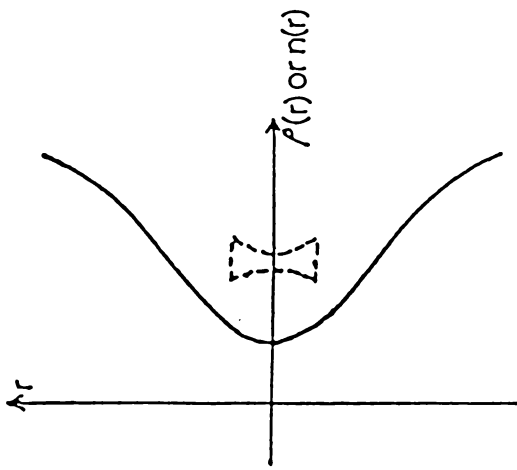


Fig.2.1 Schematic of thermal lens formation.

Refractive index profile resulting from temperature variation of density along the radial coordinate and the Equivalence between thermal lens and concave lens $n(r) \approx n(0) + \frac{r^2}{2} \left(\frac{\partial^2 n}{\partial r^2} \right)_{r=0}$.

Raman scattering from benzene by placing a 1 cm Brewster cell inside the cavity of a He-Ne laser to make use of the high intracavity circulating power (0.8W). With the sample cell in the cavity, the laser output exhibited power build up and decay transients with time constant of a few seconds. In the steady state, the beam spot size at the mirror is changed as if a diverging lens of focal length 1 metre is formed in the sample. The workers concluded that a thin thermal lens is formed in the sample by the heating action of the Gaussian beam. They have given a detailed analysis of the time development of the focal length of the thermal lens and have shown how the very weak absorption coefficient of the sample can be determined by measuring the focal length of the thermal lens²³. The schematic of the formation of the thermal lens is given in Fig.2.1. Near the centre of the Gaussian beam the power profile of the laser and hence the temperature profile due to the absorption are nearly parabolic (quadratic). Since the value of $\frac{dn}{dT}$ is negative for most media the refractive index profile closely approximates that of a high quality diverging lens.

2.41 Focal Length of the Thermal Lens

Born and Wolf²⁴ have given the method of evaluating the focal length of a cylindrically symmetric index distribution where the refractive index can be expanded in a Taylor

series about $r = 0$

$$n(r) = n(0) + r \left(\frac{\partial n}{\partial r} \right)_{r=0} + \frac{r^2}{2!} \left(\frac{\partial^2 n}{\partial r^2} \right)_{r=0} + \dots \quad (2.11)$$

For the cylindrical distribution, since n is extremum at $r = 0$, the first derivative $\left(\frac{\partial n}{\partial r} \right)_{r=0}$ vanishes. The path of a paraxial ray will be a circular path with curvature

$$\frac{1}{R} = \frac{1}{n} \frac{\partial n}{\partial r} = \frac{r}{n} \left(\frac{\partial^2 n}{\partial r^2} \right)_{r=0} \quad (2.12)$$

where the terms beyond quadratic in the Taylor series are neglected. From simple geometrical optics considerations, the focal length of the index distribution is shown to be^{22,23}

$$F = - \left[1 \left(\frac{\partial^2 n}{\partial r^2} \right)_{r=0} \right]^{-1} \quad (2.13)$$

In the case of temperature variation of refractive index originating from radial temperature distribution, the chain rule equation (2.10) yields

$$F = - \left[1 \frac{dn}{dT} \left(\frac{\partial^2 T}{\partial r^2} \right)_{r=0} \right]^{-1} \quad (2.14)$$

where the condition $\left(\frac{\partial T}{\partial r} \right)_{r=0} = 0$ has been made use of. Since both $\frac{dn}{dT}$ and $\left(\frac{\partial^2 T}{\partial r^2} \right)_{r=0}$ are negative ($T = T_{\max}$ at $r = 0$), the

focal length is negative, i.e., for all media which expand upon heating the thermal lens will be a diverging lens. In the previous example of benzene, the temperature gradient across the beam radius was calculated to be $\frac{\Delta T}{w} \approx 1.1 \times 10^{-2} \text{ K cm}^{-1}$. Approximating $(\frac{\partial^2 T}{\partial r^2})_{r=0} \sim \frac{\Delta T}{w^2}$, the equation for focal length yields $F = -2.3 \times 10^4 \text{ cm}$.

In deriving the focal length of the thermal lens, the refractive index distribution is assumed to be constant along the beam path in the sample. This requires that the beam spot size remains constant in the sample cell. This is one of the restrictions imposed on the thin lens approximation. The mathematical condition imposed for the restriction is that the sample path length is small compared to the confocal length (Rayleigh length) of the laser beam. The confocal length characterizes the distance at which the beam power density reduces to half the value at the beam waist. The confocal length of a laser beam with wavelength λ and radius at beam waist w_0 is given by

$$b = \frac{\pi w_0^2}{\lambda} \quad (2.15)$$

(At one confocal length away from the beam waist, the laser spot size becomes $\sqrt{2}w_0$). The restriction for sample path length was hold good in Gordon's experiments^{22,23}.

When the absorbed power in the sample becomes large, full wave phase shifts can occur in the wavefront of the transmitted beam. This will cause interference fringes (spherical aberration)¹. This puts restriction on the absorbed power, which is imposed by the mathematical condition that the total change in optical path length must be less than a quarter wave. i.e.,

$$l \frac{\Delta n}{\lambda} < \frac{1}{4} \quad (2.16)$$

This leads to

$$l \frac{\Delta n}{\lambda} = l \frac{dn}{dT} \frac{\Delta T}{\lambda} = \frac{\alpha P l}{2 \pi J k \lambda} < \frac{1}{4}$$

i.e., the absorbed power

$$\alpha P l < \frac{\pi J k \lambda}{2 \frac{dn}{dT}} \quad (2.17)$$

As a typical example, for benzene this condition leads to $\alpha P l < 0.5$ mW.

2.4.2 Time Development of Focal Length--Gordon's Equation

The basic derivation of the time development of the focal length of a thermal lens under the irradiation of a Gaussian beam was taken up by Gordon et al²³ and later by Whinnery²⁵ and

Swofford and Morrell²⁶. The time dependence of the focal length appears through the time dependence of $\left(\frac{\partial^2 T}{\partial r^2}\right)_{r=0}$ in equation (2.14). As the Gaussian beam is switched on in the medium, the temperature distribution in the medium and hence $\left(\frac{\partial^2 T}{\partial r^2}\right)_{r=0}$ evolves in time. Gordon's derivation in the medium and consists in finding the time dependence of $\left(\frac{\partial^2 T}{\partial r^2}\right)_{r=0}$ by solving the heat condition equation given by Carslaw and Jaeger²⁷. The expression derived by Gordon et al reads,

$$\left(\frac{\partial^2 T}{\partial r^2}\right)_{r=0}(t) = \frac{-\alpha P}{\pi J k w_1^2 (1+t_c/2t)} \quad (2.18)$$

where w_1 is the radius of the beam spot in the sample and $t_c = \frac{w_1^2}{4D}$ is the response time of the medium to the heat input. t_c is also known as the critical time. Other quantities have their usual meanings.

In the steady state ($t = \infty$) the curvature at the centre of the temperature profile is,

$$\left(\frac{\partial^2 T}{\partial r^2}\right)_{r=0}(t=\infty) = \frac{-\alpha P}{\pi J k w_1^2} \quad (2.19)$$

For the previous example of benzene, $\left(\frac{\partial^2 T}{\partial r^2}\right)_{r=0}(t=\infty) = -0.23 \text{ K cm}^{-2}$ which compares with the crude estimate of -0.11 K cm^{-2} given earlier.

Now the expression for the focal length follows directly from equations (2.14) and (2.18).

$$F(t) = \frac{\pi J k w_1^2}{\alpha P l \frac{dn}{dT}} (1 + t_c/2t) \quad (2.20)$$

With a 10 mW laser, the steady state focal length in benzene in the previous case is $F = -1.14 \times 10^2$ cm which compares with the crude estimation of -2.3×10^4 cm given earlier. In Gordon's experiment the intracavity thermal lens had a focal length of -1.42×10^2 cm.

The above expression for the time dependent focal length is derived based on several important assumptions. First, the medium is assumed to be radially infinite. Secondly, the restriction on sample path length is valid here also since model assumes constant beam size in the sample. A third important restriction is that the series expansion upto second order term in the Taylor expansion can be valid only very near the beam centre; at the wings of the Gaussian beam the gradient will be weaker than predicted by parabolic approximation. While the first two restrictions can be taken into consideration in the Gordon type experiment, the third one was realized in practice by Hu and Whinnery later (see below).

2.50 The Extracavity Method of Hu and Whinnery

After the work of Gordon et al, a number of workers used thermal lens technique for measuring weak absorptions using different probing methods like measurement of equilibrium spot size²⁸⁻³⁰, looking time development of the spot size using movie camera³¹, interferometric measurement of phase delay of on-axis and off-axis beams⁵, measurement of shift in the beat frequency between TEM₀₀ and TEM₀₁ modes³²⁻³⁶ etc. The most important advance in the thermal lens technique after Gordon's work is that of Hu and Whinnery^{37,25}. These workers demonstrated theoretically and experimentally that the maximum fractional change in the far-field intensity (that is the maximum fractional change in the radius of curvature of the beam), due to thermal lens formation, can be obtained by placing the sample at one confocal length past the beam-waist. Fig.2.2 shows the experimental setup used by Hu and Whinnery. They used an extracavity lens ($f = 20-60$ cm) to produce a beam waist (w_0) and the sample was placed at one confocal length ($b = \frac{\pi w_0^2}{\lambda}$) away from the beam waist. A shutter placed at the beam waist allows rapid unblocking of the initially blocked laser beam. The intensity changes at the beam centre in the far field is monitored using a pinhole-photo diode assembly and a storage oscilloscope. The fractional change in the far-field intensity is independent of the beam width in the sample since an increase in the strength of the thermal lens

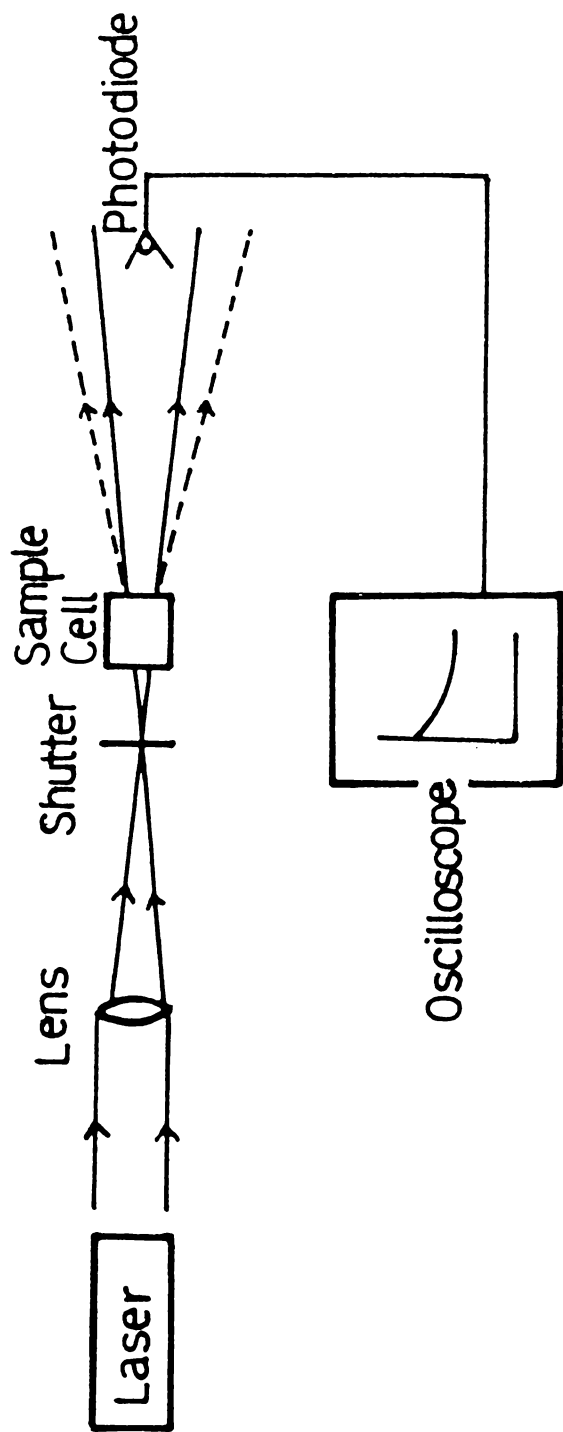


Fig.2.2 Experimental set-up of single beam extracavity technique of Hu and Whinnery. The pinhole is placed in front of the photodetector if the detector area is considerable. However, for ordinary photodiodes the pinhole need not be used.

by reducing the spot-size in the cell also increases the initial far-field spot size.

The thermal lens signal detected through the pinhole of radius a is

$$P_{\text{det}} = \int_0^a \frac{2P}{\pi w_2^2} \exp\left(-\frac{2r^2}{w_2^2}\right) 2\pi r dr \approx 2P \frac{\pi a^2}{\pi w_2^2} \quad \text{for } a \ll w_2 \quad (2.21)$$

where P is the laser beam power and w_2 is the beam radius at the detector plane.

Hu and Whinnery presented a detailed mathematical analysis, starting from Gordon's expression for the time dependent focal length (equation 2.20) and proved that the relative increase in the far-field beam size is maximized when the sample is placed at one confocal length away from the beam waist. Under this condition, the fractional change in the beam size is shown to be

$$\left[\frac{w_2(t) - w_2(0)}{w_2(0)} \right] = \left[\frac{-\alpha P l \frac{dn}{dT}}{2\lambda J k (1+t_c/2t)} \right] \quad (2.22)$$

The far field beam intensity is inversely proportional to the beam area there. Thus

$$\frac{P_{\text{det}}(t=0)}{P_{\text{det}}(t)} = \frac{w_2^2(t)}{w_2^2(t=0)} = \left[1 - \frac{\alpha P l \frac{dn}{dT}}{2\lambda J k (1+t_c/2t)} \right]^2 \quad (2.23)$$

$$\approx \left[1 - \frac{\alpha P l \frac{dn}{dT}}{\lambda J k (1+t_c/2t)} \right] \quad (2.24)$$

where the terms containing α^2 has been neglected. In the steady state ($t = \infty$)

$$\frac{P_{\text{det}}(t=0)}{P_{\text{det}}(t=\infty)} = \left[1 - \frac{\alpha P_1 \frac{dn}{dT}}{J \lambda k} \right] \quad (2.25)$$

which yields

$$\alpha = - \left[\frac{P_{\text{det}}(t=0) - P_{\text{det}}(t=\infty)}{P_{\text{det}}(t=\infty)} \frac{\lambda J k}{P_1 \frac{dn}{dT}} \right] \quad (2.26)$$

Thus the measurement of the steady state relative change in the detected power of the transmitted laser beam (which is independent of the initial spot size in the sample) directly yields the sample absorptivity value. As a typical example, for benzene, the steady state fractional change in intensity when using a path length of 1 cm and a power of 10 mW (He-Ne 6328Å) is ~ 0.045 i.e., 4.5 per cent.

The formula derived by Hu and Whinnery is widely used for the measurement of weak absorptivities. It is very important therefore that one should be aware of the basic assumptions under which the formula is derived, so that the required experimental conditions can be realized. First of all, the restriction on the sample path length applies here also since the analysis is based on Gordon's equation for focal length. An additional

limitation existing in the Hu and Whinnery configuration is that the cell path length is to be small compared with the confocal length of the focused beam which is usually less than that of the unfocused beam.

Also for the maximum sensitivity condition (sample placed at one confocal length past the beam waist) to be meaningful, the cell path length must be much small compared to the confocal length of the focused beam. (In the setup used by Hu and Whinnery a beam waist of $w_0 = 0.01$ cm was produced by a lens of focal length 60 cm to get a confocal length $b = 5.2$ cm, and a 1 cm cell was used for the sample). Secondly, the neglect of the term containing α^2 is going from equation (2.23) to (2.24) makes the formula valid only for small α values and hence small relative intensity changes. A relative intensity change of 10% would lead to an error of 0.25% in the measured value of α and a relative intensity change of 25% would lead to an error of 1.5% in the measured value of α . Another important point to be considered in the Hu and Whinnery technique is that the measurement of steady state far-field intensity $P_{\text{det}}(t=\infty)$ requires the knowledge of how fast the thermal lens develops in time. In terms of the critical time ($t_c = \frac{w_1^2}{4D}$), 80% of the signal develops in time $2t_c$, while a time of $9t_c$ is required to observe 95% of the total signal (equation 2.24). The delay between the initial and the steady state

intensities can be reduced by reducing t_c (i.e., by tight focusing the beam) which again restricts the sample path length. (In a typical experimental condition of Hu and Whinnery, a lens of focal length 60 cm was used to produce a beam waist of $w_0 = 0.01$ cm and the critical time $t_c = 530$ milliseconds). Thus a careful choice of focal spot size and sample path length is to be made in any Hu-Whinnery type experiment.

The method of Hu and Whinnery has been used by several workers for measuring weak absorptivities in different contexts. The most noticeable among them is the work of Dovichi and Harris³⁸⁻⁴¹ who used this technique for trace analysis. The pump source used are discrete wavelength CW lasers like Ar^+ , He-Ne and He-Cd. These workers have made detailed parametric studies of the thermal lens setup and have discussed in detail how the sensitivity can be maximized by suitable choice of experimental conditions. In the initial studies³⁸ they have used 'sample and hold' amplifiers for measuring the initial and the steady state intensities ($P_{det}(t=0)$ and $P_{det}(t=\infty)$) along with the source intensity for correcting long term drifts. In later work^{40,41}, they measured the time dependent build up of the thermal lens signal instead of the steady state measurements. This method has got the advantage that even relatively large absorptivities can be measured where the equilibrium lens may be distorted by spherical aberration. A lower detection limit of $\alpha = 1.6 \times 10^{-7} \text{ cm}^{-1}$ in CCl_4 for a path length of 1 cm and

a laser power of 160 mW (488 nm of Ar⁺) has been reported in the experiment of Dovichi and Harris. These authors have also reported another interesting work, namely, the differential thermal lens calorimeter³⁹. The principle of this technique is based on the antisymmetric behaviour of thermal lens with respect to the extracavity beam waist in the Hu-Whinnery configuration³⁷. While the sample cell placed at one confocal distance after the beam waist produces maximum divergence in the laser beam, the sample cell placed at one confocal length before the beam waist produces maximum convergence to the beam. Thus if the two identical cells containing the same sample are placed at these two positions the net divergence vanishes and there will be zero detected thermal lens signal. Thus a differential thermal lens effect due to the solute alone can be observed if a solvent cell is placed at one confocal length before the beam waist and a sample cell (same path length) is placed at one confocal length past the beam waist. The cancellation of about 100% 'common mode' solvent thermal lens effect made it possible to detect absorptivities as small as $1.45 \times 10^{-6} \text{ cm}^{-1}$ in CCl₄ using a 20 mW Ar⁺ (488 nm) line³⁹. This level of sensitivity is achieved in the presence of 'common modes' of several orders of magnitude larger than the signal of interest. Dovichi and Harris³⁹ have also discussed the details of standardization and calibration of the thermal lens technique for use in quantitative analysis like trace analysis.

2.60 The Dual Beam Thermal Lens Technique

The thermal lens experiments described so far uses a single laser source to excite and probe the thermal lens effects. In many experiments, especially in absorption spectroscopy, where the pump laser is to be tuned over a wavelength range, the point by point measurement scheme of the single beam technique becomes very time consuming and cumbersome. In such cases the use of separate lasers to pump and probe the thermal lens will be more advantageous. The pump beam chopped (or repeatedly pulsed) at a suitable frequency creates a pulsating thermal lens in the sample. The weak CW probe beam on passage through the medium gets modulated by this pulsating thermal lens. This small intensity modulation can be monitored using sensitive measurement equipments like boxcar averager, transient recorder, or more frequently using a lock-in amplifier, in conjunction with a photomultiplier tube. Since only a single wavelength is always detected, the detection optics and detectors need to be optimized only for a single probe wavelength, and one need not take into account the spectral response of the optical elements and the detector.

The dual beam thermal lens technique was first used by Grabiner et al⁴² and Flynn⁴³ to monitor the energy transfer in gas phase molecules pumped by a pulsed CO₂ laser. They used a He-Ne laser as the probe source. The first report of

the application of the dual beam technique to spectroscopic measurements is that of Long et al⁴⁴. They used a repetitively chopped CW dye laser as the pump source and a He-Ne laser as the probe source. The optical arrangement used by Long et al is shown in Fig.2.3. The CW dye laser (heating beam) chopped at 13 Hz combines collinearly on an uncoated beam splitter with the He-Ne laser (probe beam). The two beams are focused by a lens of focal length 60 cm to a sample cell of path length 1 cm. Both beams are then incident on a filter which blocks the pump beam and transmits the probe beam. The probe beam then falls on the PMT photocathode through a pinhole. The detected probe beam power which is modulated at the chopping frequency by the pulsating thermal lens is monitored by a frequency tracking lock-in amplifier synchronized to the chopping frequency. The magnitude of the lock-in output (which is the r.m.s. value of the fundamental sine wave at the chopping frequency) is recorded on a strip-chart recorder, along with the relative power of the dye laser, as the dye laser is wavelength scanned. Point by point division of the lock-in signal by the corresponding relative power of the dye laser gives the absorption spectrum of the sample in arbitrary units. Long et al demonstrated the validity of the dual beam method by comparing the overtone spectra of benzene and toluene obtained by this method with those obtained by the single beam method^{44,45}.

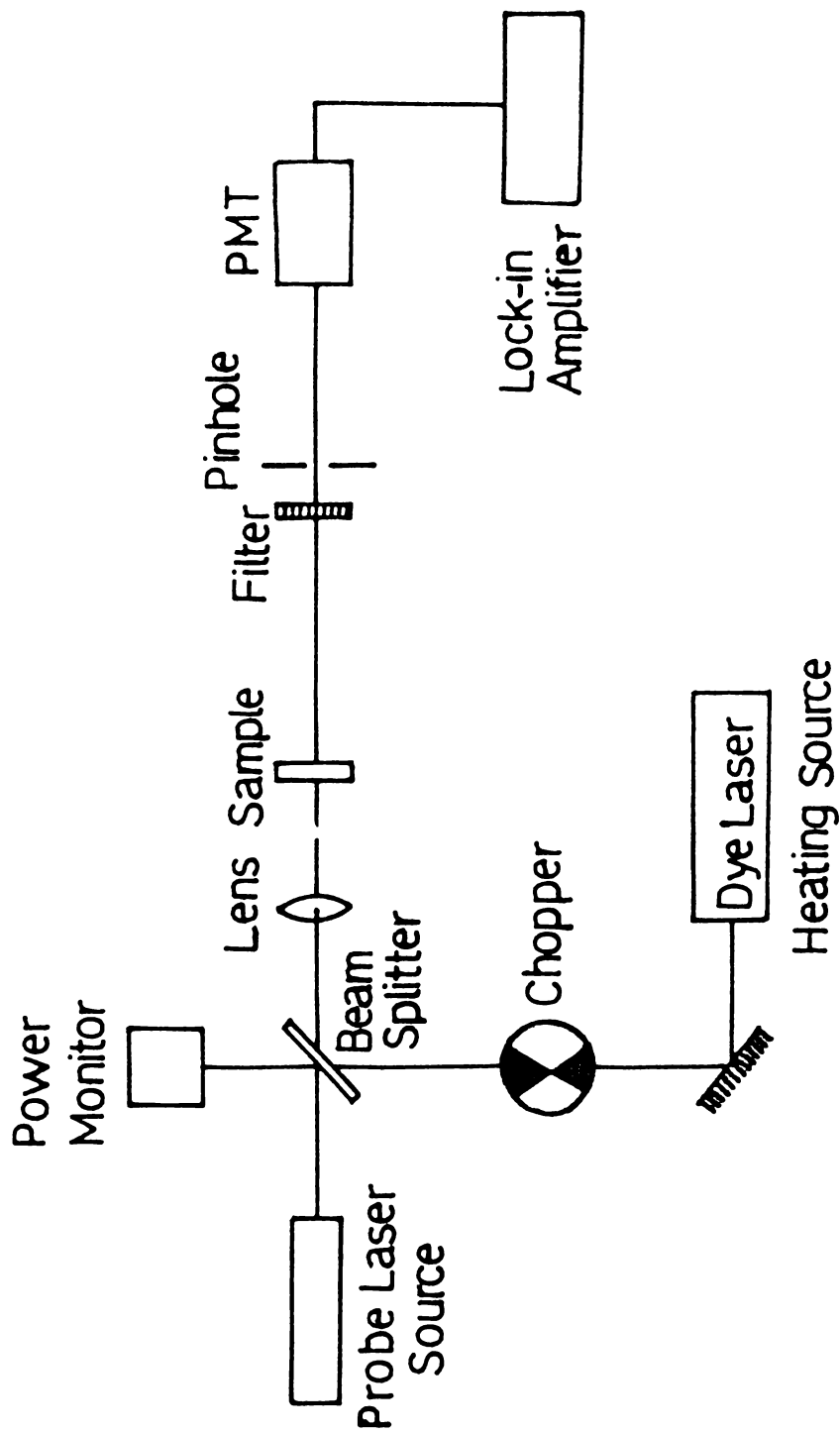


Fig.2.3 The dual beam experimental configuration of Long et al. The lock-in output is normalized by the relative power of the pump laser to get the absorption spectrum of the medium as the wavelength is scanned.

Swofford and Morrell⁴⁶ have presented the mathematical analysis of the CW dual beam thermal lens technique by extending the model of Gorden et al²³ to account for the cumulative effect of the chopped heating beam. When the sample is excited by a continuously chopped laser beam, the temperature rise during a particular chopper cycle depends not only on the heat input from that chopper cycle but also on the previous chopper cycles. The workers derived the following expression for the a.c. component of the probe power detected.

$$\frac{\Delta P_{\text{det}}(0, \tau; m)}{P_{\text{det}}(0; 0)} = \left[\frac{P_{\text{det}}(0; m) - P_{\text{det}}(\tau; m)}{P_{\text{det}}(0; 0)} \right]$$

$$= 2Z' \frac{dn}{dT} \frac{\alpha P_1}{\pi J k w_1^2} \left[\frac{1}{1 + t_c/2\tau} + \sum_{n=1}^{m-1} \frac{2(1 + 2n(\tau + \tau')/t_c)}{[1 + 2n(\tau + \tau')/t_c]^2 - (2\tau/t_c)^2} \right]$$

(2.27)

where m refers to a particular chopper cycle, τ is the chopper 'on' time, τ' is the chopper 'off' time, w_1 is the probe spot size in the sample and Z' is the distance of the sample from the probe beam waist. The authors have shown that computer generated plots of the signal defined by eqn.(2.27) with respect to time, follow quite satisfactorily the thermal lens signals observed with an oscilloscope. The agreement has been established for different power levels also.

The lock-in amplifier gives the rms value of the fundamental (sine wave at the chopping frequency) component of the above signal (2.27). However about 85% of the total calculated signal appears as the fundamental and the variation of this fraction with change of the exciting wavelength (as the pump laser is tuned) is negligible⁴⁶.

The most important point in the performance of the dual beam thermal lens spectrometer is that the linearity of the lock-in signal with respect to the incident laser power for constant $\alpha(\lambda)$ is ensured. Swofford and Morrell have addressed this point and concluded that the magnitude of the a.c. signal (eqn.(2.27)) should be less than 0.1 to ensure linearity in absorbed power.

Fang and Swofford⁴⁷ revised the model of the dual beam thermal lens technique to suit for an optically thick sample so that the restriction on the sample path length can be overcome. In their analysis, the sample is considered to be divided into several slices and the propagation through each slice is calculated using ABCD law; the output of one slice is fed as the input of the next. An iterative calculation can thus account for the propagation. These authors have also modelled the thermal lens formation resulting from elliptic Gaussian beams⁴⁷.

Fang and Swofford¹ have discussed in detail the various experimental requirements that are to be carefully

considered in carrying out thermal lens experiments in general and the dual beam experiment in particular. These are described in detail in the next chapter, in connection with the description of our experimental setup.

2.70 Thermal Lens Produced by Pulsed Lasers

We have so far considered the thermal lens effects created by CW lasers. Several researchers have reported (including the first dual beam experiment of Grabiner et al and Flynn mentioned earlier) the creation of thermal lens by a pulsed pump laser which is probed by a CW laser. The detailed theoretical analysis of pulsed dual beam thermal lens technique has been carried out by Twarowski and Kliger⁴⁸⁻⁵⁰ and later by Bailay et al^{51,52}. The availability of pulsed lasers has made it possible the study of many nonlinear effects. Two photon absorption spectroscopy is one such area. Detection of two photon absorption by thermal lens technique is ideal when the fluorescence quantum yield from the upper level is very small, in which case the efficient nonradiative decay causes significant thermal lens effect. Twarowski and Kliger studied⁴⁹ the $A_{1g} \rightarrow B_{2u}$ two photon transition in benzene using this technique. They have extended these studies to other molecular species also⁵⁰. Fang et al^{53,1} have demonstrated the use of picosecond high repetition rate (MHz) (mode locked cavity dumped) dye laser for exciting two photon absorption in organic compounds like

naphthalene, anthracene etc., the resulting thermal lens signal being synchronously detected by mechanically chopping the picosecond laser as in a CW thermal lens technique.

2.80 Applications of the Thermal Lens Effect

2.81 Absorption Spectroscopy

As described in detail in the earlier sections, the most important application of the thermal lens technique is the measurement of weak absorptions in liquid-phase substances. Weak absorption arises due to spectroscopic transitions of very low probability. Examples include vibrational overtone absorption in the ground electronic state of polyatomic molecules and multiphoton electronic absorption. Liquid-phase overtone spectra of a large number of molecules detected by laser induced thermal lens technique have been reported^{44,45,54}. The work presented in this thesis is mainly based on the CW dual beam thermal lens experiments for detecting the fifth CH overtone spectra of several organic compounds. The application of pulsed and picosecond laser induced thermal lens technique in detecting two photon absorption in organic compounds has already been discussed in previous sections.

2.82 Analytical Applications

Since the thermal lens technique can achieve very high sensitivities ($\alpha \sim 10^{-6} \text{ cm}^{-1}$), it can be used to detect strong absorbers ($\epsilon \geq 10^5 \text{ M}^{-1} \text{ cm}^{-1}$) present in concentrations

as low as 10^{-11} M suggesting its application in trace analysis. The work of Dovichi and Harris referred to in earlier sections demonstrated the use of He-Ne and Ar⁺ lasers in determining trace levels of many substances. Thermal lens technique is now-a-days widely used as a detection technique in liquid chromatography and this is the most important analytical application of this technique. The most sensitive chromatographic detection technique known to date is that based on thermal lens technique. A recent review⁵⁵ covers the various aspects of the technique and the different works appeared in this area.

2.83 Energy Transfer Studies in Gas Media

The thermal lens technique has been used to determine vibration-translation (V→T) energy transfer in gas media, which forms a very important study relating to infrared laser photochemistry. Bailey et al⁵⁶ have studied the effect of addition of non-absorbing inert gas to a cell in which a low pressure gas absorbs laser pulses to form a thermal lens. They have established that the axial temperature rise in the cell due to the laser pulse passes through a maximum due to the variation of thermal diffusivity with pressure, and thus pointed the usual incorrect interpretation in energy transfer studies. Bailey et al⁵⁷⁻⁵⁹ have also made accurate reassessment of rate constant for V → T energy transfer in many gaseous systems

using thermal lens technique. Flynn⁶⁰ has carried out experiments on $V \rightarrow V$ energy transfer between CH_3F molecules. Bailey et al⁶¹ have used a thermal lens technique to study $V \rightarrow V$ energy transfer in CO_2 . The $V \rightarrow V$ rate constant could be calculated from the analysis of the time development of thermal lens.

2.84 Bulk Thermal Properties

The time development of a thermal lens signal, both in the single beam and the dual beam methods, depends on the critical time t_c which depends on the beam diameter and the thermal diffusivity of the medium. The time development of the thermal lens signals has been used for determining the thermal diffusivities of many substances⁶². Gupta et al⁶³ have used a pulsed dual beam thermal lens technique using a flash lamp-pumped dye laser and a probe He-Ne laser. The pulsed thermal lens technique is fast and the sample heating problem can be fully eliminated.

2.85 Measurements of Absolute Quantum Yields

By observing the far field intensity changes of a laser beam caused by a thermal lens and knowing the thermal and thermo-optic properties of the medium one can compute the quantity of absorbed power converted into heat. Also measuring the total optical absorption spectrophotometrically, one can

calculate the absolute quantum yields of radiative and non-radiative transitions. Many such measurements have been reported^{37,64}.

2.86 Chemical Reactions

Thermal lensing technique has been used to monitor certain slow chemical reactions⁶⁵⁻⁶⁷. The generation of dopachrome by enzyme-catalyzed air oxidation of dopamine has been monitored by observing the thermal lens signal changes⁶⁵. The product concentrations at any time could be determined from the slope of the thermal lens signal. Daree⁶⁶ has studied the toluene-bromine exothermic reaction using a single beam thermal lens technique. He determined the velocity of the reaction, the rate constant of termination and the quantum yield by the time resolved thermal lens technique. A recent paper⁶⁷ describes the application of thermal lens technique to infrared multiple photon photochemistry of cyclobutanone in the estimation of transient temperatures.

REFERENCES

1. H.L.Fang and R.L.Swofford in "Ultrasensitive Laser Spectroscopy", D.S.Kliger (Ed.), (Academic Press Inc., New York, 1983), p.175, and refs. therein.
2. A.C.Boccara, D.Fournier and J.Badoz, Appl.Phys.Lett.36, 130 (1980).
3. J.C.Murphy and L.C.Aamodt, J.Appl.Phys.51, 4580 (1980).
4. W.B.Jackson, N.M.Amer, A.C.Boccara and D.Fournier, Appl.Opt.20, 1333 (1981).
5. J.Stone, J.Opt.Soc.Am.62, 327 (1972).
6. J.Stone, Appl.Opt.12, 1828 (1973).
7. H.Aung and M.Katayama, Jpn.J.Appl.Phys.14, 82 (1975).
8. H.Aung and M.Katayama, Chem.Phys.Lett.33, 502 (1975).
9. A.Miller, E.K.Hussmann and W.L.Mclaughlin, Rev.Sci.Instrum.46, 1635 (1975).
10. D.Baysens and P.Calmettes, J.Chem.Phys.66, 766 (1977).
11. R.N.Zitter, D.F.Koster, A.Cantoni and A.Ringwelski, High Temp.Sci.12, 209 (1980).
12. G.Abbate, U.Bernini, G.Brescia and E.Raggozino, Opt.Laser Technol.13, 97 (1981).

13. M.J.Pelletier, H.R.Thorsheim and J.M.Harris, Anal.Chem. 54, 239 (1982).
14. G.Da Costa, and J.Calatroni, Appl.Opt.17, 2381 (1978).
15. C.K.N.Patel and A.C.Tam, Rev.Mod.Phys.53, 517 (1981) and refs.therein.
16. M.J.Adams, Prog.Analyt.Atom.Spectrosc.5, 153 (1982).
17. A.C.Tam in "Ultrasensitive Laser Spectroscopy", D.S.Kliger (Ed.), (Academic Press, New York, 1983), and refs.therein.
18. A.Jujishima, H.Masuda, K.Honda and A.J.Bard, Anal.Chem. 52, 682 (1980).
19. P.J.Severin and H.van Esveld, Appl.Opt.20, 1833 (1981).
20. K.I.White, Opt.Quantum Electron.8, 73 (1976).
21. P.Halander, I.Lundstrom and D.Mc Queen, J.Appl.Phys.52, 1146 (1981).
22. J.P.Gordon, R.C.C.Leite, R.S.Moore, S.P.S.Porto and J.R.Whinnery, Bull.Am.Phys.Soc. (2)9, 501 (1964).
23. J.P.Gordon, R.C.C.Leite, R.S.Moore, S.P.S.Porto and J.R.Whinnery, J.Appl.Phys.36, 3 (1965).
24. M.Born and E.Wolf, "Principles of Optics", (Pergamon, Oxford, 1970), p.124.

25. J.R.Whinnery, *Acc.Chem.Res.*7, 225 (1974).
26. R.L.Swofford and J.A.Morrell, *J.Appl.Phys.*49, 3667 (1978).
27. H.S.Carslaw and J.C.Jaeger, "Operational Methods in Applied Mathematics", (Dover, New York, 1963).
28. R.C.C.Leite, R.S.Moore and J.R.Whinnery, *Appl.Phys.Lett.*5, 141 (1964).
29. D.Solimini, *J.Appl.Phys.*37, 3314 (1966).
30. D.Solimini, *Appl.Opt.*5, 1931 (1966).
31. R.L.Carman and P.L.Kelly, *Appl.Phys.Lett.*12, 241 (1968).
32. Y.Kohanzadeh and D.H.Auston, *J.Quantum Electron.*6, 475 (1970).
33. R.Banilis, A.Burgos, H.Mancini and E.Quel, *Jpn.J.Appl.Phys.*13, 486 (1973).
34. A.Burgos, H.Mancini, E.Quel and J.Westfried, *Opt.Commun.*20, 434 (1977).
35. C.C.Davis, *IEEE J.Quantum Electron.* QE-15, 26 (1979).
36. C.C.Davis and S.J.Petuchowski, *Appl.Opt.*20, 2539 (1981).
37. C.Hu and J.R.Whinnery, *Appl.Opt.*12, 72 (1973).
38. N.J.Dovich and J.M.Harris, *Anal.Chem.*51, 728 (1979).

39. N.J.Dovichi and J.M.Harris, *Anal.Chem.*52, 2338 (1980).
40. N.J.Dovichi and J.M.Harris, *Anal.Chem.*53, 106 (1981).
41. N.J.Dovichi and J.M.Harris, *Anal.Chem.*53, 689 (1981).
42. F.R.Grabiner, D.R.Siebert and G.W.Flynn, *Chem.Phys.Lett.*
17, 189 (1972).
43. G.W.Flynn in "Chemical and Biochemical Applications of
Lasers", C.B.Moore (Ed.), (Academic Press, New York,
1974), Vol.1, p.163.
44. M.E.Long, R.L.Swofford and A.C.Albrecht, *Science* 191, 183
(1976).
45. R.L.Swofford, M.E.Long and A.C.Albrecht, *J.Chem.Phys.*65,
179 (1976).
46. R.L.Swofford and J.A.Morrell, *J.Appl.Phys.*49, 3667 (1978).
47. H.L.Fang and R.L.Swofford, *J.Appl.Phys.*50, 6609 (1979).
48. A.J.Twarowski and D.S.Kliger, *Chem.Phys.*20, 253 (1977).
49. A.J.Twarowski and D.S.Kliger, *Chem.Phys.*20, 259 (1977).
50. A.J.Twarowski and D.S.Kliger, *Chem.Phys.Lett.*50, 36 (1977).
51. R.T.Bailey, F.R.Cruickshank, D.Pugh and W.Johnstone,
*Chem.Phys.Lett.*59, 324 (1978).

52. R.T.Bailey, F.R.Cruickshank, D.Pugh and W.Johnstone, J.Chem.Soc.Faraday.Trans.(2)76, 633 (1980).
53. H.L.Fang, T.L.Gustafson and R.L.Swofford, J.Chem.Phys.78, 1663 (1983).
54. Also see the references of Chapters 4 and 5.
55. M.D.Morris and K.Peck, Anal.Chem.58, 811A (1986).
56. R.T.Bailey, F.R.Cruickshank, D.Pugh, R.Guthrie, W.Johnstone, J.Mayer and K.Middleton, J.Chem.Phys.77, 3453 (1982).
57. A.T.Bailey, F.R. Cruickshank, D.Pugh and W.Johnstone in "Lasers in Chemistry", M.West (Ed.), (Elsevier, London, 1977), p.257.
58. R.T.Bailey, F.R.Cruickshank, D.Pugh, R.Guthrie and I.J.M.Wier, Mol.Phys.48, 81 (1983).
59. R.T.Bailey, F.R.Cruickshank, R.Guthrie, D.Pugh, and I.J.M.Wier in "Time Resolved Vibrational Spectroscopy", (Academic Press, London, 1983), p.121.
60. Ref.43, p.189.
61. R.T.Bailey, F.R. Cruickshank, D.Pugh and K.Middleton, J.Chem.Soc.Faraday Trans (2),81, 255 (1985).
62. Calmettes and Laj, J.Phys.(Paris) C 1, 125 (1972).

63. M.C.Gupta, S.D.Hong, A.Gupta and J.Moacanin, Appl.Phys. Lett.37, 505 (1980).
64. J.H.Brannon and D.Megde in "Advances in Laser Chemistry", A.H.Zewail (Ed.), (Springer Verlag, 1978), p.292.
65. J.P.Hanshalter and M.D.Morris, Appl.Spectrosc.34, 445 (1980).
66. K.Daree, Opt.Commun.4, 238 (1971).
67. J.R.Quckert and R.W.Carr, J.Phys.Chem.90, 4286 (1986).

Chapter 3

EXPERIMENTAL TECHNIQUES

3.10 Introduction

The present chapter contains the details of the dual beam thermal lens setup used for recording the fifth overtone spectra which includes the details of the experimental configuration, components of the apparatus and the various experimental considerations that are to be carefully executed. A brief description of the spectrophotometric measurements of the lower overtones is given towards the end of the chapter.

3.20 Thermal Lens Experimental Configuration

The main components of a basic dual beam thermal lens setup are:- (1) a pump laser beam which produces the thermal lens, (2) a mechanical chopper to modulate the pump beam, (3) a probe laser beam to monitor the thermal lens and (4) a detector assembly and associated electronics to measure the strength of the thermal lens. The dual beam thermal lens setup used for the present work is a modified version of the setup of Fang and collaborators. The block diagram and the photographs of the experimental arrangement are shown in Figs.3.1 and 3.2.

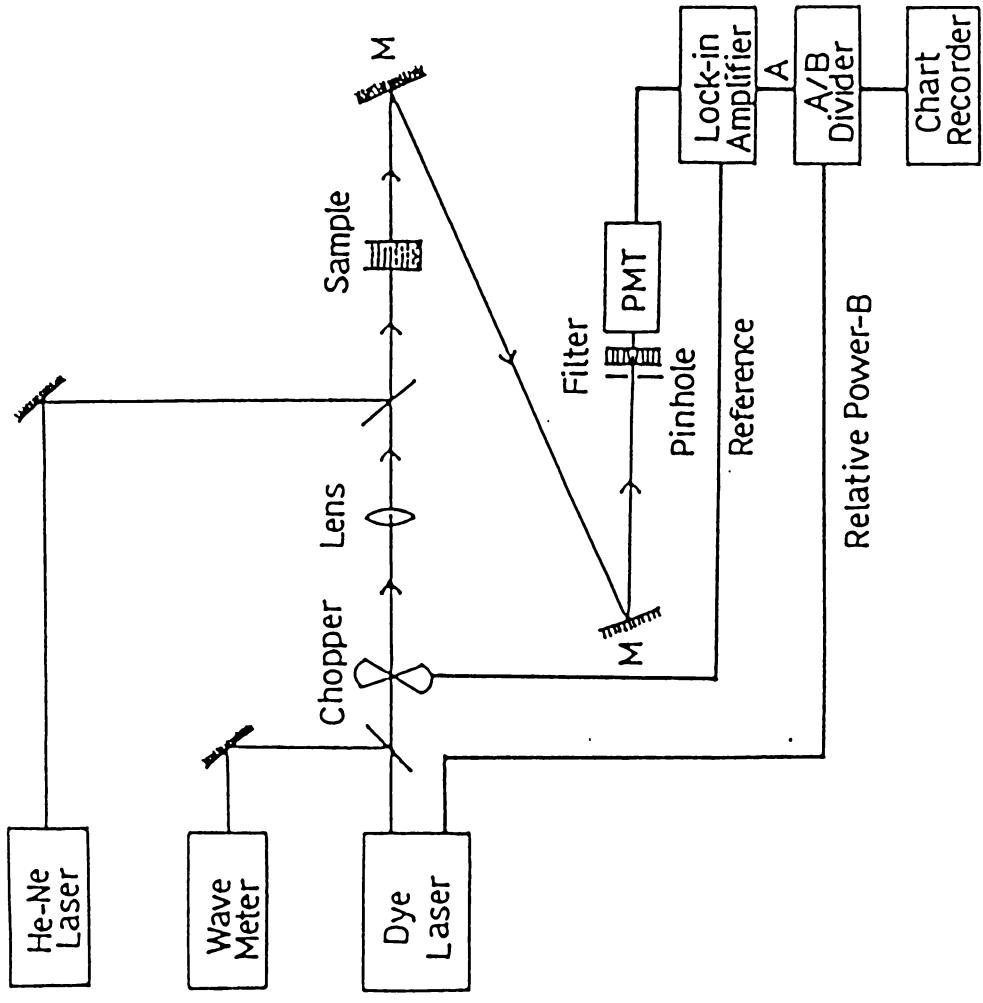
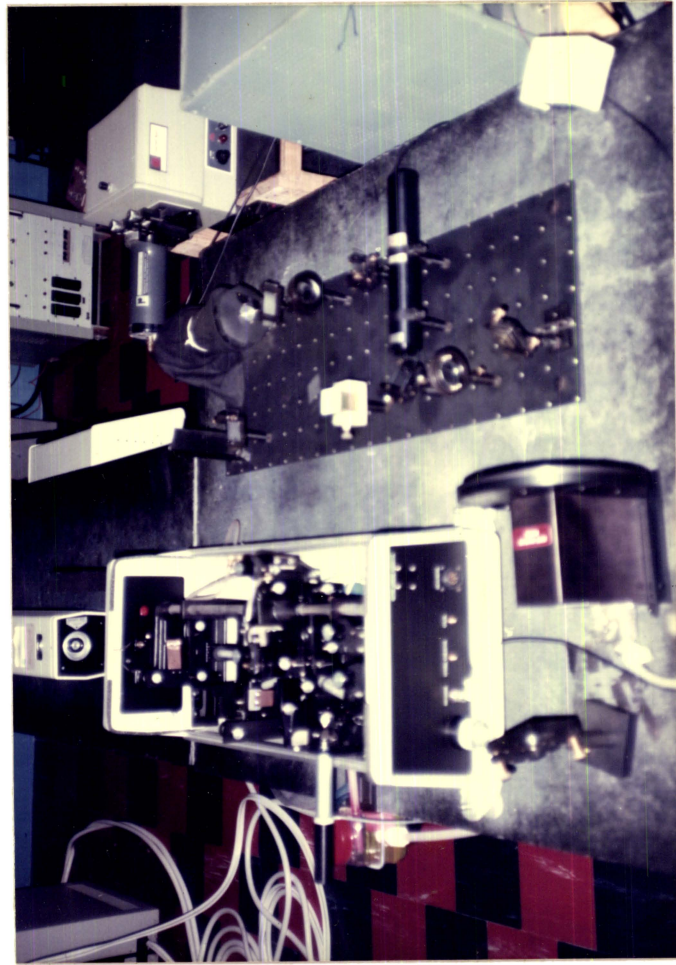
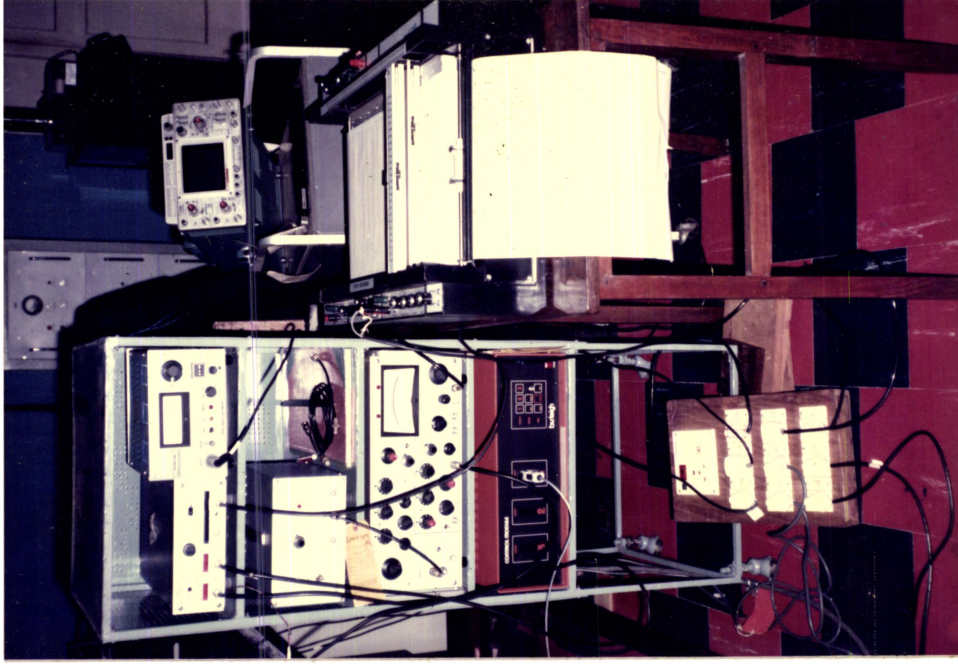


Fig. 3.1 Block diagram of the dual beam thermal lens set-up for the present work.



(a)



(b)

Fig.3.2 Photograph of the dual beam thermal lens setup (a) Optical arrangement
(b) Detection Electronics.

The experiment uses a Rhodamine 6G dye laser (Spectra Physics 380A Ring Dye Laser) as the pump source for creating thermal lens effect. An output power of 50-100 mW is found to be suitable for many of the experiments. The dye laser beam is chopped (10 Hz - 25 Hz) and is focused to the sample cell of path length 1 cm by a convex lens of focal length 15 cm. A 2 mW He-Ne beam passing through the sample collinear to the pump beam probes the pulsating thermal lens formed in the sample. The modulated He-Ne beam then falls on a PMT (EMI 9684) placed at a distance of 130 cm from the sample cell after passage through a concave lens of focal length 15 cm placed at one focal length away from the PMT. The output of the PMT is synchronously detected by a lock-in amplifier (EG&G 124 A). The output of the lock-in amplifier and the relative power of the dye laser (amplified by a factor of ten) obtained from the wavelength corrected detector in the dye laser are fed to a ratiometer (EG&G 193) for power normalization. The wavelength of the dye laser is scanned across the tuning range of the Rhodamine 6G dye using an inch-worm translator (Burleigh IW - 602) which turns the birefringent filter. The output of the ratiometer as a function of the wavelength is recorded on a strip chart recorder (Digital Electronics Series 2000). Wavelength measurements are made using a Burleigh WA 20 vacuum wavemeter.

The finer details of the main components of the thermal lens apparatus are given below.

3.21 The Pump Source--Ring Dye Laser

The excitation source used is a Rhodamine 6G CW dye laser (Spectra Physics 380 A Ring Dye Laser). This dye laser is pumped by an Argon ion laser (Spectra Physics 171-17). The dye laser is pumped by all lines from the Argon ion laser since Rhodamine 6G absorbs many of the Argon lasing lines and thus will help in operating the ion laser at lower discharge currents compared with that required for single line operation. The cavity configuration of the ring dye laser is schematically shown in Fig.3.3. The dye laser contains five mirrors--the pump mirror m_p which focuses the argon laser beam onto the dye jet and the resonator mirrors $m_1 - m_4$ which make the beam configuration in the form of the figure "8" pattern. The unidirectional device allows oscillation only in one (counter clockwise) direction. This is used for avoiding spatial hole burning¹. Under optimum conditions the dye laser has an efficiency of ~ 25 per cent.

The wavelength selection of the dye laser output is done using several elements in the cavity. The birefringent filter when rotated tunes the output wavelength coarsely over the full tuning range of the dye. Fine frequency tuning can be done using the scanning elalon and the galvanometer plates.

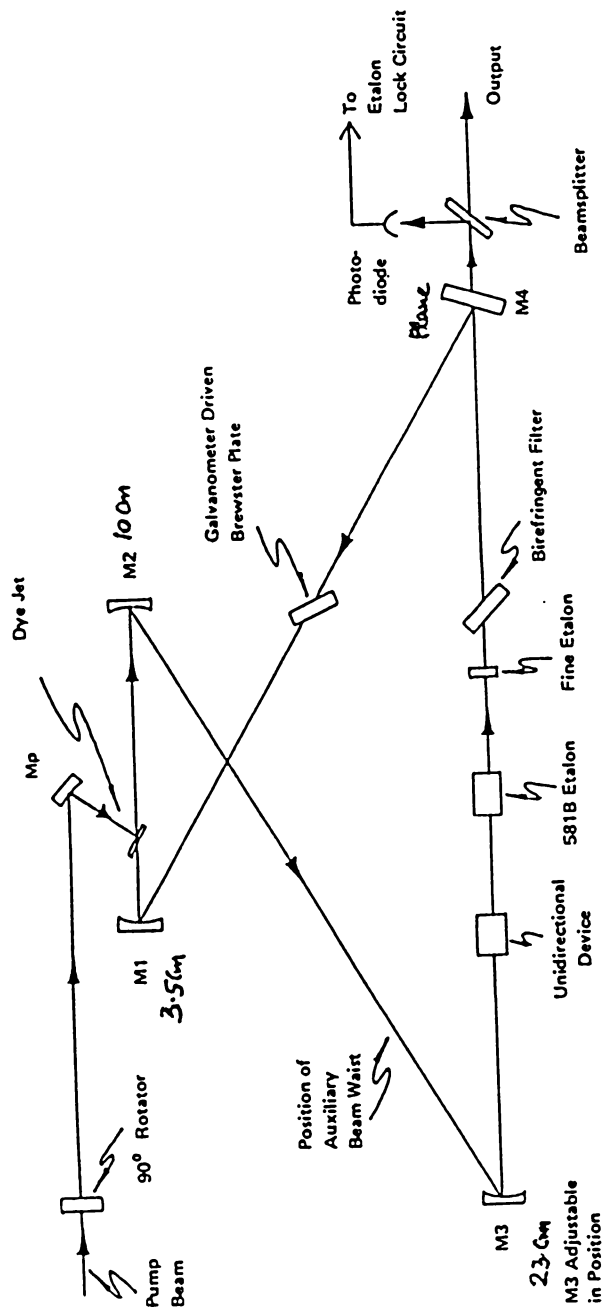


Fig. 3.3 Beam path in the Spectra-Physics 380A Ring Dye Laser cavity.

However, for the present experimentation, the thick (scanning) etalon and the thin etalon are removed from the cavity. This is because, for recording the broadband liquid-phase spectra, the band width ($0.024 \overset{\circ}{\text{A}}$) obtainable by using the birefringent plate alone in the cavity is more than sufficient. Also, removal of the fine tuning elements will increase the output power of the dye laser. Wavelength scanning is done by rotating the birefringent filter using an inchworm translator (Burleigh IW 602) driven by a Burleigh CE 1000 control module. For most of the experiments an output power of 50 - 100 mW is used. The tuning range of the Rhodamine 6G dye laser is 570-630 nm. The laser is always operated in the fundamental transverse (TEM_{00}) mode.

3.22 The Chopper

An EG&G 192 Variable frequency chopper is used to modulate the pump source. The minimum chopping frequency obtainable from this chopper is 5 Hz when using a two-apertured blade. We have used chopping frequencies ranging from 10 Hz to 25 Hz for the different samples under investigation. The chopper blade used is symmetric, that is the 'on' time is equal to the 'off' time. A reference output compatible for the lock-in amplifier is obtainable from the chopper driver.

3.23 The Probe Source

The probe source used for the dual beam thermal lens experiment is a 2 mW He-Ne laser (Coherent) which operates in

the fundamental transverse (TEM_{00}) mode. The output stability of the He-Ne laser is ~ 3 per cent. The main source of fluctuation of the output power of the He-Ne laser is due to the fluctuations in line voltage. A power line isolator (Hill-105-1 India) is used for avoiding such spikings from the line voltage.

3.24 The Detector Assembly

The probe beam after passing through the pulsating thermal lens is detected in the far field using a photomultiplier (red sensitive cathode - EMI 9684 tube). The PMT is fitted with a pinhole of 1 mm diameter and a He-Ne laser line filter (Melles Griot Model 03 FIL008). Behind the filter, a ground glass diffuser is also fixed so that the photocathode gets a uniform illumination by the probe beam. The output of the PMT is terminated to a $10\text{ k}\Omega$ shielded resistance.

3.25 The Lock-in Amplifier

The lock-in amplifier used for the present experiments is an EG&G 124 A high sensitivity instrument. This lock-in amplifier has a maximum sensitivity of 100 nV in direct mode with a model 117 differential preamplifier. This combination is used for all the experiments in the present investigation. The lock-in amplifier has different signal amplifier modes like high pass, band pass, low pass and notch modes. For the

thermal lens experiment the band pass mode is used (with Q ranging from 10 to 50) to avoid the probe beam noise induced overload.

3.26 Ratiometer and Recorder

As the dye laser is wavelength scanned, the output power varies along the dye gain curve and the lock-in output is to be normalized for the laser power variation. We have used an EG&G 193 ratiometer for this purpose. The relative power output from the dye laser is obtained from the wavelength corrected photodiode² in the dye laser. The ratiometer has input options of 1 volt and 10 volt maximum. The signal from the photodiode is amplified by a factor of ten using a d.c. amplifier. The recorder output from the lock-in amplifier (10 volts full scale) is fed directly to the A input and the amplified relative power is fed to the B input of the ratiometer. The A/B output of the ratiometer is given to the strip chart recorder (Digital Electronics - 2000 series). The recorder trace gives the normalized absorption spectrum of the sample in arbitrary units.

3.27 The Wavemeter

A Burleigh WA 20 vacuum wavemeter is used for measuring the absolute wavelength of the dye laser output. The wavemeter consists of a scanning Michaelson interferometer with

built in He-Ne laser. The interference fringes created are counted electronically and compared to the count for the reference He-Ne beam. The wavelength or wave number can be digitally displayed. There are two count settings for high and low resolution. For the present investigations on liquid-phase spectra the low resolution count setting is sufficient which measures wavelength with $\pm 0.1 \overset{\circ}{\text{A}}$ resolution.

3.30 Experimental Considerations

As already explained, the recording of the absorption spectra using the dual beam setup is accomplished by scanning the dye laser wavelength and recording the normalized lock-in signal by a strip chart recorder. However there are several experimental requirements to be satisfied³ in the experimental arrangement shown in Fig.3.1. First of all, the spatial mode quality of the pump laser is very important. For the thermal lens experiment, the pump beam is to be operated in the TEM₀₀ mode. Higher order cavity modes when present in the beam increases the total output power of the beam but they do not enhance thermal lens formation since these modes have no significant power at the beam centre of the Gaussian beam profile. Thus the correction of the observed thermal lens signal for total pump beam power will degrade the signal to noise ratio. Moreover, when higher order modes are present in the beam, the corresponding profiles will produce additional refractive index

534.321.4:535.316:535.374

A B D

gradients in the sample, which will distort the thermal lens created by the fundamental Gaussian beam. The ring dye laser used for the present work, when properly aligned, gives out high quality TEM₀₀ output. With its four cavity mirrors and one pump mirror, the alignment of the ring dye laser needs much skill and this is one of the most difficult parts of the experiment. However, once aligned properly, the mode quality and output power of the dye laser remains steady for a long time compared with the measurement time of the thermal lens signal.

Once the fundamental transverse mode is obtained for the pump laser, the next consideration is the choice of the correct power level and path length. A decreased pump power will reduce the strength of the thermal lens signal and hence will cause a reduced S/N ratio. An increased pump power will certainly increase the thermal lens signal, but one has to make sure that the linear behaviour of the thermal lens signal is maintained upto the maximum pump power used. Swofford and Morrell have addressed this point in their analysis of the dual beam technique⁴ and has concluded that the magnitude of the a.c. component should be less than 0.1 to assure linearity in absorbed power. We have checked the linear behaviour for every sample before recording the spectra and found that the behaviour is linear upto 100 mW for all the samples studied for a path length of 1 cm. We have used a

power range of 50-100 mW for almost all the samples studied with a path length of 1 cm. This small path length is used since we have focused the pump beam in the cell and a larger path length will destroy the approximation of constant spot size in the cell³.

The chopper performance is an important experimental parameter. If the chopper is open for less than the critical time t_c , the growing thermal lens causes a decrease of $\sim 60\%$ of the value of the equilibrium change in probe beam power. When the chopper is closed the thermal lens gets relaxed and the signal regains original value. If the chopper is on for two times the critical time the change in detected probe power will be $\sim 80\%$ of the equilibrium change. Variations in chopper speed will lead to fluctuations in the signal. The chopper used for the present work has a frequency stability of 0.2% with frequency drift of only less than 0.2%/°C after one hour warm up. Thus the signal fluctuations due to deviations in chopping speed is completely eliminated by allowing one hour warm up for the unit.

The choice of chopping frequency can only be done by trial. This is because the critical time t_c is unknown due to lack of knowledge of thermal diffusivities of the compounds. Slower chopping speeds will certainly lead to larger signals, but the S/N ratio will be seriously affected

by the flicker noise ($1/f$ noise) of the probe source. This problem can be overcome by using a very narrow bandwidth lock-in operation, but the amplifier settling time will be correspondingly increased. This will increase the measurement time. By trial we have found that chopping frequencies in the range 10-25 Hz are suitable for the present experimentation. The lock-in amplifier is operated always in the band pass mode with 'Q' ranging from 10 to 50 and the output filter time constant as 1 second or 3 seconds.

There are several optical considerations introduced by the dual beam arrangement. The probe source instability is one of the important requirements of the dual beam method. The output of the coherent He-Ne laser used for the present experiments when directly connected to a.c. line voltage shows power variations corresponding to the spikings in line voltage. We have used a power line isolator (Hill Model 105-1 India) for isolating the laser from such spikings in line voltage. However the laser output is again slightly modulated by ripples at 50 Hz and 100 Hz. The noise arising from this modulation could be eliminated by the band pass operation of the lock-in amplifier. Another important requirement is the stability against relative motion of the pump and probe beams. This factor becomes more critical when both the beams are focused in the sample cell as done in earlier works³⁻⁵, where even the

smallest relative motion will cause fluctuations in the detected probe power. The use of a vibration isolation system will completely eliminate this difficulty. However, we could rectify the problem by using a focused pump beam and an unfocused probe beam. This optical arrangement could significantly improve the stability of the thermal lens signal against relative motions of the two beams. To make the spot size of the probe laser at the pinhole-PMT assembly sufficiently large so that the detected power is only a small fraction of the total beam power, a concave lens is placed in front of the PMT. In the present setup a concave lens of focal length 15 cm is placed at a distance one focal length before the PMT.

The samples under investigation should be well-filtered and allowed for attaining steady state in the sample cell for a few minutes to avoid signal distortions due to suspended particles and air bubbles. We have used 10 μm Whatman filter papers for filtering the samples. For every sample, a settling time of atleast five minutes is allowed for reaching equilibrium state free of movements and convections.

Cell window absorption is another factor which can cause measurement difficulties. This is because some type of glasses can weakly absorb visible light and this in turn causes a thermal lens from the sample cell. Also the heat thus generated can flow into the sample causing distortion to the

sample thermal lens. However, fused silica cells are very much less absorptive than borosilicate glass. Hence we have used fused silica spectrophotometric cells (path length 1 cm). To ensure that cell window absorption does not cause serious problems, the thermal lens signal with cell alone in the position is looked for, and found to be negligible over a wide range of pump beam power levels.

The usual difficulties which one always come across when detecting coherent, monochromatic optical beams are also to be taken into account in the dual beam experiment. All plane parallel surfaces in the beam path, including the sample cell are tilted slightly to avoid the creation of interference fringes in the beam incident on the detector. When such interference patterns are present on the detector, small mechanical vibrations can cause fluctuations in the thermal lens signal. Surface scatter from optical components will also cause difficulties due to the speckle pattern resulting from the surface scattering. Movements of this speckle pattern by mechanical vibrations will cause fluctuations in the signal. The diffraction pattern created by the edges of the aperture (pinhole) can also cause signal fluctuations. To avoid such problems, we have fixed a ground glass diffuser behind the filter so that the photocathode is uniformly illuminated by the probe beam. If one uses absorptive filters for blocking the pump

laser at the detector the heating effect on the filter can produce spurious signals. This is because, such absorptive filter act as low finesse etalons and will create moving fringe patterns upon heating by the pump beam. To avoid such problems, we have used a thin film interference notch filter (laser line filter) for the 6328 Å wavelength. To avoid exposure to high intensity pump beam we have fixed this filter behind the pinhole. The probe beam thus passes through the pinhole, filter, diffuser and then falls on the PMT photocathode.

When the experimental parameters are chosen as described above, the thermal lens signal strength as measured by the lock-in amplifier (across 10 k Ω from PMT) ranges from 100 μ V to 10 mV for the different samples studied.

The choice of scanning speed for the dye laser is to be compatible with the chopping frequency used in the experiment, but this parameter is not difficult to choose and control since the speed of the inchworm translator is continuously variable. We have used scanning speeds of 2-6 nm/min. for the experiments.

Before carrying out experiments in new compounds we have recorded the fifth CH overtone spectra of several compounds which are already studied by other workers. The spectra

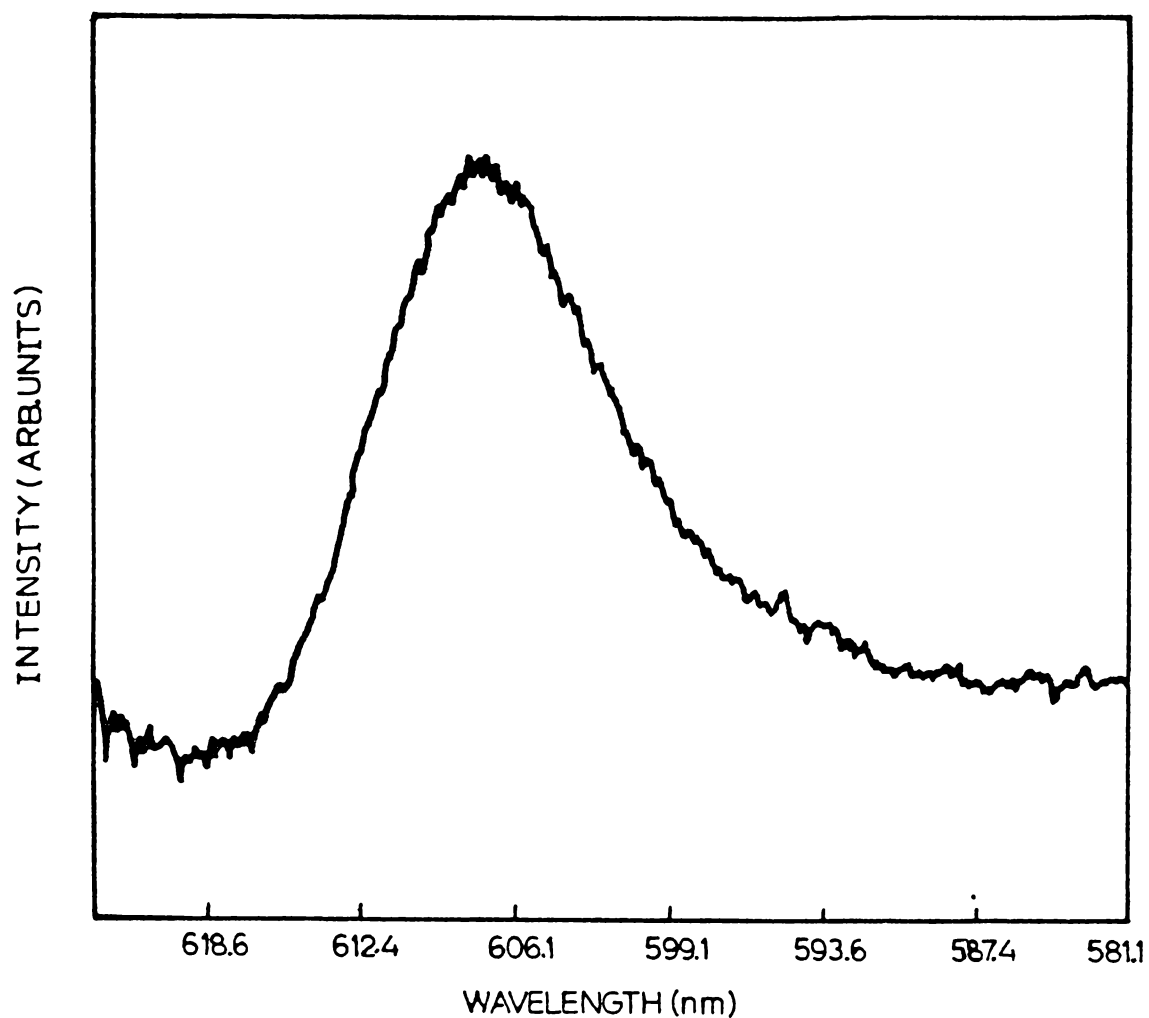


Fig.3.4 Fifth aryl CH overtone spectrum of toluene recorded by the present setup. The spectra of other compounds (not shown) also show agreement with literature values of peak positions. The present and literature values of peak positions (cm^{-1}) are Toluene - 16465 (16460^a), Chlorobenzene - 16585 (16590^a), Bromobenzene - 16565 (16565^a), 1-2 dichlorobenzene - 16600 (16606^b) and 1,3 dichlorobenzene - 16670 (16667^b).

a - ref.1, Chapter 4

b - ref.3, Chapter 4

obtained using the present setup agree well with those reported earlier. As a typical example Fig.3.4 shows the fifth aryl CH overtone spectrum of toluene along with the present and literature values of peak positions. These observations establish the performance of our setup.

3.40 Measurement of Lower Overtones

While the dual beam thermal lens technique is used for recording the fifth CH overtone spectra of several organic compounds, a Hitachi 330 UV-VIS-NIR spectrophotometer is used for recording the lower overtones in the NIR region. This spectrophotometer uses a tungsten lamp as the source of NIR. All spectra are recorded using a cell of path length 1 cm. The specific conditions under which the spectra of different samples are recorded are given in the respective sections (see Chapters 4 and 5). It is to be pointed out that even for the fourth overtone spectra ($\Delta V = 5$) the signal to noise ratio of the spectrophotometer is poor, and recording of the fifth overtone spectra using the spectrophotometer is very difficult. This indicates the necessity of high sensitivity techniques such as based on the thermal lens effect.

REFERENCES

1. Model 380 A Ring Dye Laser Instruction Manual, Spectra Physics (USA) Sec.3-1.
2. Model 380 A Ring Dye Laser Instruction Manual, Spectra Physics (USA), Sec.4-31.
3. H.L.Fang and R.L.Swofford in "Ultrasensitive Laser Spectroscopy", D.S.Kliger (Ed.), (Academic Press, N.Y., 1983).
4. R.L.Swofford and J.A.Morrell, J.Appl.Phys.49, 3667 (1978).
5. H.L.Fang and R.L.Swofford, J.Appl.Phys.50, 6609 (1979).

ANALYSIS OF CH OVERTONE SPECTRA OF
SOME AROMATIC COMPOUNDS

4.10 Introduction

4.11 Aryl CH Overtones in Substituted Benzenes

As already mentioned in Chapter 1, overtone spectroscopy has been used for characterizing the aromatic CH bonds in many substituted benzenes. The initial studies on the effect of various substituents (atoms and groups) on the benzene ring CH overtones are those of Mizugai et al.^{1,2} These workers recorded the fifth aryl CH overtone spectra of about thirty monosubstituted and about fifteen disubstituted benzenes using pulsed dual beam thermal lens technique. They observed a good correlation between the shift in the overtone energy from that of benzene and the inductive part of the Hammett σ (σ_I) of the substituent. The shift in disubstituted benzenes correlates with the sum of the σ_I values of the two substituents when they have the same polarity. When the two substituents have opposite polarities, a doublet structure is observed in the spectrum corresponding to the neighbouring CH bonds of the two substituents. The studies of Mizugai et al have shown that

an electron withdrawing substituent causes increase in the aryl CH mechanical frequency (or force constant) and hence a decrease in CH bond length while an electron donating substituent cause a decrease in the mechanical frequency.

Gough and Henry³ extended the work of Mizugai et al by studying the overtone spectra of a number of liquid phase halobenzenes and nitrobenzene in the $\Delta V = 2$ to 6 or 7 regions by conventional absorption technique. All the substituted halobenzenes show single peaks in the overtone spectra, indicating that the variation in CH bond length among the nonequivalent aryl CH bonds in these compounds is negligible. The shift in the overtone energies with respect to benzene correlates with the inductive part of Hammett σ assuming additivity of substituent effects. A doublet structure in the overtone spectra is observed only for nitrobenzene, the higher energy peak corresponding to the ortho CH bonds and the lower energy peak corresponding to the meta and para CH bonds. (The authors have confirmed these assignments in a separate study on deuterated nitrobenzenes⁴). Only the low energy peak correlated well with the Hammett σ_I value, since σ_I is defined only for meta and para positions⁵. The authors have also discussed the various specific points to be considered in correlating overtone energy shifts with Hammett σ_I values.

Nakagaki and Hanazaki⁶ reported the aryl CH overtone spectra of several methyl and chloro substituted benzenes. They

established that the red and the blue shifts with respect to benzene observed for methyl- and chloro-benzenes respectively, occur due to the change in the mechanical frequency. The observed changes are attributed to the polar effects (i.e., inductive effects represented by Hammett σ_I) of the substituents. Assuming additivity of substituent effects in the ortho, meta, and para positions, the change in the mechanical frequency with respect to benzene is calculated. The authors compared the validity of through-- σ bond inductive and through--space field (electrostatic) effect models, assuming that only one is operating at a time. They concluded that, the through-- σ bond effect is predominant in methylbenzenes and the through--space effect is predominant in chlorobenzenes.

Other reports on aryl CH overtones in substituted benzenes include the gas-phase investigations in toluene and xylenes⁷ and in trimethylbenzenes⁸. The frequency shifts in toluene and xylenes with respect to benzene indicates that the aryl CH bonds meta, para and (meta + para) to the methyl group(s) are comparable in lengths to the CH bonds in benzene. The bonds which are ortho, (ortho + meta) or (ortho + para) are predicted to be longer by 0.001 - 0.002 Å. The (ortho + ortho) bond in m-xylene is predicted to be still longer by 0.001 Å. A similar behaviour is expected in the aryl CH bond lengths of trimethylbenzenes.

The important observation in all these overtone spectral studies of substituted benzenes is that the mechanical frequency and (hence the force constant) of the aryl CH bonds show an increase upon substitution by an electron withdrawing group on the ring, and a decrease in the mechanical frequency upon substitution by an electron donating group. The anharmonicity of the aryl CH bonds remains almost same as that in benzene over a wide range of substituents. Even though the shift in the overtone energies correlates well with the Hammett σ_I values, no simple conceptual picture of the mechanism of the change in ring CH force constants upon substitution on the ring is provided in any of these previous works.

We have studied⁹ the aryl CH overtones in liquid-phase acetophenone and benzaldehyde in the $\Delta v = 2$ to 6 regions by conventional and thermal lens techniques (section 4.31). The physical mechanism of the change in the aryl CH bond length upon substitution by an electron withdrawing/electron donating group is proposed and discussed in detail in connection with the previous studies (section 4.32).

4.12 Nonequivalent Methyl CH Overtones in Anisotropic Environments

We have seen in Chapter 1 that the local mode model has been used to describe the appearance of overtone absorptions corresponding to the excitations of different types of CH bonds

in a molecule. Environmental influences, operating on CH bonds which are otherwise chemically equivalent, alter the overtone transition energies of these oscillators differently, causing the overtone peaks to get resolved. There is now a large body of evidence from fundamental IR studies of selectively deuterated samples^{10,11} as well as overtone studies¹²⁻¹⁶, that groups like C=C, C=O and atoms like O, N, S produce anisotropic environments which result in the creation of nonequivalent CH bonds in an adjacent methyl group. We have already seen in Chapter 1 the advantages of using overtone spectroscopy as a tool in such cases over the fundamental IR studies.

Fang and his collaborators have reported¹²⁻¹⁶ the visible and near infrared overtone spectra (recorded using gas-phase photo acoustic, liquid-phase thermal lens and conventional methods) of many compounds containing nonequivalent methyl CH bonds created by lone pair trans effect and π electron effects. Among the compounds containing C=C bond they have studied propylene, 2-butene, 2-methyl 2-butene and 2,3-dimethyl 2-butene¹². For all these compounds, the methyl groups attached to the C=C bond exhibited two types of conformationally nonequivalent CH bonds. The authors have shown that in all the above compounds, the low energy peak in the methyl overtone doublet corresponds to the two out-of-plane

CH bonds, and the high energy peak corresponds to the in-plane CH bond. The out-of-plane CH bonds interact strongly with the π electron cloud of the $C=C$ bond, thus lowering the transition energy whereas for the in-plane methyl CH bond which lies in the π nodal plane, there is no such interaction. Later, Fang et al have given a molecular orbital analysis of the overtone spectrum of propylene and have concluded that orbital delocalization is the mechanism responsible for the appearance of nonequivalent methyl CH bonds¹³. Among the compounds containing a hetero atom with lone pairs of electrons, Fang and co-workers studied methanol, dimethyl ether, dimethoxy ethane, dimethyl sulphide, trimethyl amine and methyl formate^{14,15}. In all the molecules studied the methyl groups adjacent to the hetero atom (O,S,N) shows two distinct bands at each overtone level. The effect of the hetero atom on the methyl group is explained as the interaction of the lone pair of electrons in the hetero atom with the CH bonds situated trans to the lone pair (lone pair trans effect). The effect is explained to originate from the donation of electron density from the lone pair to the antibonding orbitals of the CH bonds situated trans to the lone pair. This explanation is well accepted in literature^{17,18} but the exact mechanism of its operation is not understood. Among the compounds containing carbonyl ($C=O$) group, Fang et al studied acetaldehyde and acetone in detail and compared the $\Delta v = 4$ and 5 overtone spectra of these compounds

with those of 2-butanone and 3-pentanone^{12,15}. The carbonyl group contains both π electrons and lone pairs of oxygen, and hence Fang et al pointed out that in compounds like acetaldehyde both lone pair effect and π effect will be operative on a methyl group adjacent to a carbonyl. Based on the overtone and the earlier fundamental IR studies, Fang et al assigned the high energy peak in the methyl overtone spectra to the in-plane CH bond and the low energy peak to the two out-of-plane CH bonds. In analyzing the spectrum of acetaldehyde, the authors speculated that the in-plane methyl CH is effected by a trans effect of lone pairs either directly through the interactions with an oxygen lone pair or indirectly through interactions involving aldehydic CH which in turn is strongly influenced by the trans effect of oxygen lone pair. On the other hand, the out-of-plane CH bonds are more likely to be affected by the carbonyl π electrons. On going from acetaldehyde to acetone the high energy peak (in-plane CH bond) is virtually unaffected, while for the low energy peaks (out-of-plane CH bonds) both the mechanical frequency and the anharmonicity are significantly reduced. This could not be explained by simple trans effect since the in-plane CH bond (and hence the high energy component) would be most strongly influenced by trans substitution. Fang et al argued that the shorter C=O bond length in acetaldehyde compared to acetone could result in stronger interaction of π electrons and the out-of-plane CH bonds resulting in an

increased mechanical frequency and anharmonicity with respect to acetone. A comparison of the overtone spectra of acetone with those of 2-butanone and 3-pentanone in the $\Delta V = 4$ and 5 regions revealed that the high energy (in-plane CH bond) peak disappears when the methyl group is separated from the carbonyl by a methylene group. The low energy peak (out-of-plane) is almost unchanged on transition from acetone to 2-butanone and 3-pentanone. The disappearance of the high energy peak is interpreted by Fang et al as resulting from the loss of bond strengthening mechanism which operates on the in-plane CH bond when the methyl group is adjacent to the carbonyl.

Our studies on the overtone spectrum of acetophenone has revealed that this compound contains nonequivalent methyl CH bonds. To the authors knowledge this is the first report⁹ of the observation of nonequivalent methyl CH bonds in this compound. While our analysis supports the arguments of Fang et al on out of plane CH bonds, the local mode parameters of the in-plane CH bond requires an interpretation based quantum mechanical resonance among highly polar valence bond structures. The observation and analysis of the nonequivalent methyl CH bonds in acetophenone is detailed in section 4.33.

4.20 Experimental

The following liquid samples are used for the experiments--high purity acetophenone (99.9% from Sisco Research Laboratories, India), high purity benzaldehyde (99.5% from

Glaxo BDH India), spectrograde carbon tetrachloride (99.9% from Sisco Research Laboratories, India), high purity styrene (> 99% from Fluka AG, Germany) and high purity (solid) polystyrene (> 99% from Polypenco UK). The fifth CH overtone spectra of acetophenone, benzaldehyde, styrene and polystyrene are recorded from pure samples using the dual beam thermal lens technique described in Chapter 3. The first through fourth overtone spectra of these compounds are recorded in a Hitachi-330 UV-vis-NIR spectrophotometer. Except at the first overtone ($\Delta V = 2$) level where carbon tetra chloride is used to dilute acetophenone and benzaldehyde, other overtone peaks are recorded from pure samples. A path length of 2 cm is used for polystyrene and 1 cm for other samples for both the thermal lens and the conventional techniques. All spectra are recorded at $26 \pm 2^\circ\text{C}$.

4.30 Results and Discussion

4.31 Aryl CH Overtones in Acetophenone and Benzaldehyde

The thermal lens spectra of the two compounds in the Rhodamine 6G region (Fig.4.1) is entirely due to the fifth overtone ($\Delta V = 6$) excitation of the aryl CH bonds. The NIR spectra (Figs.4.2-4.4) show absorption due to both aryl and methyl CH overtones in the $\Delta V = 2, 3$ and 4 regions. The discussion on the methyl CH overtones in acetophenone is given in section 4.33. Aldehydic CH overtones in benzaldehyde

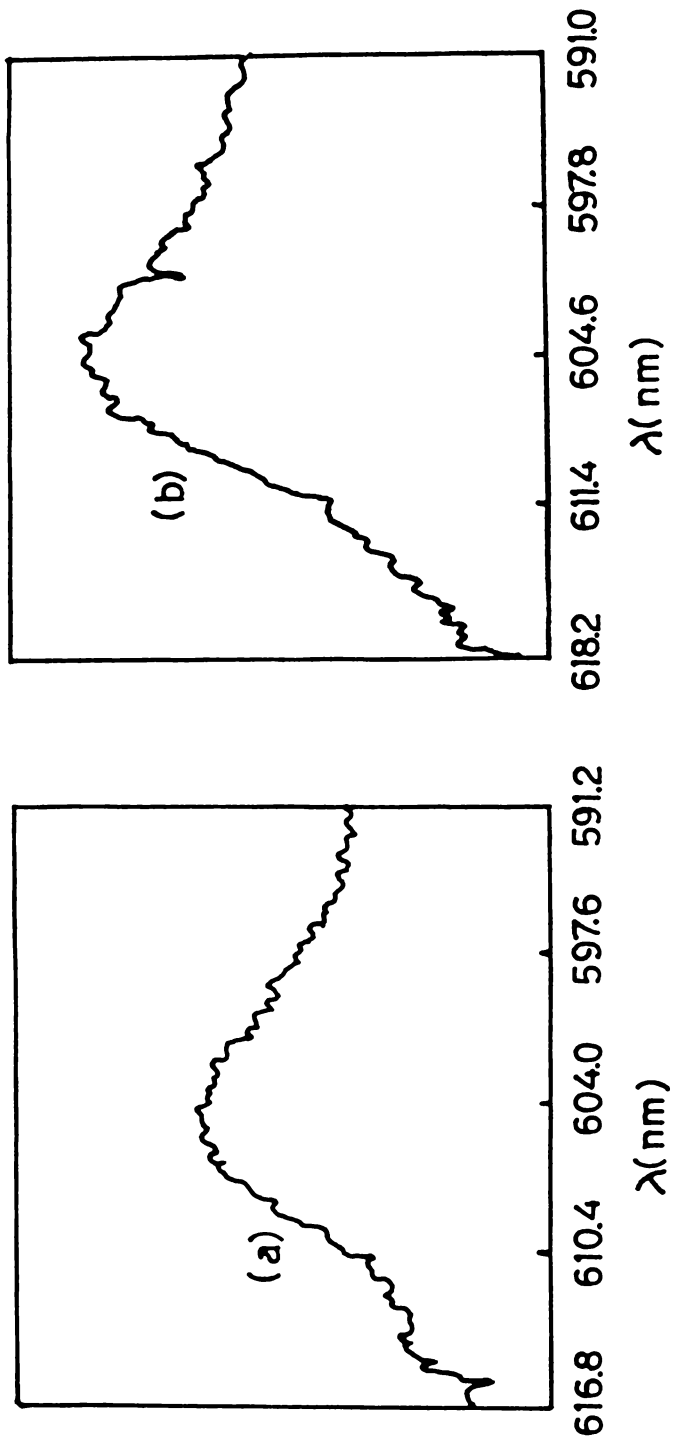


Fig.4.1 Overtone spectra of (a) acetophenone and (b) benzaldehyde in the $\Delta V = 6$ region recorded in pure liquid by dual beam thermal lens technique.

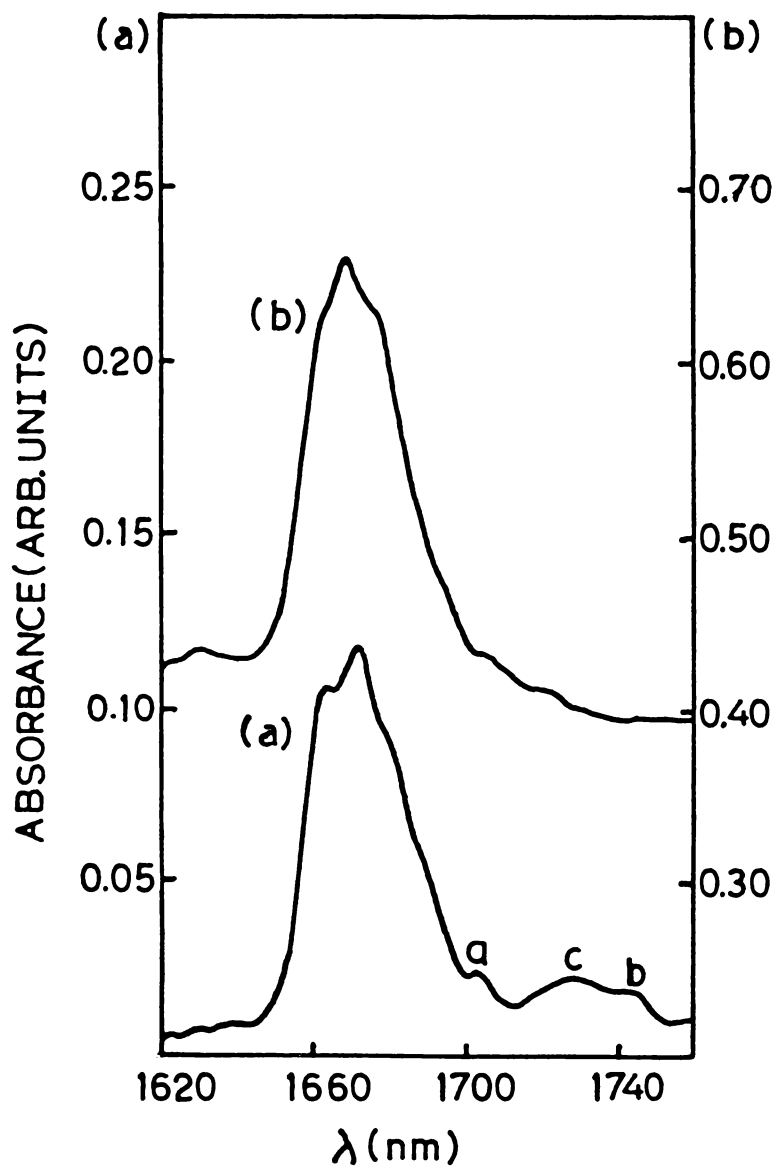


Fig.4.2 Overtone spectra of (a) acetophenone and (b) benzaldehyde in the $\Delta V = 2$ region. Samples dissolved in carbon tetrachloride. Reference - carbon tetrachloride. C - combination (see text).

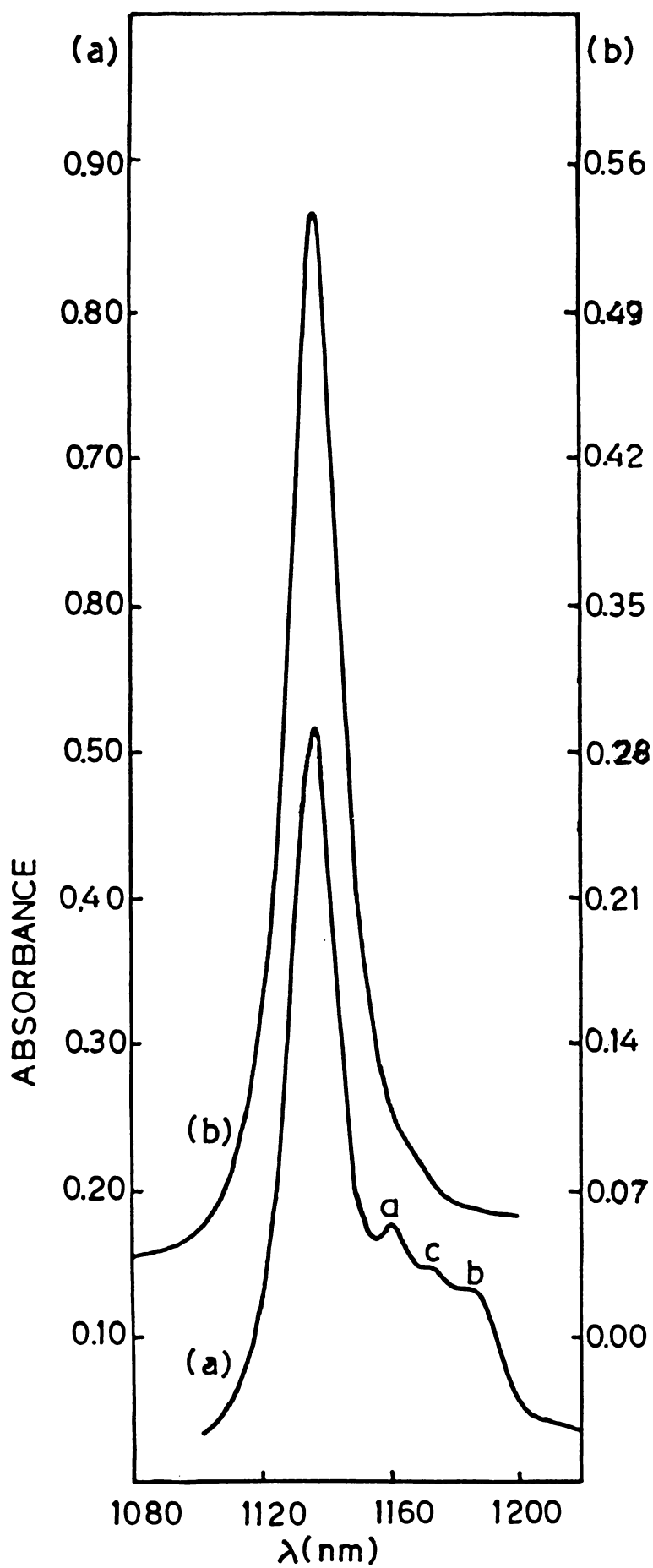


Fig.4.3 Overtone spectra of (a) acetophenone and (b) benzaldehyde in the $\Delta V = 3$ region. Pure samples; Reference - air
c - combination (see text).

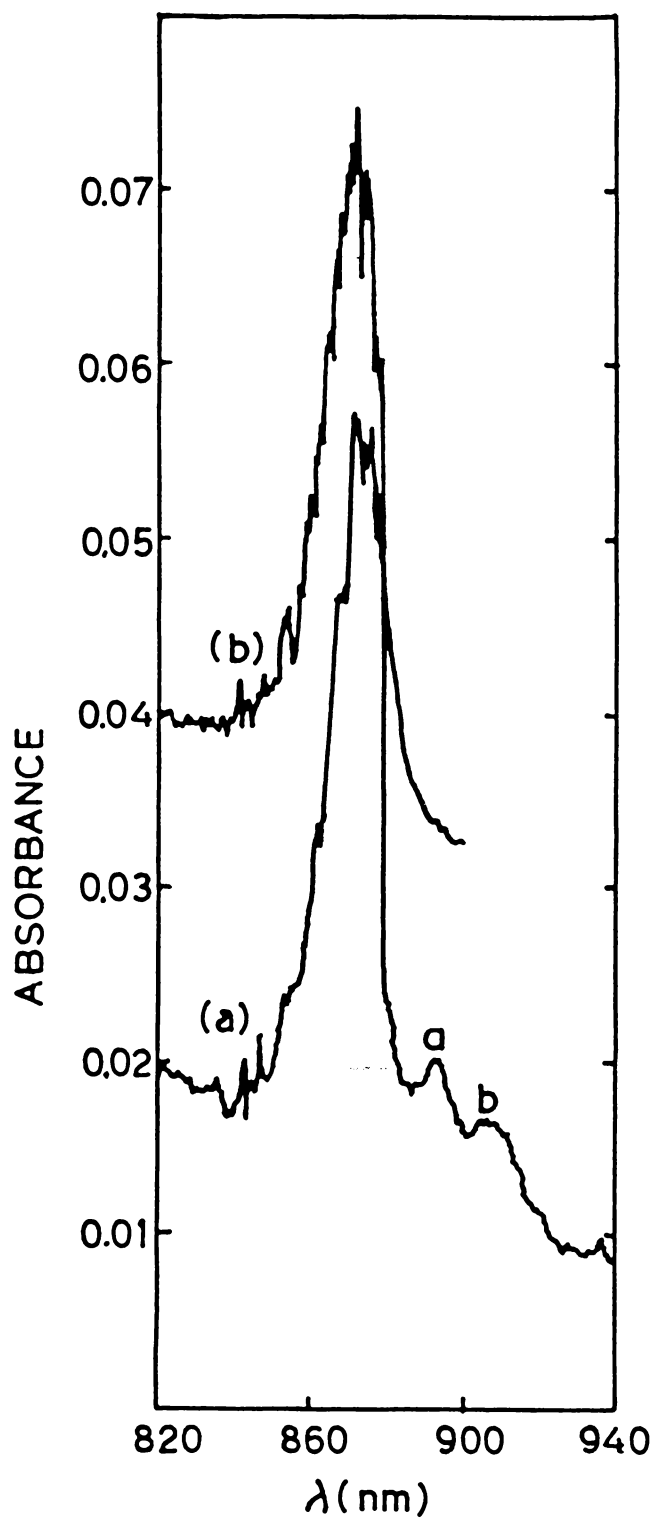


Fig.4.4 Overtone spectra of (a) acetophenone and (b) benzaldehyde in the $\Delta V = 4$ region. Pure samples; Reference - air.

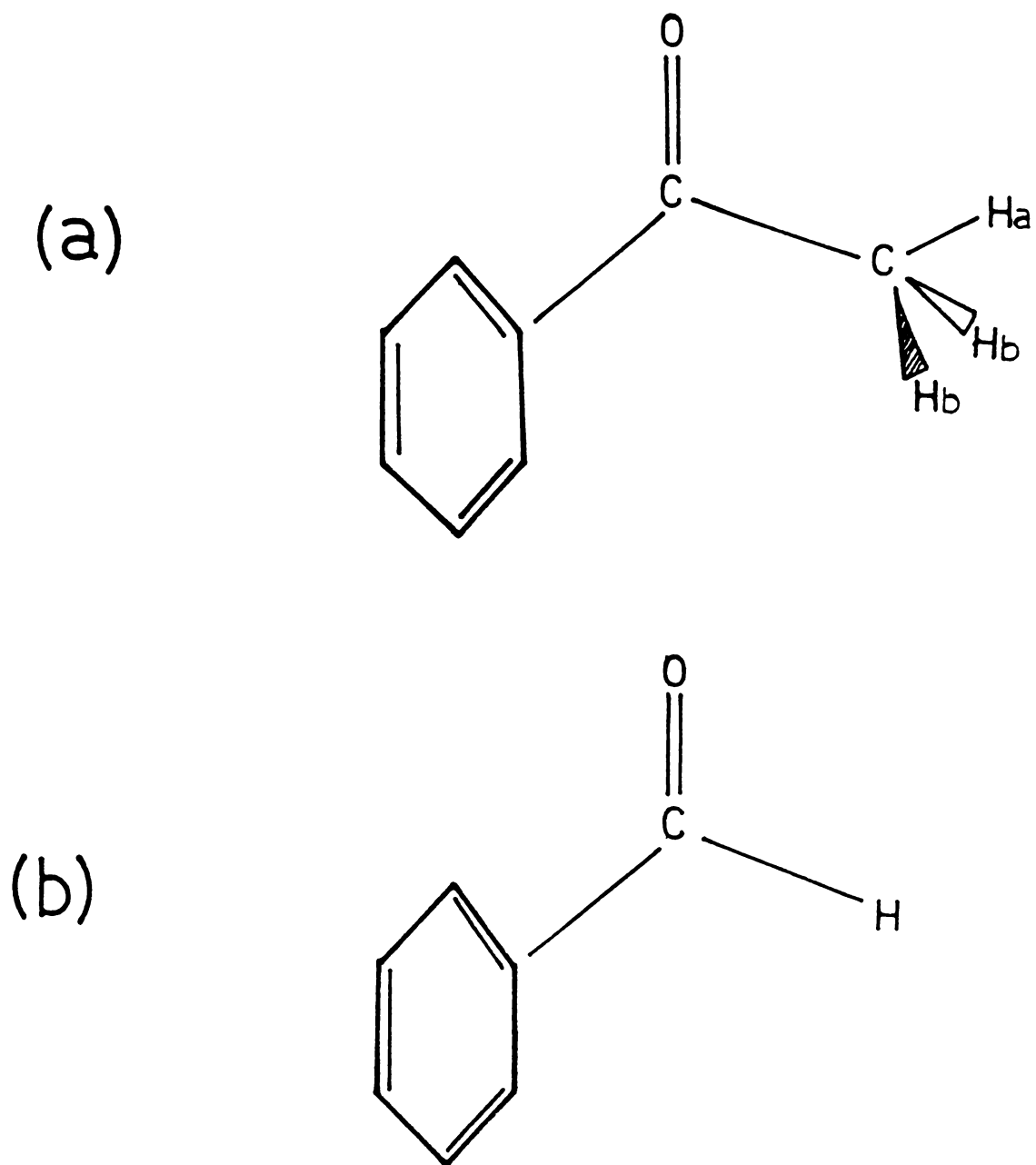


Fig.4.5 Molecular structure of (a) acetophenone and (b) benzaldehyde.

are not studied in the present work due to the poor signal to noise ratio of these overtones.

The aryl CH overtones in the $\Delta V = 2-6$ regions are represented by the Birge-Sponer relation,

$$\Delta E_{v,0} = V(A + VB) \quad (4.1)$$

A plot of $\frac{\Delta E}{V}$ versus V gives the local mode parameters viz., the mechanical frequency $X_1 = (A-B)$ and the anharmonicity $X_2 = B$ of the CH bonds. Table 4.1 shows the peak positions of the overtones and the local mode parameters. The introduction of $-C(=O)CH_3$ and $-C(=O)H$ groups to the benzene ring shifts the aromatic CH overtone energies to higher values with respect to benzene. It is also observed that (table 4.1) the anharmonicities of the aryl CH bonds in acetophenone and benzaldehyde are not very different from that in benzene¹⁹. Mizugai and Katayama¹ have reported the fifth aryl CH overtone spectrum of acetophenone and benzaldehyde recorded by pulsed dual beam thermal lens technique, where the peak positions are shown to be blue shifted with respect to benzene. Comparison of the present near infrared and visible overtone peak positions for the two compounds shows that the overtone energies of benzaldehyde are slightly higher than those of acetophenone. However the fifth overtone

Table 4.1

Observed overtone energies (cm^{-1}), Mechanical frequencies X_1 (cm^{-1}), Anharmonicity X_2 (cm^{-1}), Correlation coefficients γ , and CH bond Dissociation energies ΔE_{max} (k Cal/mole) for CH overtone spectra of Acetophenone and Benzaldehyde. Morse potential is assumed in calculating dissociation energies.

	$\Delta V=2$	$\Delta V=3$	$\Delta V=4$	$\Delta V=5$	$\Delta V=6$	X_1	X_2	γ	ΔE_{max}
Benzene ^a	5983	8760	11442	14015	16467	3140.1	-57.6	--	118.55
Acetophenone									
Aryl CH	5981	8787	11468	--	16528	3165±10	-59±1.5	-0.99963	116.9
Methyl CH ^a	5869	8613	11211	--	--	3133±8	-66±1	-0.99978	102.1
Methyl CH ^b	5734	8432	11032	--	--	3027.5±8	-54±1.5	-0.99971	117.6
Benzaldehyde									
Aryl CH	5995	8799	11468	--	16541	3174±12	-60±2	-0.99922	115.5

a. Data from ref.4b.

Note: The correlation coefficient $\gamma = -1$ indicates perfect straight line fit.

data of Mizugai and Katayama shows that the transition energies are almost equal for the two components. This shows that our data of the overtone energies is more accurate than that obtained by the point by point thermal lens measurement of the earlier workers. The slightly higher overtone energies of benzaldehyde than those of acetophenone is due to the slightly higher mechanical frequency (table 4.1) in this compound. The observation is also in agreement with the fact that the electron withdrawing power of the $-C(=O)H$ is slightly larger than that of the $-C(=O)CH_3$ group due to the presence of the electron donating $-CH_3$ group in the latter. The observation also corroborates with the slightly higher Hammett σ_I value of the $-C(=O)H$ group²⁰. Since the aryl CH mechanical frequencies of the two compounds show only a small difference, it is clear that the major influence originates from the $>C=O$ group. The physical mechanism of the increase in the aryl CH force constant is discussed in the next section.

The correlation between the aryl CH bond length and the shift in overtone energy from benzene reads^{7,8,21,22}

$$r_{CH}^{LM} (\text{\AA}) = 1.084 - 8 \times 10^{-5} \frac{\Delta\omega}{\nu} (\text{cm}^{-1}) \quad (4.2)$$

This equation predicts that the aryl CH bond length in acetophenone and benzaldehyde are $\sim 0.001 \text{\AA}$ smaller than in benzene. The difference in bond length between the two compounds is smaller than the uncertainty in the correlation.





One would expect that the ortho, meta and para bonds are likely to be affected differently by a substituent, the ortho being affected most. The present liquid-phase data give only an average effect over the different CH bonds. A gas-phase study would therefore be of interest to distinguish the inequivalent ring CH bonds in these compounds.

4.32 The Proposed Mechanism of the Change in the Aryl CH Bond Length

It is known that a group having electron withdrawing tendency relative to hydrogen atom, if attached to a benzene ring, will attract the mobile ring π electrons to a larger extent and the rigid σ electrons to a lesser extent²³. The total inductive effect consist of the electrostatic (through-space field effect) effects, through-- σ bond effects and π inductive effects²⁴. The simplified component interaction models for the propagation and distribution of electronic effects are given by Wells et al²⁴ and are reproduced in table 4.2. In the symbolic diagrams of the table, X represents the substituent and R represents the reacting group which can be in the ortho-meta-or para-positions. The first and the second interactions are inductive, while the third and the fourth are resonance types. Considering the inductive effects (the overtone energies correlate with the inductive part of Hammett σ rather than with the total Hammett σ), the interaction

Table 4.2

Simplified Component Interaction Models for Propagation and Distribution of Substituent Electronic Effects (From ref.24)

No.	Interaction Type	Symbol	Model of Interaction	Atoms in System	Effect Type
1.	Classical Inductive		Direct R with X (a) by electrostatic field effect (r^{-1}) (b) by σ bond transmission	6	I
2.	π -Inductive or Inducto-Electrometric		R to C_1 by σ bond and/or field. C_1 to other sites of the ring by π electron delocalization. From ring sites to X by field, σ bond or π delocalization	6 or 7	I
3.	Resonance or Mesomeric polar		R to ring C's by π delocalization. From these to X by field and/or σ bond.	7	R
4.	Direct conjugation Or Electromeric		Direct R with X by π delocalization	8	R

through the σ bond of the ring system is termed classical inductive effect whereas the interaction occurring through the π cloud of the ring is termed non-classical or π -inductive effect or inducto-electromeric effect. The classical and non-classical effects are mixed and are difficult to characterize separately; the principal effect of the mixing of classical and π -inductive effects is to make the total inductive effects equal in meta and para positions²⁴. In overtone spectroscopy of aryl CH bonds, the 'reacting group' R shown in the symbolic diagram can be regarded as concerned CH bond. Surprisingly enough, the important contribution of π -inductive effect has not been considered so far in interpreting the substituent effects in overtone spectra. Moreover as mentioned earlier the physical mechanism of aryl CH bond shortening/lengthening was not provided in any of the previous reports. We propose the following physical picture for the change in the aryl CH bond length. An electron withdrawing group reduces the electron density at the ring carbon atoms through inductive effects (classical and π -inductive effects). This in turn produces a net positive charge on the ring carbon atoms. This causes a greater attraction of the carbon atom for the valence electron cloud of the hydrogen atom. The net result is an increase in the CH force constant and the mechanical frequency and a decrease in the bond length. A reverse effect is expected for an

electron donating group. Similar effects are reported in the earlier infrared studies on halomethanes²⁵.

The mechanism of the change in aryl CH bond length upon substitution on the benzene ring proposed here needs further discussion in connection with the previous works. As already seen, the work of Mizugai et al^{1,2} established that an electron withdrawing group cause an increase of the aryl CH force constant. These authors stated that, since σ_I is a measure of the free energy effect of the substituent relative to hydrogen atom resulting from its power to attract or repel electrons through space and through σ bonds of the benzene system, the results of the overtone studies revealed that the CH bond force constants increases upon a decrease of the σ electron density of the carbon atoms. They also stated that they could not give an explanation for such a behaviour¹. In the later work of Gough and Henry³ the σ_I parameter, which is measurable only for meta and para positions was considered to be associated with field effect (through - space, electrostatic effect); a CH bond ortho is a substituent experiencing both through-- σ bond and through-space inductive effects. It was concluded that in both field and through-bond effects the CH bonds reflect primarily the changes induced in the σ bond framework. In both the above works are given neither the importance of the π -inductive effects nor the physical picture of the increase/decrease of the aryl CH force constant.

Nakagaki and Hanazaki⁶ compared the validity of through- σ bond inductive and through-space field effect models in several methylated and halogenated benzenes. They found that the through- σ bond inductive effect is predominant compared to through-space field effects in methylbenzenes while both through-bond and through-space effects have almost equal contributions in chlorobenzenes. However for chlorobenzenes the best fit transmission factor ϵ obtained in the assumed bond model was larger than that reported in earlier works. The workers therefore concluded that long range electrostatic field effect (through-space effect) is the predominant mechanism operating in halobenzenes. For methylbenzenes, the value of the residual sum of squares⁶ for the through- σ bond model is less than half of the value for the through-space model. This confirms the relative validity of through- σ bond mechanism in methylbenzenes.

For halobenzenes the values of the residual sum of squares for the through- σ bond and through-space effects are equal⁶. Also the best fit ϵ value is much higher than the earlier reported value. This shows that the residual sum of squares for the through- σ bond model would be much larger than that for the best fit ϵ value, if the literature value of ϵ is adopted. If the electrostatic field effect is the predominant mechanism, the residual sum of squares would have

been much smaller (compare with the value for the through-bond model in methyl benzenes⁶). The above observations lead to the conclusion that in halobenzenes, along with the long range electrostatic field effect and through- σ bond effect, the π -inductive effect is also contributing to the electron withdrawing property.

In all the above discussions as well as in previous overtone studies, the resonance contribution to Hammett σ is not taken into account, primarily because overtone energy shifts correlate with the inductive part of Hammett σ . However certain discrepancies observed especially in halobenzenes^{1,3} seems to indicate the role of resonance in the overtone energy shifts. The straight line of correlation of $\Delta\omega$ versus σ_I for these compounds makes a negative Y intercept. This shows that a negative shift in the overtone energy with respect to benzene is possible in the absence of the inductive effect thus indicating the role of resonance effect (which is opposite in sign to the inductive effect for halogens) in the frequency shift. Another interesting observation in halobenzenes is that the relative shifts between fluoro-, chloro-, bromo- and iodo-benzenes are far greater than predicted by the variation in σ_I ^{1,3}. Gough and Henry³ attributed this observation to the probable non-additivity of the substituent effects. But the fact that monosubstituted halobenzenes also show the same behaviour points to the need for much detailed investigations

of the contributions of the inductive and the resonance effects and the influence of lone pairs of halogens on the overtone energies.

4.33 Nonequivalent Methyl CH Bonds in Acetophenone

In the overtone spectrum of acetophenone the bands indicated by 'a' and 'b' on the low energy side of the aryl CH overtones (Figs.4.2-4.4) individually fit into Birge-Sponer plots. Their local mode parameters are given in table 4.1. These two bands arise from the two different types of methyl CH bonds present in the molecule. A band appearing between 'a' and 'b' bands in the $\Delta v = 2$ and 3 regions can only be assigned to a combination band either from the ring or from the methyl group, involving $(n - 1)$ quanta of CH stretch and two quanta of CH bend. The intensity of this middle band decreases as we pass from the $\Delta v = 2$ to $\Delta v = 3$ region and disappears completely in the $\Delta v = 4$ region. As observed in other carbonyl compounds^{12,15}, the nonequivalence of the two methyl CH bonds originates from the anisotropic environments created by the oxygen lone pair and carbonyl π electron cloud. In acetophenone (Fig.4.5a) the phenyl ring, the C=O group, and one of the methyl CH bonds are in a plane. Also the in-plane methyl CH bond is cis to the C=O bond²⁶. Thus the relative configuration of C=O and the methyl group is the same as that in acetone and acetaldehyde¹⁵. We assign the high

energy component 'a' of the methyl CH band to the in-plane CH bond and the low energy component 'b' to the two out-of-plane CH bonds. This assignment is in line with the predictions of the trans effect theory and observations in compounds like acetone and acetaldehyde in the fundamental¹¹ and overtone^{15,16} regions. As can be seen from table 4.3 the in-plane CH_a bond has very large mechanical frequency and anharmonicity compared with acetone and acetaldehyde. Also, the mechanical frequency and anharmonicity of the out-of-plane CH_b bonds are lowered with respect to acetone. It is known¹⁵ that on going from acetaldehyde to acetone the in-plane CH_b peak the mechanical frequency and anharmonicity are reduced. Fang et al have stated that this cannot be explained by simple trans effect. They have also pointed out that the smaller C=O bond length in acetaldehyde could result in an increased π electron interaction with the out-of-plane CH_b bonds. Considering the situation in acetophenone, it is known²⁷ that the C=O bond length in aryl alkyl ketones is larger than in dialkyl ketones. This is evident from the decreased C=O group frequencies in aryl alkyl ketones. Thus our observation that the mechanical frequency and the anharmonicity of the out-of-plane CH_b bonds show decrease as we pass from acetone to acetophenone is in line with the arguments of Fang et al, that is, in acetophenone the larger C=O bond length compared with acetone results in a decreased interaction

Table 4.3

Comparison of Methyl CH Local Mode Parameters of
Acetaldehyde, Acetone and Acetophenone

Molecule	X_1	X_2	ΔE_{\max}
Acetaldehyde ^a			
CH _a	3084±13	-55±2	119.2
CH _b	3083±9	-63.3±2	103.0
Acetone ^a			
CH _a	3082±9	-54±1	121.3
CH _b	3047±15	-58±2	111.9
Acetophenone			
CH _a	3133±8	-66±1	102.1
CH _b	3027.5±8	-54±1.5	117.6

a. Data from ref.22.

of π cloud with the out-of-plane CH_b bonds. This results in a decreased mechanical frequency and anharmonicity of the out-of-plane CH_b bonds with respect to those in acetone. Another observation, as already pointed out, is that both the mechanical frequency and the anharmonicity of the in-plane CH_a bond are much larger than in acetone and acetaldehyde (table 4.3). It is known²⁷ that dipolar structures with decreased $\text{C}=\text{O}$ bond order (increased $\text{C}=\text{O}$ bond length) (Fig.4.6) contribute much to the aryl alkyl ketone structures. These structures are such that the carbonyl oxygen is very rich in electron density. The interaction of this electron cloud seems to be the main reason for the very large mechanical frequency and anharmonicity of the in-plane CH_a bond. The in-plane phenyl ring may also affect the strength of the in-plane CH_a bond. It can be seen from atable 4.3 that the dissociation energy of the CH_a bond in acetophenone is less than that of the CH_b bonds. This is contrary to similar observations in other carbonyl compounds¹⁵. The CH_a potential in acetophenone is much shallower. due to the large anharmonicity of this bond. For obtaining more complete information on the spectral and structural aspects one has to carry out measurements in selectively deuterated gas-phase samples. Also the bond strengthening mechanisms in carbonyl compounds needs detailed theoretical investigations using MO theory.

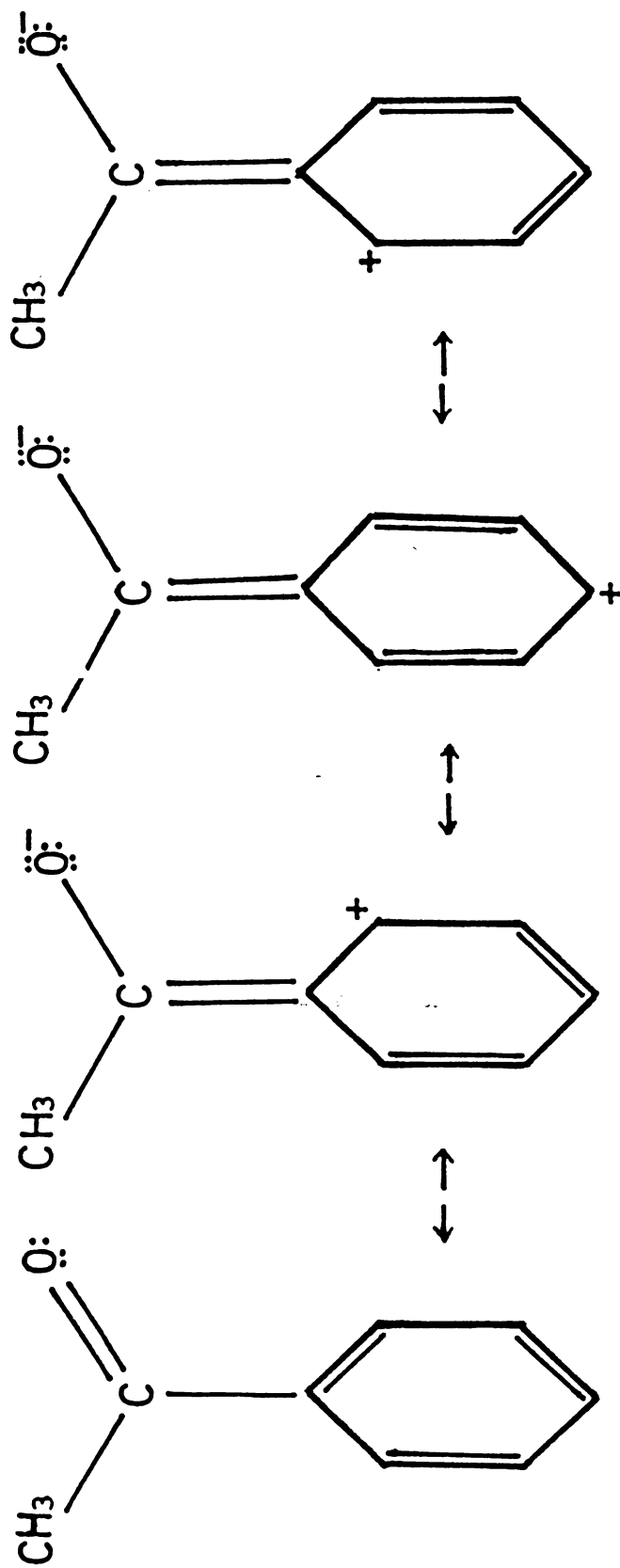


Fig.4.6 Dipolar resonance contributions to the structure of acetophenone. The dipolar structures (second through fourth) puts large electron density at the carbonyl oxygen and have larger C—O bond lengths.

4.34 Aryl CH Overtones in Styrene and Polystyrene

In this section we present the aryl CH overtone spectra of liquid styrene and solid polystyrene recorded by the dual beam thermal lens ($\Delta V = 6$) and conventional absorption ($\Delta V = 3-5$) techniques. To the authors knowledge our work reports the first thermal lens overtone spectrum of a solid as well as that of a polymer.

The thermal lens and the near infrared absorption spectra of the two compounds are shown in Figs.4.7-4.10. The overtone peak positions and the aryl CH local mode parameters are given in table 4.4. A comparison between the spectra of styrene and polystyrene reveals that the main peaks in both the compounds arise from aromatic CH overtones. In addition to aryl CH overtones, the near infrared spectrum of polystyrene shows the overtone bands of the CH bonds of the side chain.

Styrene molecule contains aromatic and olefinic CH bonds (Fig.4.11). The overtones of these two types of CH bonds appear in the same spectral regions²² and hence the olefinic CH overtones are masked by the more intense aryl CH overtones. The local mode parameters of the aryl CH bonds in both styrene and polystyrene are close to these in benzene. However, a comparison of the aryl CH overtone peak positions of the two compounds with those of benzene (table 4.4) shows that

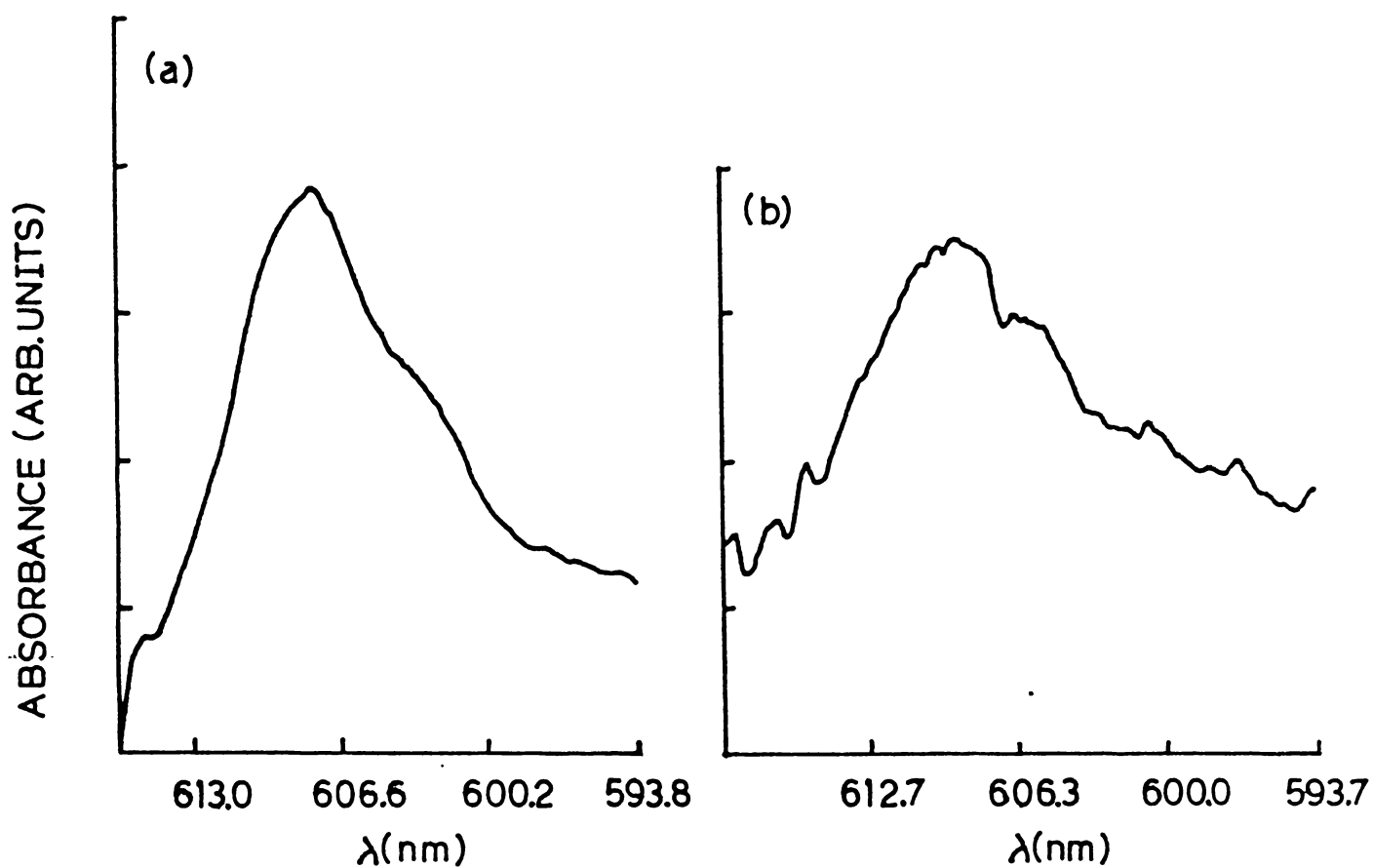


Fig.4.7 Aryl CH overtone spectrum in the $\Delta v = 6$ region recorded by the dual beam thermal lens technique (a) styrene, (b) polystyrene. Pure samples are used.

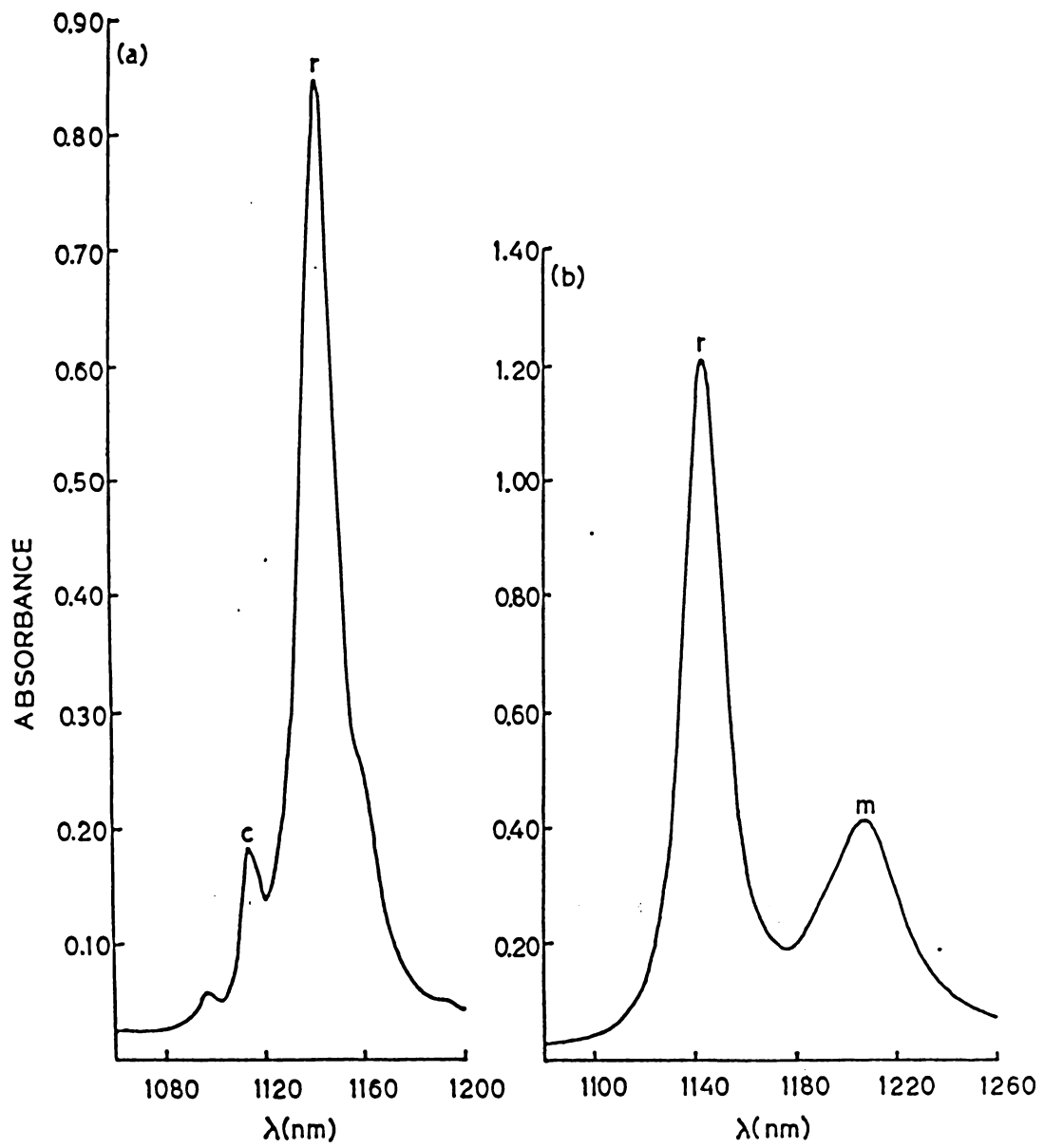


Fig.4.8 Overtone spectrum of (a) styrene and (b) polystyrene in the $\Delta V = 3$ region. (r) Aryl CH band (m) methylene CH band. Pure samples. Reference - air.

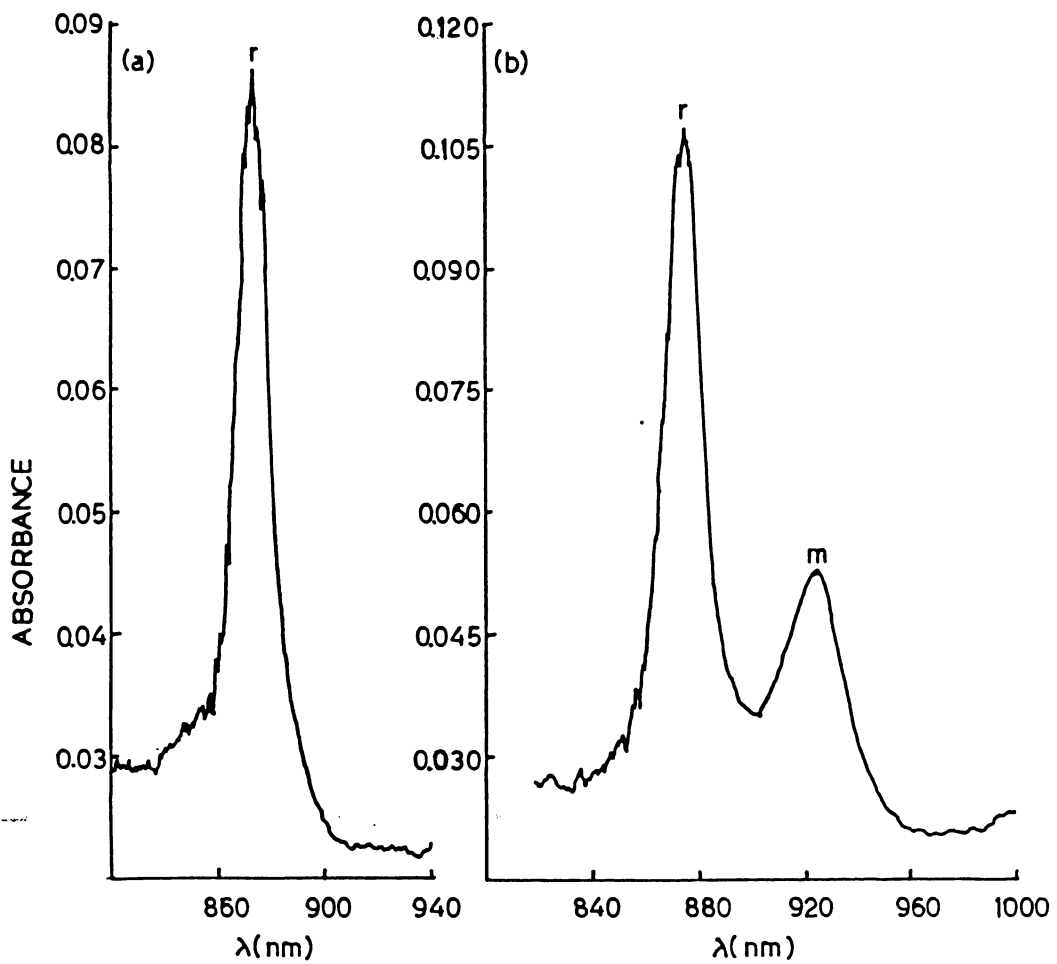


Fig.4.9 Overtone spectra of (a) styrene and (b) polystyrene in the $\Delta v = 4$ region. (r) Aryl CH band, (m) methylene CH band. Pure samples. Reference - air.

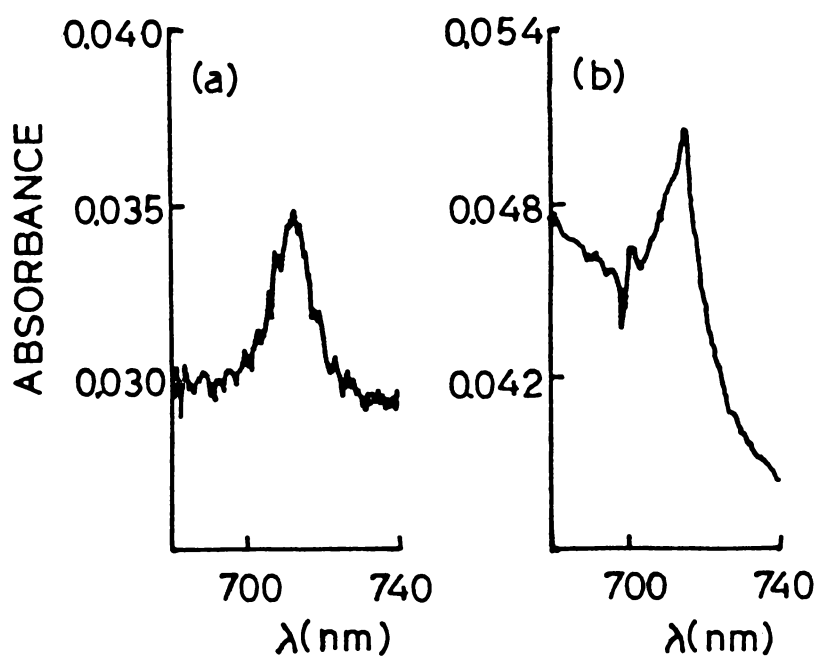


Fig.4.10 Overtone spectra of (a) styrene and (b) polystyrene in the $\Delta v = 5$ region. Only aryl CH bands could be clearly detected. Pure samples; Reference - air.

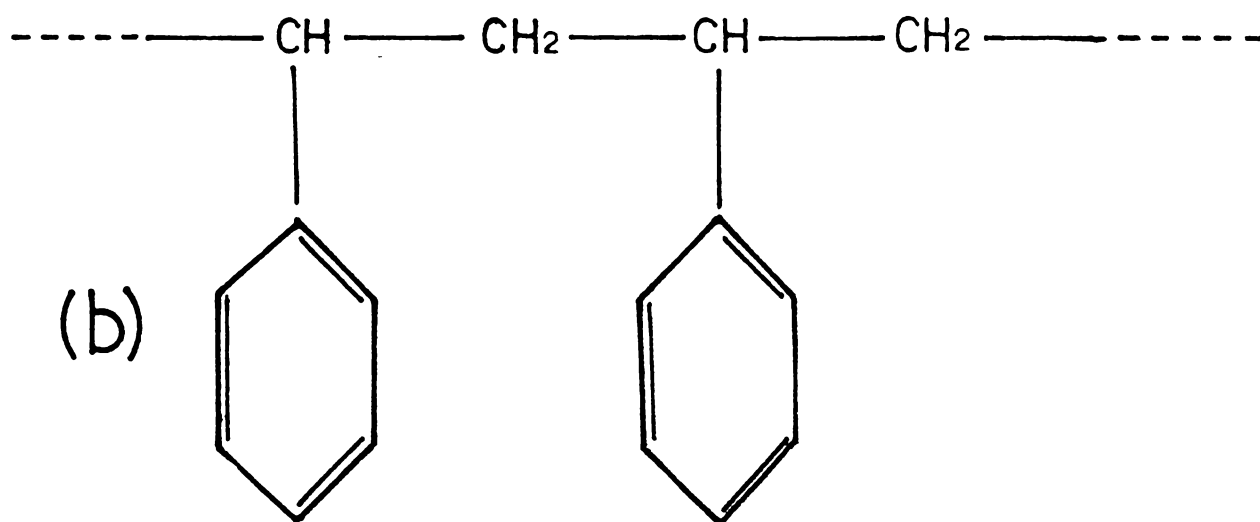
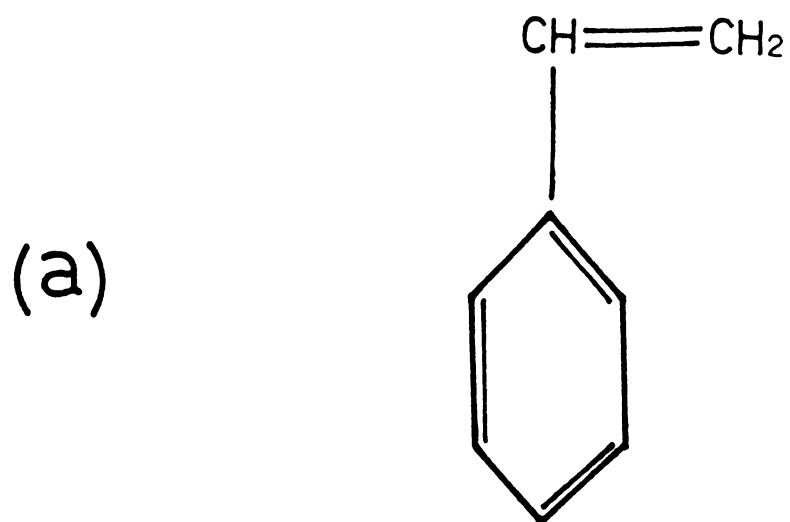


Fig.4.11 Molecular structure of (a) styrene
(b) polystyrene.

Table 4.4

Peak positions of bands observed in pure overtone regions of styrene and polystyrene, their assignments and aryl CH local mode parameters

	$\Delta V=3$	$\Delta V=4$	$\Delta V=5$	$\Delta V=6$	X_1	X_2	γ
Benzene ^a	8760	11442	14015	16467	3148.1	-57.6	--
Styrene	8757	11435	14035	16449	3151±9	-58±2	-0.999906
Polystyrene	8741	11429	13986	16430	3149±8	-59±2	-0.999996
	8285	10811	--	--	--	--	--
Methylenic Methy- lenic							
Secondary CH bonds in propane ^b	8307	10846	--	--	--	--	--

a. From ref.19.

b. From ref.29.

the shifts in the peak positions are -3 cm^{-1} ($\Delta V = 3$), -7 cm^{-1} ($\Delta V = 4$), $+20 \text{ cm}^{-1}$ ($\Delta V = 5$) and -18 cm^{-1} ($\Delta V = 6$) for styrene and -19 cm^{-1} ($\Delta V = 3$), -13 cm^{-1} ($\Delta V = 4$), -29 cm^{-1} ($\Delta V = 5$) and -37 cm^{-1} ($\Delta V = 6$) for polystyrene. The shifts in the styrene peaks are comparable to the experimental uncertainties in peak positions. Also there is no regularity in the magnitude and sign of the shifts. Thus we can conclude that the overtone energies of the aryl CH bonds in styrene are not affected by the $-\text{CH}=\text{CH}_2$ group. The polystyrene peaks on the other hand, shows increasing negative shifts, with respect to benzene, towards higher overtones. Even if the shifts are small, the good least square correlation of the Birge-Sponer plot (table 4.3) and the regularity in the magnitude and sign of the shifts clearly indicates that there is a small but detectable effect on the ring CH bonds. The correlation between overtone energy and CH bonds length (eqn.4.2) predicts that the aryl CH bond length in polystyrene is $\sim 0.0005 \text{ \AA}$ longer than in benzene. Except for $\Delta V = 4$, all other overtone data predict the same change in CH bond length. However, to the author's knowledge, no experimental data is available on the aryl CH bond length in polystyrene.

In the present work, the overtone spectrum of styrene is measured in the liquid phase and that of polystyrene is measured in the solid phase. Greenlay and Henry have reported²⁸ that in 3-methyl pentane a transition from liquid to solid phase

renders the CH vibrations more harmonic. In the case of polystyrene the nonobservation of a change in anharmonicity from styrene reveals that there is no appreciable modification of the aryl CH potential curve from that in styrene. If at all there is a change in anharmonicity due to change of phase, this change might have been cancelled by a change in the opposite direction due to some steric effects occurring in the polymer structure. However an overtone spectroscopic study of the compounds in the same phase is necessary to confirm such an argument.

In the $\Delta V = 3$ and 4 regions of the polystyrene spectrum, a band appears on the low energy side of the aryl CH bands. The peak positions of these bands are close to the overtone energies of secondary CH oscillators in alkanes²⁹ (table 4.4) and are thus identified to be the overtones of the sp^3 CH_2 and CH bonds of the side chain. The above bands clearly distinguish the overtone spectrum of polystyrene from that of styrene and can be used to probe polymerization. Overtone bands have been used to probe polymerization of ethylene³⁰. Probing polymerization using overtone bands is a very convenient means since the fundamental spectra are often congested by the presence of many modes of vibration as can be realized from the fundamental IR spectra of styrene³¹ and polystyrene³², where a comparison is difficult.

REFERENCES

1. Y.Mizugai and M.Katayama, J.Am.Chem.Soc.102, 6424 (1980).
2. Y.Mizugai, M.Katayama and N.Nakagawa, J.Am.Chem.Soc.103, 5061 (1981).
3. K.M.Gough and B.R.Henry, J.Phys.Chem.87, 3433 (1983).
4. K.M.Gough and B.R.Henry, J.Phys.Chem.87, 3804 (1983).
5. Lloyd N.Ferguson, "The Modern Structural Theory of Organic Chemistry", (Prentice Hall Inc.,N.J. USA, 1963).
6. R.Nakagaki and I.Hanazaki, Spectrochim.Acta.40A, 57 (1984).
7. K.M.Gough and B.R.Henry, J.Phys.Chem.88, 1298 (1984).
8. M.K.Ahmed and B.R.Henry, J.Phys.Chem.90, 1737 (1986).
9. T.M.A.Rasheed, K.P.B.Moosad, V.P.N.Nampoori and K.Sathianandan, J.Phys.Chem. in press (1987).
10. D.C.Mc Kean, J.L.Duncan and L.Batt, Spectrochim.Acta.29A, 1037 (1973).
11. D.C.Mc Kean, Spectrochim.Acta.31A, 861 (1975).
12. H.L.Fang and R.L.Swofford, Appl.Opt.21, 55 (1982).
13. H.L.Fang, R.L.Swofford, M.McDevitt and A.B.Anderson, J.Phys.Chem.89, 225 (1985).

14. H.L.Fang, D.M.Meister and R.L.Swofford, *J.Phys.Chem.*88, 405 (1984).
15. H.L.Fang, D.M.Meister and R.L.Swofford, *J.Phys.Chem.*88, 410 (1984).
16. I.A.Findsen, H.L.Fang, R.L.Swofford and R.R.Birge, *J.Chem.Phys.* 84, 16 (1986).
17. L.J.Bellamy and D.W.Mayo, *J.Phys.Chem.*80, 1217 (1976).
18. L.J.Bellamy, *Appl.Spectrosc.* 33, 439 (1979).
19. C.K.N.Patel, A.C.Tam and R.J.Kerl, *J.Chem.Phys.*71, 1470 (1979).
20. R.W.Taft Jr., "Steric Effects in Organic Chemistry", M.S.Newman (Ed.), (Wiley, N.Y.,1956), p.594.
21. Y.Mizugai and M.Katayama, *Chem.Phys.Lett.*73, 240 (1980).
22. J.S.Wong and C.B.Moore, *J.Chem.Phys.*77, 603 (1982).
23. David A.Shirley, "Organic Chemistry", (Holt, Rinehart and Winston Inc., N.Y., 1964), p.640.
24. P.R.Wells, S.Ehrensens, and R.W.Taft in "Progress in Physical Organic Chemistry", (John Wiley & Sons, Interscience Publishers, N.Y., 1968), Vol.6, p.157.
25. W.Kaye, *Spectrochim.Acta.*6, 257 (1954).

26. V.M.Potapov, "Stereochemistry", (MIR Publishers, Moscow, 1978), p.487.
27. Margreta Avram, and G.H.D.Mateescu, "Infrared Spectroscopy-- Applications in Organic Chemistry", (Wiley Interscience, N.Y., 1972), p.357.
28. W.R.A.Greenlay and B.R.Henry, Chem.Phys.Lett.53, 325 (1978).
29. H.L.Fang and R.L.Swofford, J.Chem.Phys.73, 2607 (1980).
30. H.W.Siesler and K.Holland-Moritz, "Infrared and Raman Spectroscopy of Polymers", (Marcel Dekker Inc., N.Y., 1980), p.331.
31. John R.Dyer, "Applications of Absorption Spectroscopy of Organic Compounds", (Prentice Hall Inc., Englewood Cliffs, N.J., USA, 1965), pp.24-25.
32. L.J.Bellamy, "The Infrared Spectra of Complex Molecules", (Chapman and Hall, London, 1975), p.101.

Chapter 5

ANALYSIS OF CH OVERTONE SPECTRA OF SOME ALIPHATIC COMPOUNDS

5.10 Introduction

The characterization of CH bonds in aliphatic compounds using overtone absorption spectroscopy has revealed much information on the strength of individual CH bonds, the effect of substituents on the strength of individual CH bonds, the coupling of the CH stretching to other molecular motions, the details of coupling between equivalent CH oscillators attached to a common carbon atom and the creation of non-equivalent CH bonds in methyl groups subjected to anisotropic environments and many other structural and spectroscopic details.

The local mode parameters of a CH bond can be well studied by analyzing the overtone spectra of compounds containing solitary CH bonds. Quack and co-workers have presented^{1,2} detailed analysis of the high resolution gas-phase CH overtone spectra of compounds like CF_3H and $(\text{CF}_3)_3\text{H}$ obtained by Fourier transform (NIR) and photoacoustic (visible) techniques. They have shown that the overtone spectral structure can be interpreted using a tridiagonal Hamiltonian involving stretch-bend

Fermi interaction between states with a common chromophore quantum number $N = (V_s + \frac{1}{2} V_b)$. These authors also studied the dynamics of the CH overtones using the tridiagonal Hamiltonian obtained from the spectroscopic data and have shown that the Fermi interaction plays a key role in the local mode dynamics (see Chapter 1, sec.1.32). Zewail and co-workers also demonstrated^{3,4} the presence of stretch-bend interactions in the overtone spectra of deuterated methanes obtained by photoacoustic spectroscopy.

One of the criteria for observing mode selective rupture of an X-H bond by overtone excitation is that the X-H local mode under question is not to be coupled to other vibrational modes by Fermi resonance and that the molecule contains only one X-H oscillator of that particular type⁵. Another possibility of mode selective chemical reaction by overtone pumping is that the local mode is mixed with another vibration which in turn can be a reaction coordinate (eg. dissociation of H_2O_2 by overtone pumping of OH bond; the overtone energy is transferred to the O-O stretching mode leading to the fragmentation into two OH bonds⁶⁻⁸). In either case one has to understand from the overtone spectra the details of the strength of the X-H bond, its coupling with other molecular motions and the dependence of the strength of such couplings on the overtone quantum level. Among the different overtone photochemistry

experiments reported to-date, more than half of them involve molecules in which olefinic CH bonds are excited^{9,10}. Hence an understanding of the olefinic CH local mode parameters and the couplings to other vibrations will be of interest in any overtone photochemical studies involving them.

Considering the above facts we have studied¹¹ the CH overtone spectrum of trichloroethylene in the $\Delta V = 2-6$ regions. Trichloroethylene contains only a single CH bond, also it is an olefinic molecule. The overtone spectrum presented here demonstrates that the CH bond strength in this molecule is much greater than its parent molecule ethylene. This is shown to be due to the electron withdrawing effect of the chlorine atoms. The fifth CH overtone data is used to predict the change in CH bond length from that in ethylene. The spectrum also demonstrates that in the second overtone region ($\Delta V = 3$) the CH overtone is Fermi resonant with the CH deformation mode. There are no measurable Fermi interactions in other overtone quantum levels. The Fermi interaction matrix element has a magnitude close to that found in dichloromethane. The analysis of the overtone spectrum of trichloroethylene is given in sec.5.31.

Haloalkanes form a class of compounds that has been subjected to many spectroscopic studies in the overtone¹²⁻¹⁸ and fundamental¹⁹⁻²¹ regions. Henry and co-workers¹² have

investigated the mass effects in the applicability of the local mode description by studying the spectra of all the dihalo-methanes upto the fourth overtone region. Fang et al¹³ measured the conventional (NIR) and thermal lens (visible) overtone spectra of di- and tri-, chloro- and bromo-, methanes and identified pure CH overtones and local-normal combination bands in the spectra. These authors reported the first observation of Fermi resonance in the overtone spectra of CHCl_3 and CHBr_3 . Henry et al¹⁴ demonstrated the use of overtone spectra for conformational analysis by studying the spectra upto the fourth overtone regions of 1, 1,2,2 tetrahalo- and pentahalo - (chloro and bromo) ethanes. Mortensen et al¹⁵ calculated the overtone spectra of the dihalo (chloro, bromo and iodo) methanes using a coupled C_{2v} model Hamiltonian (Chapter 1, sec.1.22). The observed splittings between the symmetric and antisymmetric states have been correctly explained by this model Hamiltonian. Recently Ahmed and Henry¹⁶ used the same Hamiltonian to interpret the CD overtone spectra of deuterated dihalomethanes where the coupling occurs between the CD oscillators.

We have studied¹⁸ the overtone spectra of two larger haloalkanes - 1,2 dichloro- and 1,2 dibromo-ethanes in the $\Delta v = 2-5$ regions. Pure local mode overtones, local-local combinations and local-normal combinations are observed in the spectra. We have shown that the local mode model Hamiltonian used by Mortensen et al can be used to interpret the local

mode overtones and local-local combinations in the spectra. Possible assignments of the observed local-normal combinations are also given. The analysis of the haloethane spectra is given in sec.5.32.

As explained in detail in Chapters 1 and 4, when a methyl group is subjected to anisotropic environments created by oxygen lone pair and π electron clouds the CH bonds in this methyl group become nonequivalent. The methyl group now loses its original C_{3v} symmetry. The methyl group in methanol contains two types of CH bonds and its overtone spectrum is analysed under C_s symmetry²². Thus whether a particular methyl group contains nonequivalent CH bonds or not can be identified from the structure of the overtone spectrum of the molecule. It should be pointed out that the fundamental absorption spectra are difficult to use for searching local symmetry. The various overtone spectroscopic studies on nonequivalent methyl CH bonds have already been discussed in Chapters 1 and 4. 2-butanone molecule contains two methyl groups; one adjacent to the carbonyl group and the other separated from the carbonyl by a methylene group. Fang et al²³ have compared the third and fourth overtone spectra of 2-butanone with those of acetone and acetaldehyde.

We have studied²⁴ the overtone spectrum of 2-butanone in the $\Delta V = 2-5$ regions. It is shown that the methyl group away from the carbonyl is not effected by the anisotropic

environments and that it maintains C_{3v} symmetry. The peak positions of the local mode overtones and local-local combinations calculated by the C_{3v} local mode Hamiltonian agree with the observations. The overtones of the in-plane CH_a bond and the methylene CH bonds appear as shoulders to the main peaks. The CH_b overtones coincide with the C_{3v} CH overtones. The analysis of the 2-butanone overtone spectrum is given in sec.5.33.

5.20 Experimental

The following samples are used for the experiments:- high purity trichloroethylene (99.9% extra pure AR from Sisco Research Laboratories India), high purity 1,2 dichloroethane (99.5% from Sisco Research Laboratories India), high purity 1,2 dibromoethane (99.0% from E Merck Germany), high purity 2-butanone (99.5% from Sisco Research Laboratories India) and spectrograde carbon tetrachloride (99.9% from Sisco Research Laboratories, India). The $\Delta V = 6$ overtone spectrum of trichloroethylene is recorded using the dual beam thermal lens technique described in Chapter 3. The $\Delta V = 3-5$ spectra of trichloroethylene, haloethanes and 2-butanone are recorded from pure liquids in a Hitachi - 330 UV-vis-NIR spectrophotometer. The $\Delta V = 2$ spectra of the samples are recorded from solutions in carbon tetrachloride to avoid saturation in

absorbance signals. All spectra are recorded using a path length of 1 cm and at $26 \pm 2^\circ\text{C}$.

5.30 Results and Discussion

5.31 Overtone Spectrum of Trichloroethylene

The overtone spectrum of trichloroethylene in the $\Delta v = 2-6$ regions are shown in Figs.5.1-5.5. The assignments of the peak positions are given in table 5.1.

5.31a Pure CH Overtones

Trichloroethylene molecule contains only a single CH bond (Fig.5.7) and the entire overtone spectrum appears due to the excitation of this oscillator. The $\Delta v = 2, 4, 5$ and 6 overtone peaks fit into a Birge-Sponer plot with good correlation. The $\Delta v = 3$ overtone is shifted to high energy side due to Fermi resonance (see the next section). The CH local mode parameters obtained from the above fit along with the correlation coefficient are also given in table 5.1. It is to be pointed out that the fundamental CH stretching frequency observed in trichloroethylene (3096 cm^{-1})²⁵ is close to the extrapolated value (3092 cm^{-1}) of the Birge-Sponer plot. This is due to the fact that the single CH oscillator in trichloroethylene exhibits local character even in the fundamental region due to the large separation in frequency with

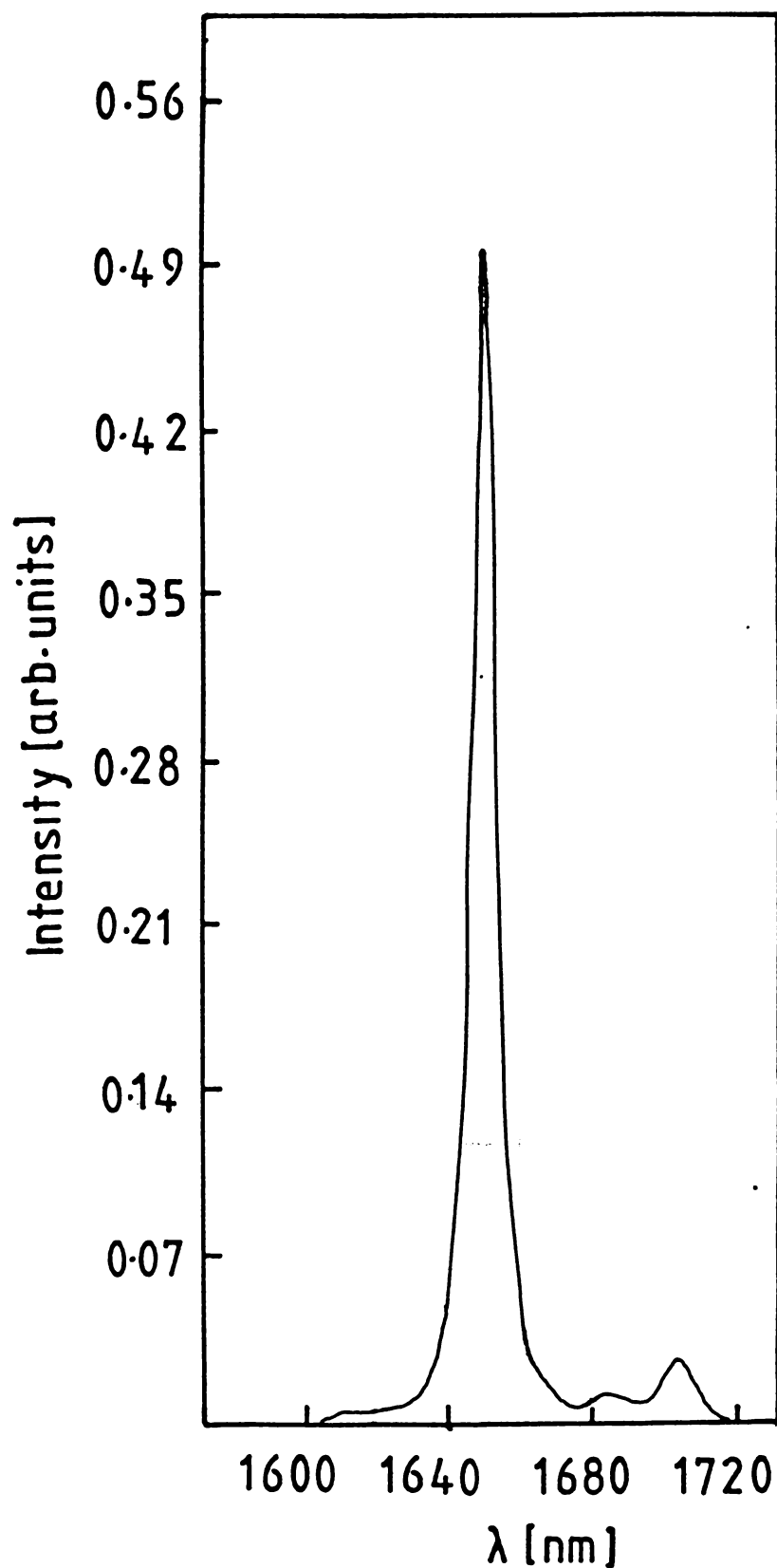


Fig.5.1 Overtone spectrum of trichloroethylene in the $\Delta V = 2$ region. Sample dissolved in carbon tetrachloride. Reference - carbon tetrachloride.

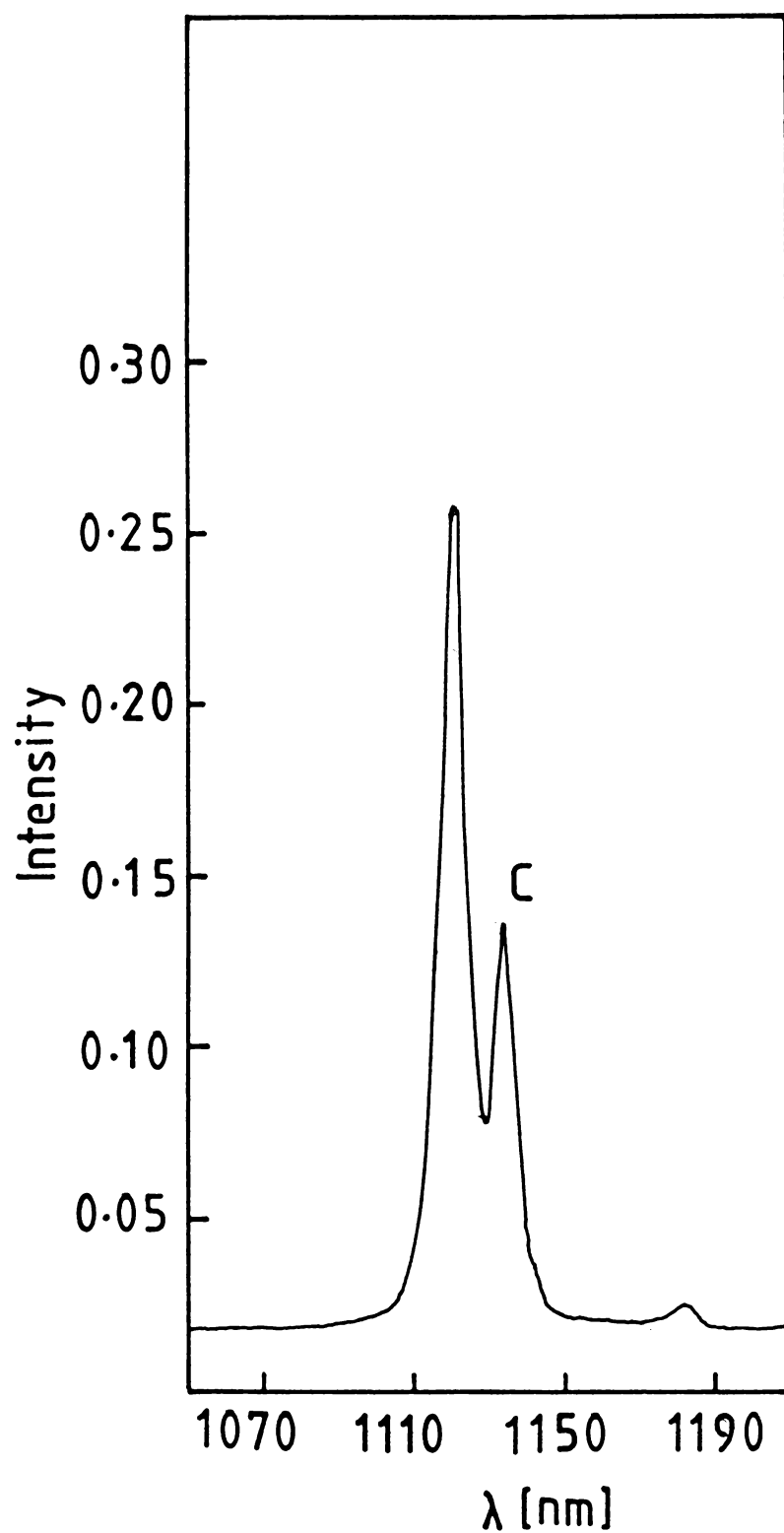


Fig.5.2 Overtone spectrum of trichloroethylene in the $\Delta v = 3$ region. Pure liquid; Reference - air.

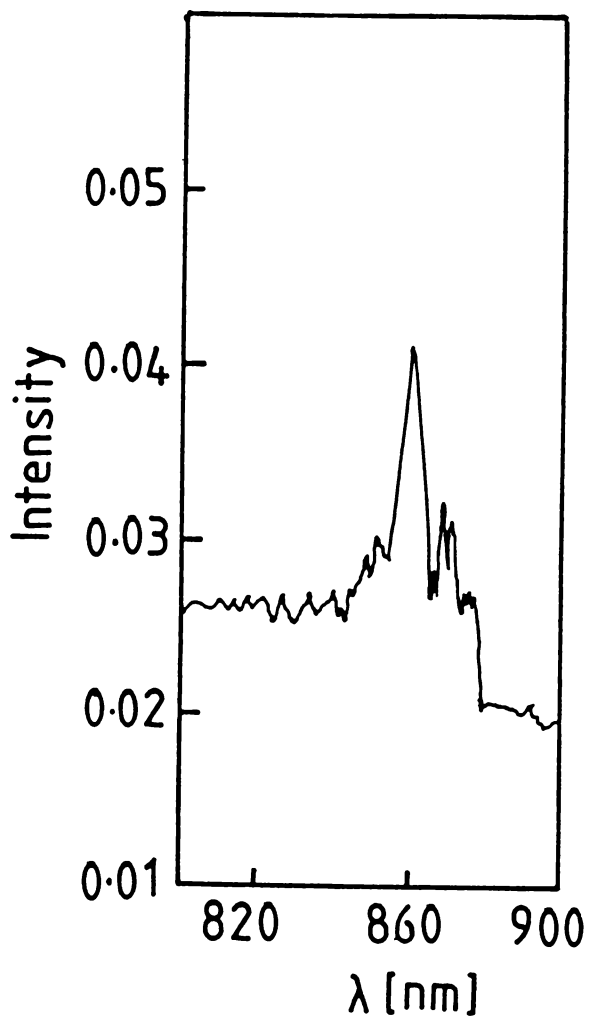


Fig.5.3 Overtone spectrum of trichloroethylene in the $\Delta V = 4$ region. Pure liquid; Reference - air.

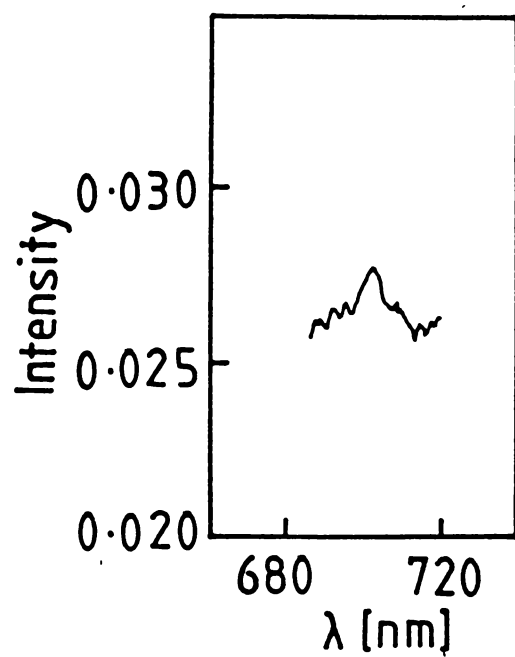


Fig.5.4 Overtone spectrum of trichloroethylene in the $\Delta v = 5$ region. Pure liquid; Reference - air.

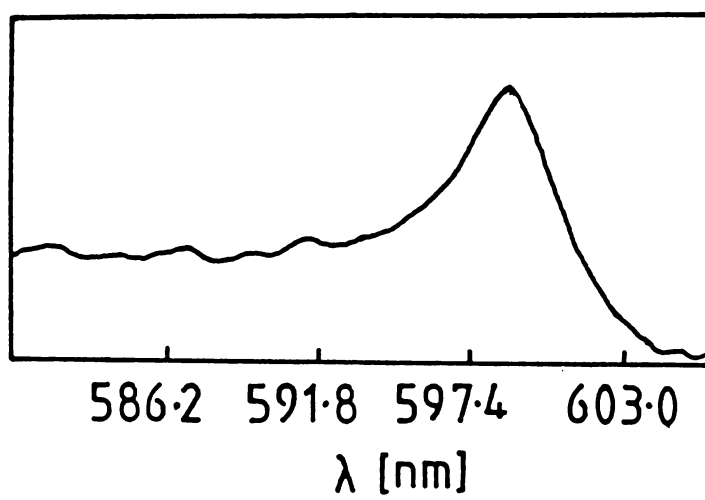


Fig.5.5 Overtone spectrum of trichloroethylene in the $\Delta v = 6$ region recorded by the dual beam thermal lens technique. Pure liquid.

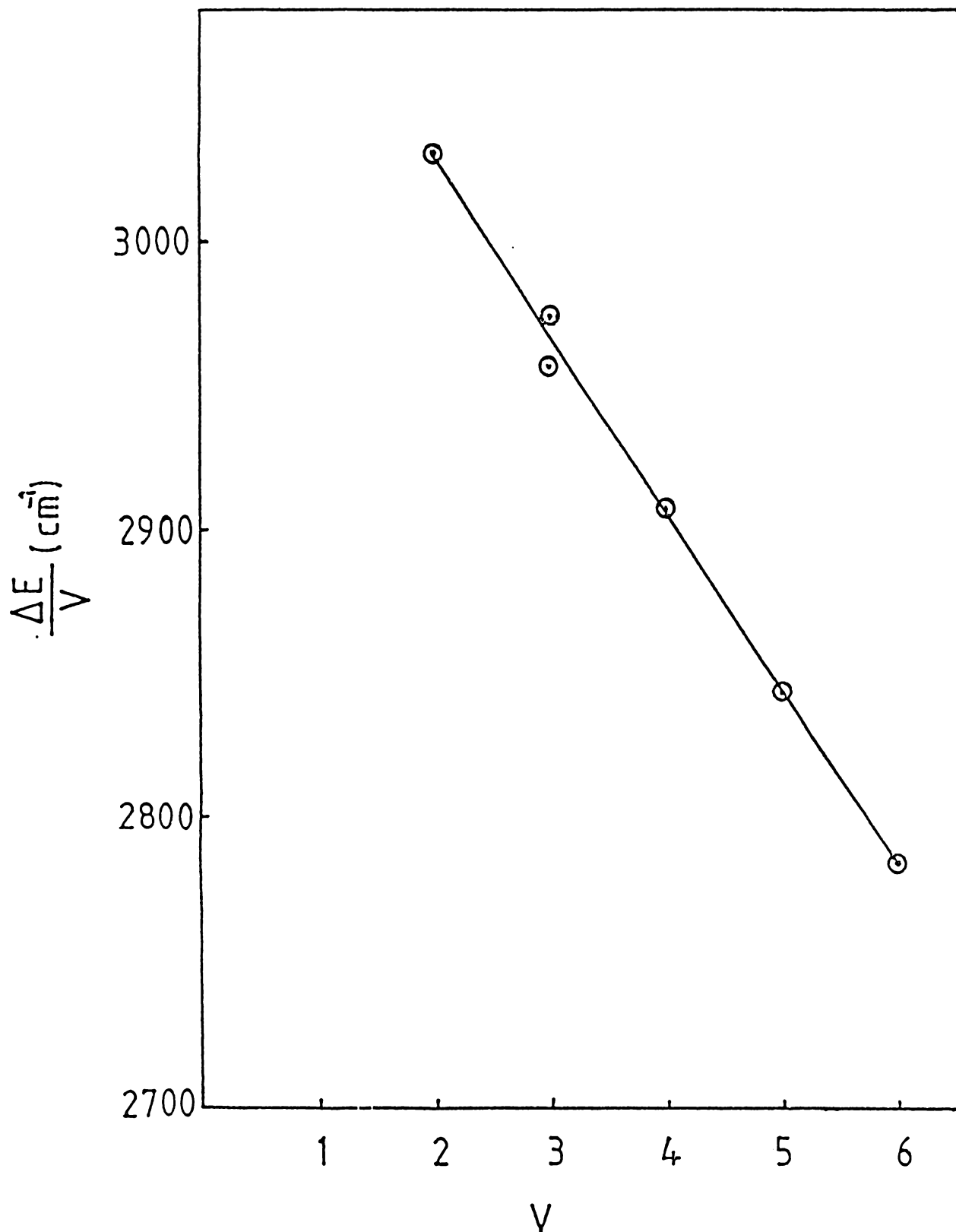


Fig.5.6 Birge-Sponer plot of overtone energies in trichloroethylene. The $\Delta V = 3$ region shows Fermi shifted pure overtone (upper point) and combination (lower point) states.

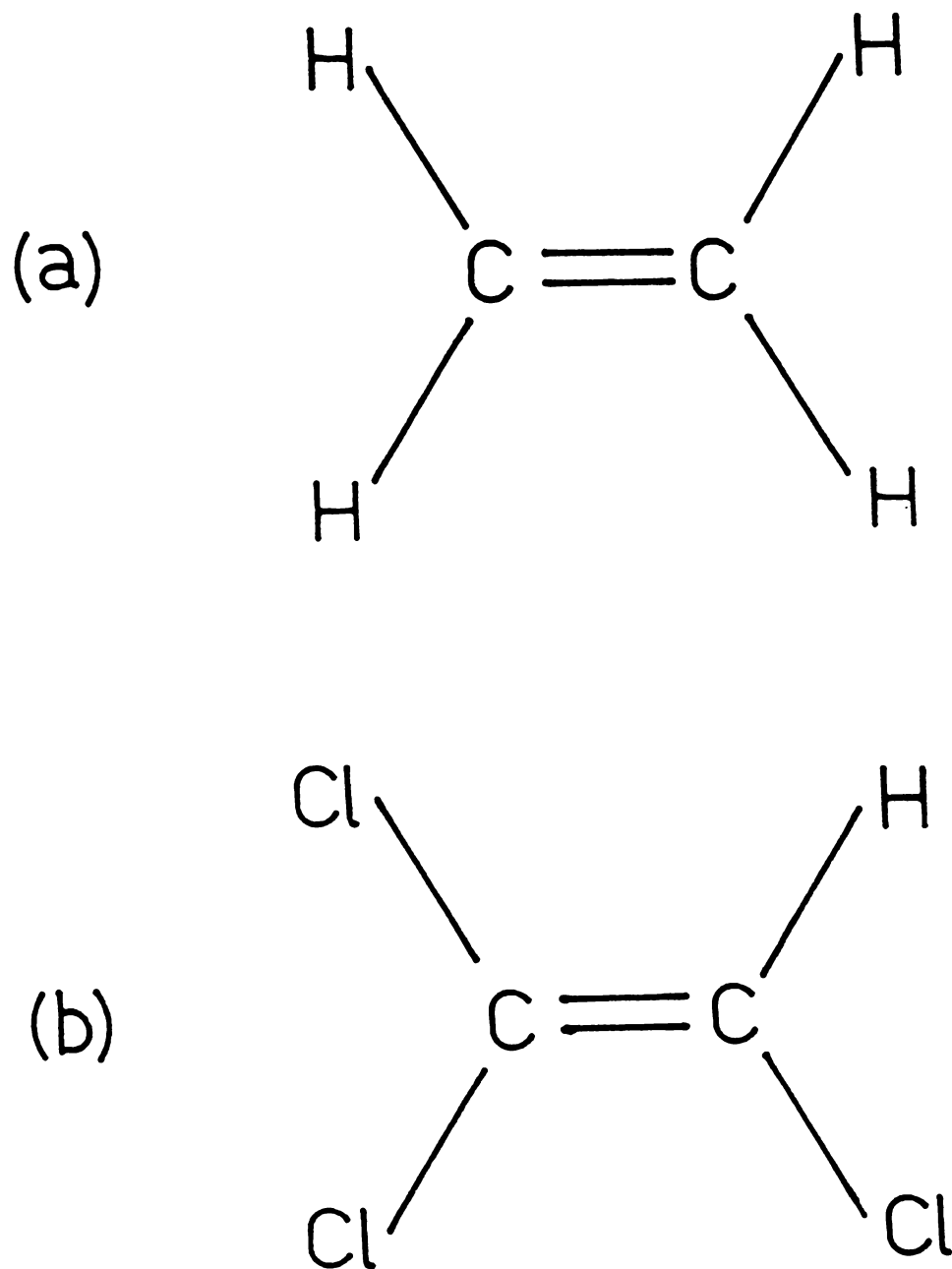


Fig.5.7 Molecular structure of (a) ethylene
(b) trichloroethylene.

Table 5.1

Observed peak positions and Assignment of
Overtone Spectrum of Trichloroethylene.

The local mode parameters are:

$$\omega = 3216 \pm 5 \text{ cm}^{-1} \text{ and}$$

$$-\omega x = -62 \pm 1.5 \text{ cm}^{-1} \text{ with correlation } \gamma = -0.99963$$

Peak position (cm^{-1})	Assignment
5872	Combination
5938	Combination
6061	$\Delta v_s = 2$ overtone
8460	Combination
8811	Combination*
8921	$\Delta v_s = 3$ overtone*
11628	$\Delta v_s = 4$ overtone
14224	$\Delta v_s = 5$ overtone
16700	$\Delta v_s = 6$ overtone

* Fermi shifted positions.

other vibrations. The local mode parameters of ethylene are not available in literature and hence a comparison could not be made. However the fifth CH overtone data of ethylene is available²⁶ and a comparison shows that the fifth overtone of trichloroethylene is blue shifted with respect to ethylene by 150 cm^{-1} . Since the anharmonicity of the CH bond is not expected to vary upon halogen substitution²⁷ the blue shift in the overtone energy clearly indicates an increase in the mechanical frequency and hence a decrease in the CH bond length. The correlation between fifth overtone energy and CH bond length given in by Wong and Moore²⁶ reads

$$r_{\text{CH}}^{\text{LM } \circ} (\text{A}) = (1.328 \pm 0.024) - \frac{\nu_{v=6} (\text{cm}^{-1})}{(69160 \pm 690)} \quad (5.1)$$

Even though there is considerable scatter in the data used to deduce the above equation, Wong and Moore have demonstrated that small changes in the CH bond length can be well predicted from the observed changes in overtone energy. A change of 0.001 \AA on CH bond length causes only a shift of $\sim 10 \text{ cm}^{-1}$ in the fundamental but a shift of $\sim 70 \text{ cm}^{-1}$ in the fifth overtone region. The above correlation predicts that the CH bond length in trichloroethylene is $\sim 0.002 \text{ \AA}$ smaller than that in ethylene. However to the author's knowledge, no experimental data is available on the CH bond length of trichloroethylene and hence we could not verify the result predicted by the overtone data.

Earlier infrared studies by McKean on fundamental isolated CH stretching frequencies in various halogenated ethylenes²⁸ have shown that halogen substitution generally increases the isolated CH stretching frequency. McKean has analyzed the observations by considering cis, trans and α effects of the C-X (X = F, Cl, Br, I) defined as the difference between $\nu_{\text{CH}}^{\text{iso}}$ in the cis trans and α positions relative to the halogen and the value of $\nu_{\text{CH}}^{\text{iso}}$ in ethylene. The cis, trans and α effects are shown to be almost additive. Among the halogens, fluorine behaves somewhat anomalously due to the increased trans effect of lone pairs. The substituent S values²⁸ of F and Cl show that cis and trans effects for chlorine are almost equal and the α effect is slightly higher, whereas for fluorine the trans effect is much larger than the cis and α effects. It is thus clear that the trans effect of lone pairs is not dominant for chlorine substitution. We can therefore conclude that the major effect of chlorine substitution in ethylene is similar to the effect of halogen substitution on methane²⁹ and benzene (Chapter 4). The blue shift in the CH fundamental frequencies in halomethanes with respect to methane is interpreted as due to the electron withdrawing property (-I effect) of halogens arising from their electronegativity. The halogen atoms reduce the electron density at the CH carbon atom which in turn result in an attraction of the valence cloud of the hydrogen atom towards the carbon

atom. This results in a decrease in CH bond length and an increase in CH mechanical frequency.

5.31b Fermi Resonance in the $\Delta V = 3$ Region

The CH overtone transitions $\Delta V = 2, 4, 5$ and 6 perfectly fit into a Birge-Sponer plot. The $\Delta V = 3$ overtone energy deviates from the Birge-Sponer plot (Fig.5.6) due to the Fermi resonance with a combination band involving two quanta of CH stretch and two quanta of CH bend (see below). In the $\Delta V = 2$ region, the combination band is well separated from the pure overtone (Fig.5.2) and thus level matching does not occur. We could not observe the combination band in the $\Delta V = 4$ region due to the poor signal to noise ratio of the spectrophotometer in that region. However the perfect Birge-Sponer fit (Fig.5.6) obtained for $\Delta V = 2, 4, 5$ and 6 transition energies indicates that these levels are not affected by Fermi resonance and the effect is dominant only in the $\Delta V = 3$ region. Recent high resolution studies^{1,2} have shown that the Fermi interactions between overtone and combination states involve all the states with a common chromophore quantum number. However with the present low resolution liquid-phase spectrum, the interactions can be approximated to a two level case. The perturbed energies are then given by³⁰

$$E_{\pm} = E_{12}^0 \pm \frac{1}{2} (4W_{12}^2 + \delta^2)^{\frac{1}{2}} \quad (5.2)$$

where the subscripts 1 and 2 are used for $|3_s\rangle$ and $|2_s, 2_b\rangle$ states, E_{12}° is the average energy of the unperturbed levels, W_{12} is the off-diagonal Fermi interaction matrix element and δ is the difference ($E_1^{\circ} - E_2^{\circ}$) of the unperturbed (zero order) energies. Following the method used by Perry et al³, the zero order pure overtone energy of $\Delta V = 3$ is obtained by extrapolation of the Birge-Sponer plot. The Fermi resonance shift is the difference between the observed and the extrapolated values. Since the Fermi shifts are equal for a two level interaction, we can use the shift obtained by the extrapolation to correct the observed energy of $|2_s, 2_b\rangle$ to get the zero order energy of this state. With the knowledge of the two zero order energies the Fermi interaction matrix element is calculated from eqn.5.2. This yields a value of 37.5 cm^{-1} for the magnitude of the matrix element. This value is comparable to the stretch-bend Fermi interaction matrix element observed in dichloromethane (33 cm^{-1}).¹⁷

The method followed here helps in identifying the normal mode involved in the Fermi interaction. The zero order energy of the combination band obtained above is 8826.6 cm^{-1} . Since the anharmonicity of the low frequency mode is expected to be small, the above value must be close to the energy of the $\Delta V = 2$ pure overtone plus two quanta of the low frequency motion. This yields $2\nu_b \sim 2765.5 \text{ cm}^{-1}$, ie., $\nu_b \sim 1383 \text{ cm}^{-1}$.

This is close to the value of CH deformation frequency (1385 cm^{-1}) observed in trichloroethylene²⁵. At this point if we assume that the low frequency motion involved in the Fermi resonance interaction is C=C stretch i.e., the Fermi resonance is between $\Delta V = 3$ pure CH overtone and $\Delta V = 2 + 2 \nu_{\text{C=C}}$ combination ($\nu_{\text{C=C}} = 1590 \text{ cm}^{-1}$) as is in the case of cyclobutene⁵, we will get the result that the off-diagonal anharmonicity constant is $> 100 \text{ cm}^{-1}$, and if we assume that the combination band involved is $\Delta V = 2 + \nu_{\text{C=C}} + \delta_{\text{CH}}$, we will get the result that the off-diagonal anharmonicity constant is $> 50 \text{ cm}^{-1}$. Since such high values are not observed for the cross anharmonicity constants, we can conclude that the low frequency motion involved in the Fermi resonance is the CH deformation mode. Also the diagonal bending anharmonicity and the off-diagonal stretch-bend anharmonicity are negligibly small.

The reason for the occurrence of the Fermi resonance only in the $\Delta V = 3$ region is now evident. The diagonal CH stretching anharmonicity constant causes significant harmonic suppression of the pure overtone energies. A nonzero stretch-bend anharmonicity constant (which is found negative in most cases) will cause similar suppression in the combination band energy. The net effect is the occurrence of a slow tuning of the combination energy over the overtone energy and this Fermi

interaction occurs for a few quantum levels³. In the present case of trichloroethylene the absence of off-diagonal anharmonicity causes larger separation of the two bands with change in quantum number and the energy matching occurs only at the $\Delta V = 3$ region. In other words, the tuning becomes faster. This observation again confirms our conclusion that the stretching state in Fermi coupled to combination involving two quanta of CH deformation mode rather than those involving $2 \nu_{C=C}$ or $(\nu_{C=C} + \delta_{CH})$. The wave functions for the mixed states are^{3,30}

$$\begin{aligned}
 |\psi^+\rangle &= \alpha |3_s\rangle + \sigma \beta |2_s, 2_b\rangle \\
 |\psi^-\rangle &= -\sigma \beta |3_s\rangle + \alpha |2_s, 2_b\rangle
 \end{aligned}
 \tag{5.3}$$

where σ is the sign of W_{12} (which cannot be determined from spectroscopic data¹⁻³) and the coefficient α and β are given by

$$\alpha = \left(\frac{\Gamma + \delta}{2} \right)^{\frac{1}{2}}
 \tag{5.4}$$

$$\beta = \left(\frac{\Gamma - \delta}{2} \right)^{\frac{1}{2}}$$

where $\Gamma = (4 W_{12}^2 + \delta^2)^{\frac{1}{2}}$ (5.5)

and $\alpha^2 + \beta^2 = 1$ (5.6)

The ratio of the intensities is given by

$$\frac{I_+}{I_-} = \frac{\alpha^2}{\beta^2} \quad (5.7)$$

In the present case of trichloroethylene the above relations yield $\alpha^2 = 0.87$; $\beta^2 = 0.13$.

Thus $I_+/I_- \simeq 6.7$.

The $\Delta V = 3$ spectrum clearly shows that $I_+ > I_-$.

However a measurement of the integrated intensities of the two bands is not attempted.

5.32 Overtone Spectra of 1,2 Dichloro- and Dibromo-Ethanes

The overtone spectra of 1,2 dichloro- and dibromoethanes in the $\Delta V = 2-5$ regions are shown in Figs.5.8-5.13. The spectra show pure local mode overtones, local-local combinations and local-normal combinations. The peak positions of the bands and their assignments are given in table 5.2.

5.32a Pure CH Local Mode Overtones and Local-Local Combinations

The vibrational overtone spectra of 1,2 dichloroethanes can be analysed using local mode picture and kinetic and potential energy coupling between CH oscillators attached to a common carbon atom. For interpreting the overtone spectra

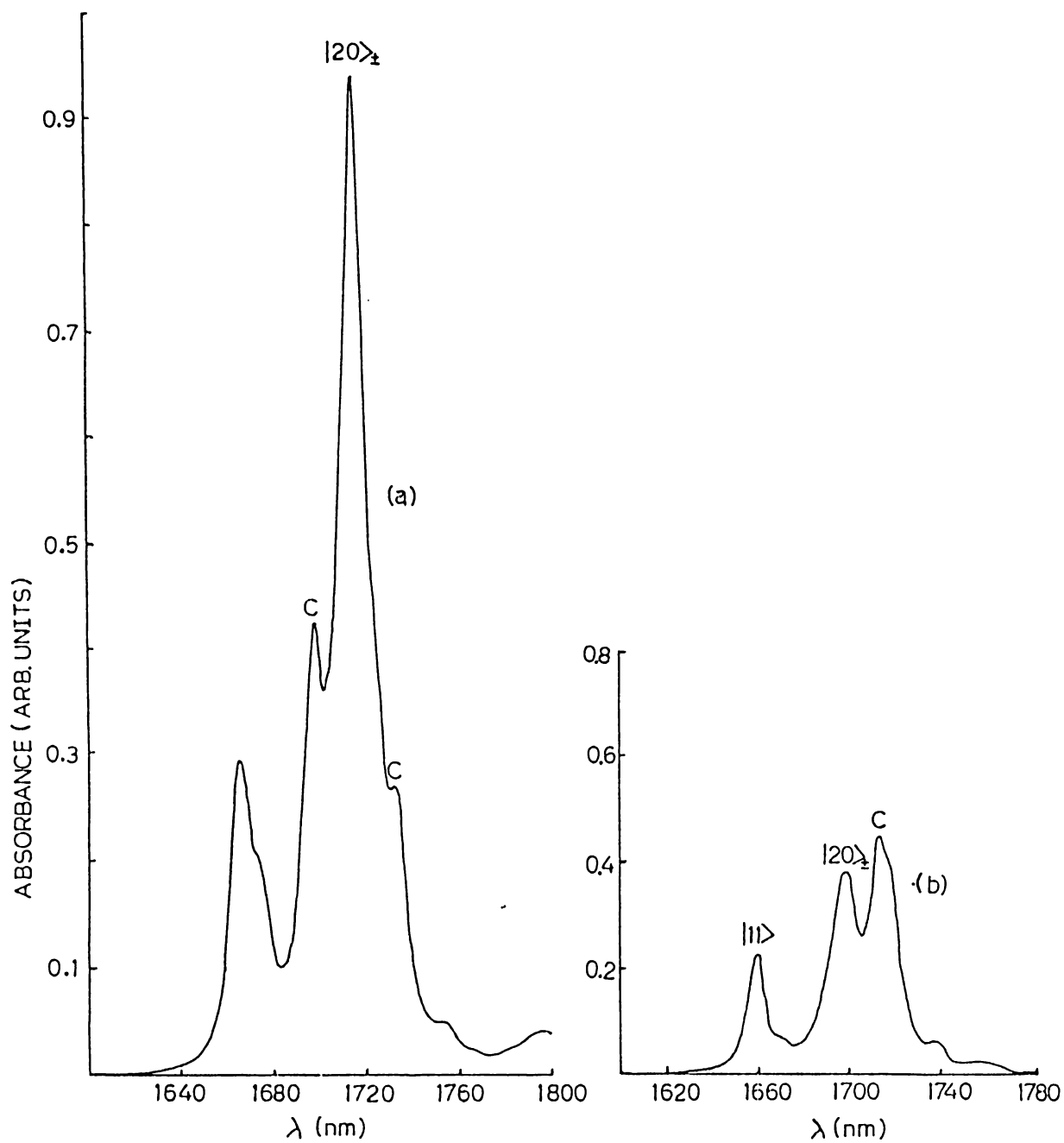


Fig.5.8 Overtone spectrum of (a) 1,2 dichloroethane and (b) 1,2 dibromoethane in the $\Delta v = 2$ region. Compounds dissolved in carbon tetrachloride; Reference - carbon tetrachloride.

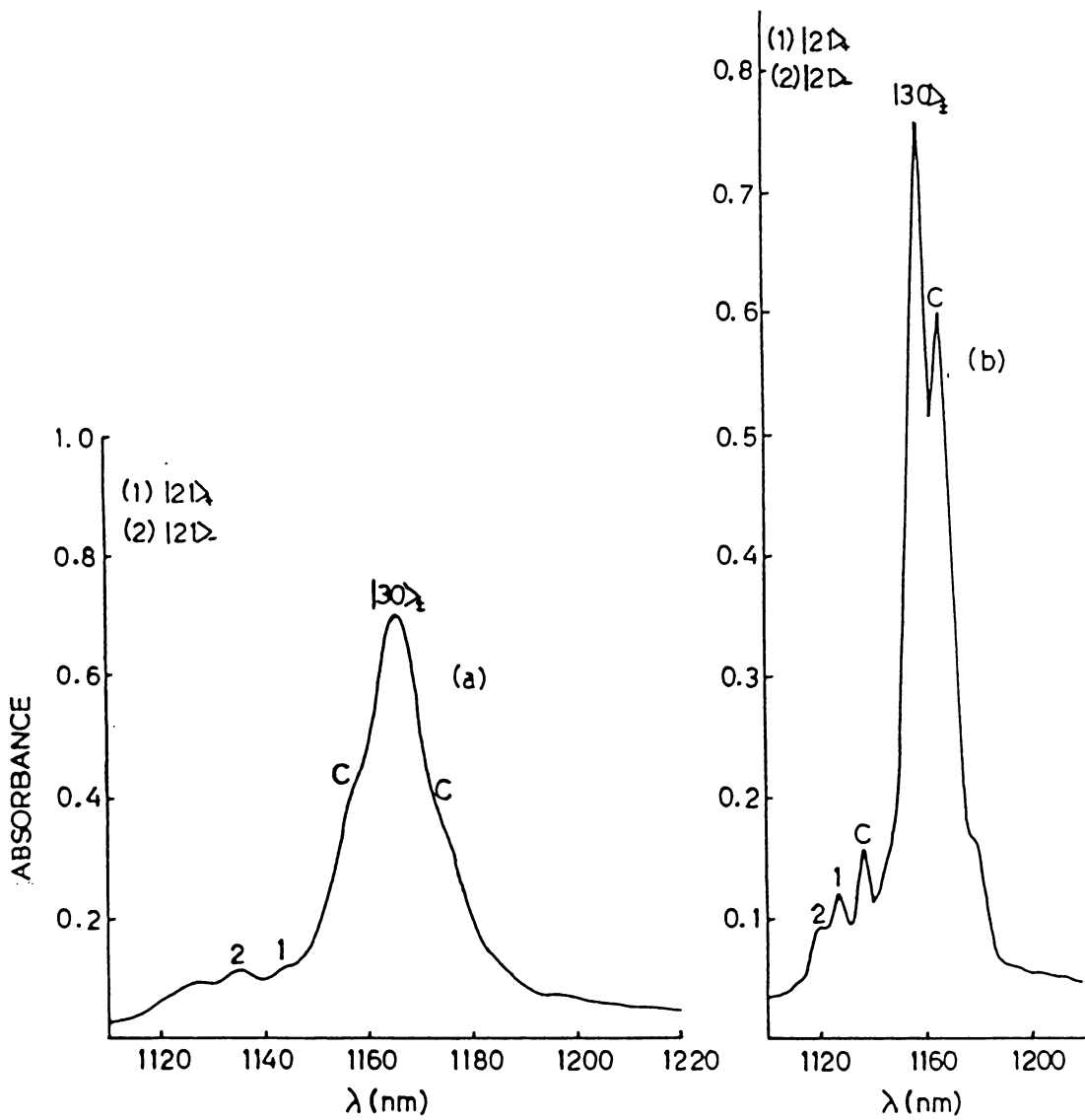


Fig.5.9 Overtone spectrum of (a) 1,2 dichloroethane and (b) 1,2 dibromoethane in the $\Delta V = 3$ region. Pure liquids; Reference - air.

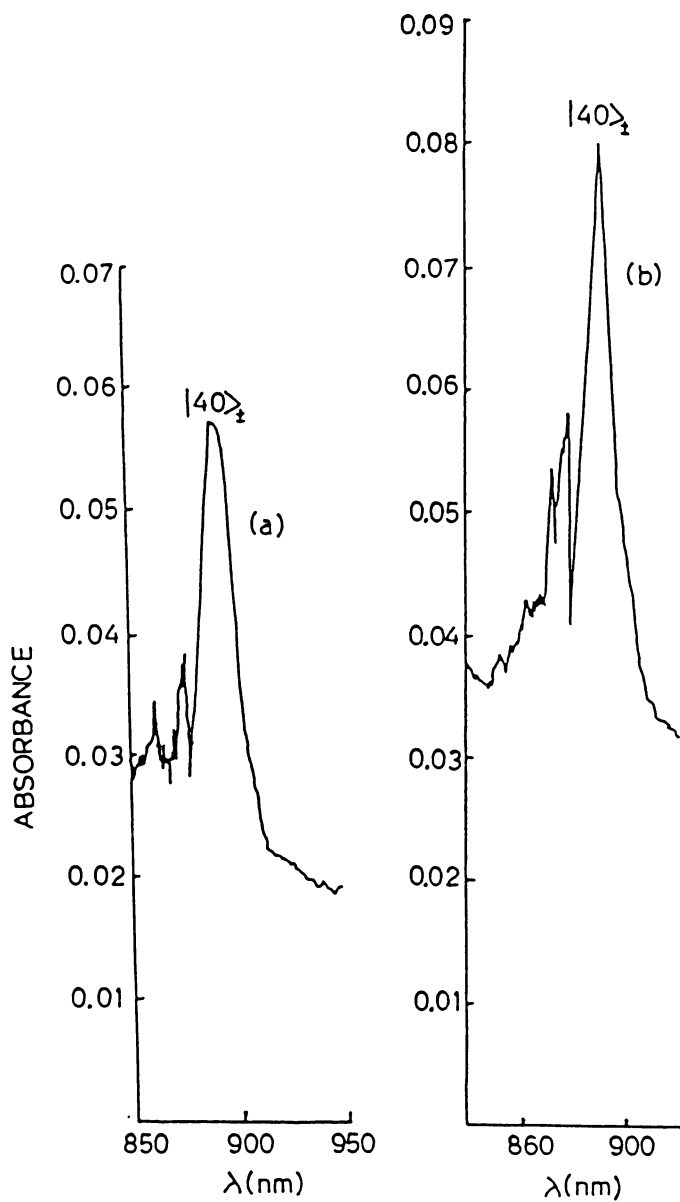


Fig.5.10 Overtone spectrum of (a) 1,2 dichloroethane and (b) 1,2 dibromoethane in the $\Delta v = 4$ region. Pure liquids; Reference - air.

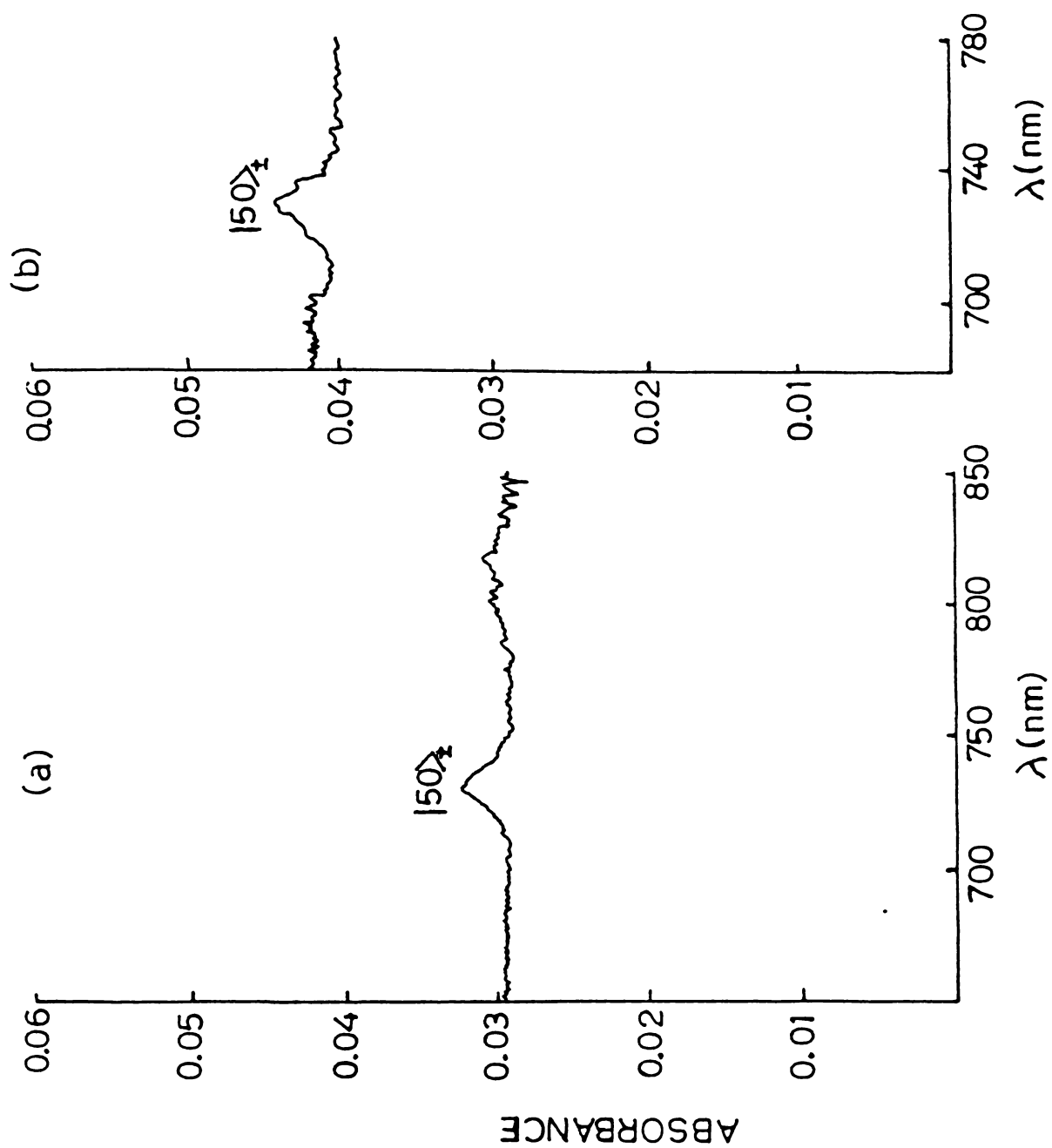


Fig.5.11 Overtone spectrum of (a) 1,2 dichloroethane and (b) 1,2 dibromoethane in the $\Delta V = 5$ region. Pure liquids; Reference - air.

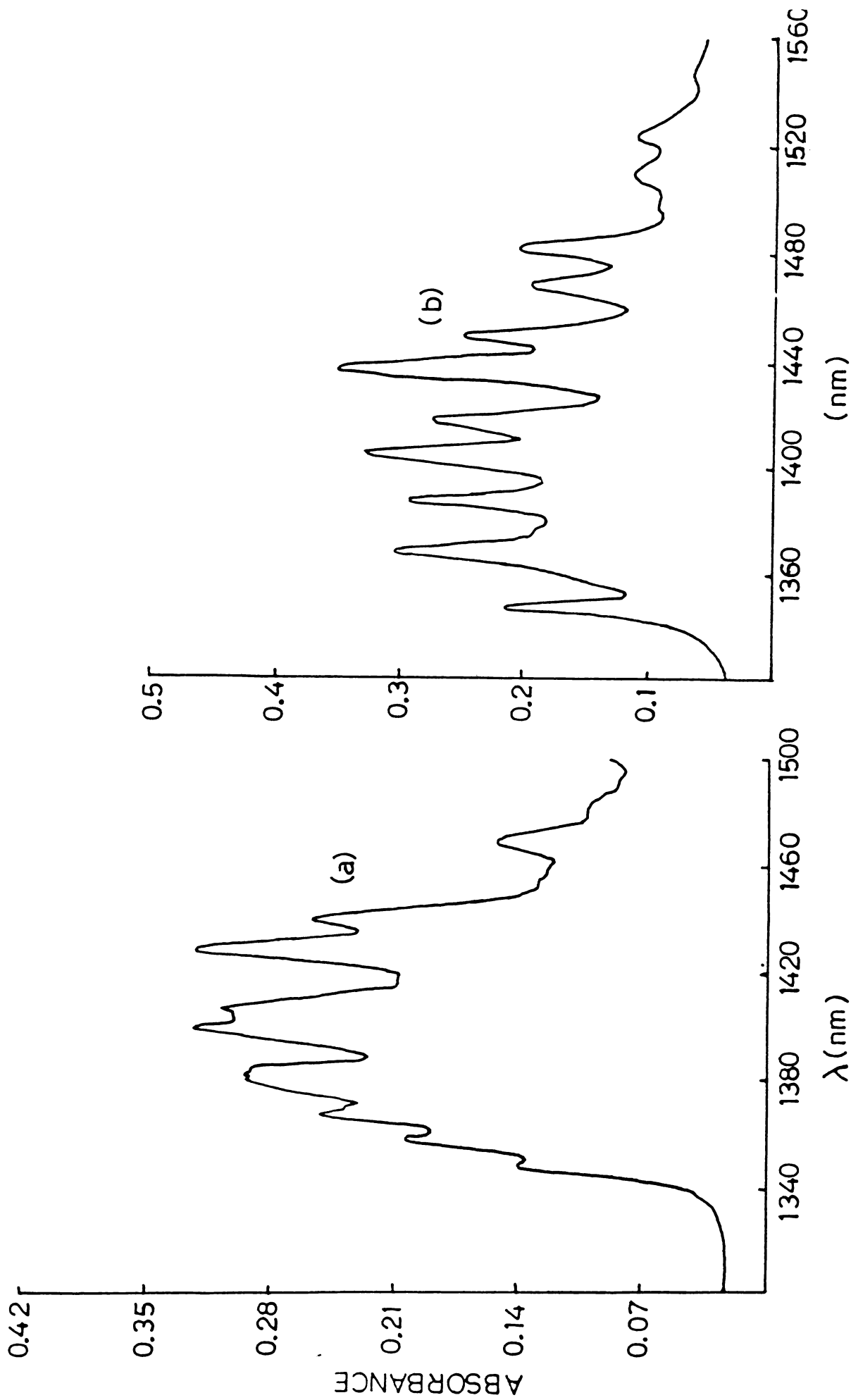


Fig.5.12 Local-Normal combination structure of (a) 1,2 dichloroethane and (b) 1,2 dibromoethane involving $\Delta V = 2$ plus one low frequency quantum. Pure liquids; Reference - air.

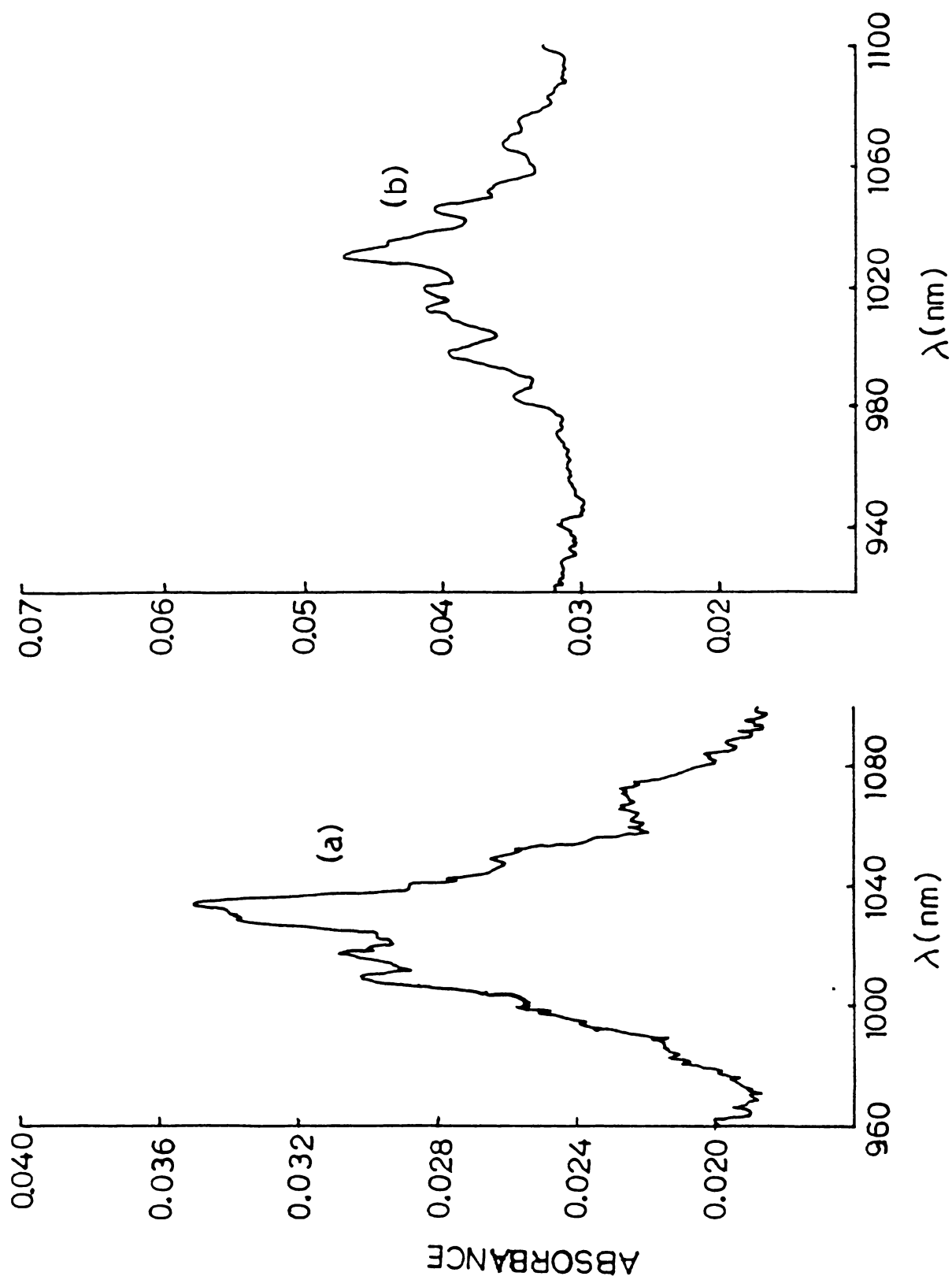


Fig.5.13 Local-Normal combination structure of (a) 1,2 dichloroethane, and (b) 1,2 dibromoethane involving $\Delta V = 3$ plus one low frequency quantum. Pure liquids; Reference - air.

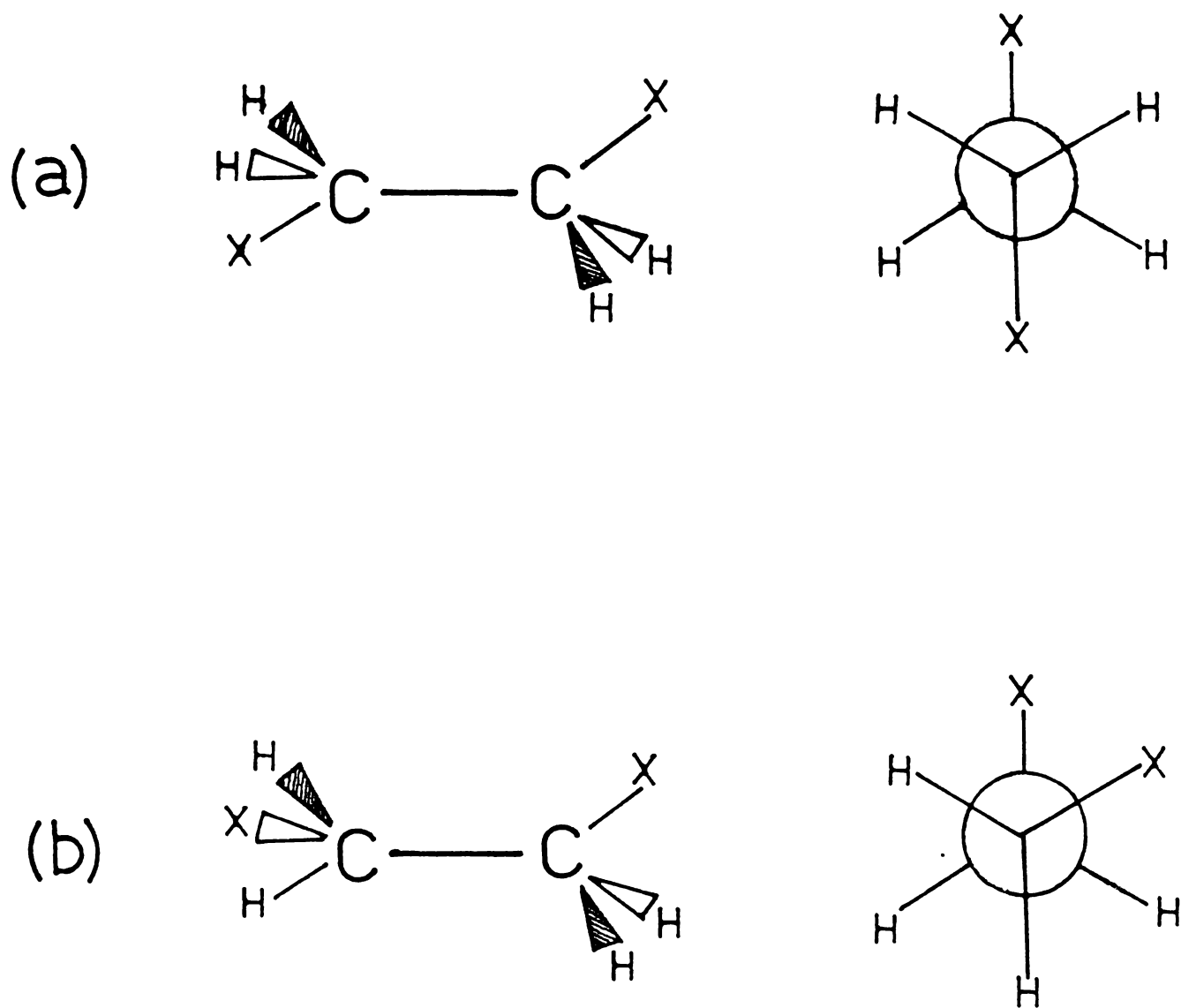


Fig.5.14 Structure of 1,2 dihaloethanes (a) trans conformation and (b) gauche conformation with corresponding Newmann projections.

Table 5.2

Vibrational peak assignments for dihaloethanes

CH ₂ Cl-CH ₂ Cl		CH ₂ Br-CH ₂ Br	
Peak position (cm ⁻¹)	Assignment	Peak position (cm ⁻¹)	Assignment
(1)	(2)	(3)	(4)
5764	$ 10\rangle_{\pm} + 2\nu'_2, 2\nu'_{15}(C)$	5841	$ 10\rangle_{\pm} + 2\nu_2, 2\nu'_2, 2\nu_{15}, 2\nu'_{15}(C)$
5814	$ 20\rangle_{\pm}$	5893	$ 20\rangle_{\pm}$
5874	$ 10\rangle_{\pm} + 2\nu_2, 2\nu_{15}$	6028	$ 11\rangle$
5988	?	6477	$ 20\rangle_{\pm} + \nu_{17}, \nu'_{17}$
6803	$ 20\rangle_{\pm} + \nu_{13}$	6575	$ 20\rangle_{\pm} + (\nu_3 - \nu_{17})$
6944	$ 20\rangle_{\pm} + \nu_8$	6640	$ 20\rangle_{\pm} + \nu_9$
6993	$ 20\rangle_{\pm} + \nu'_8$	6557	$ 20\rangle_{\pm} + \nu'_9$
7105	$ 20\rangle_{\pm} + \nu_3, \nu'_{16}$	6826	$ 20\rangle_{\pm} + \nu_{13}$
7143	$ 20\rangle_{\pm} + \nu'_8 + \nu'_{10}$	6911	$ 20\rangle_{\pm} + \nu_4, \nu'_4$
7233	$ 20\rangle_{\pm} + \nu'_2 + \nu'_{15}$	6969	$ 20\rangle_{\pm} + \nu_8$

(1)	(2)	(3)	(4)
7313	$ 20\rangle_{\pm} + 2\nu_5$	7062	$ 20\rangle_{\pm} + \nu'_8$
7360	$ 20\rangle_{\pm} + \nu'_{13} + \nu'_{17}$	7128	$ 20\rangle_{\pm} + \nu_3, \nu'_{16}$
7414	$ 20\rangle_{\pm} + \nu'_5 + \nu'_9$	7215	$ 20\rangle_{\pm} + 2\nu_5$
8574	$ 30\rangle_{\pm}$	7321	$ 20\rangle_{\pm} + \nu_2, \nu'_{15}, \nu'_2, \nu'_{15}$
8734	$ 21\rangle_+$	7429	?
8818	$ 21\rangle_-$	8576	$ 20\rangle_{\pm} + 2\nu'_2, 2\nu'_{15}(c)$
8869	?	8628	$ 30\rangle_{\pm}$
9547	$ 30\rangle_{\pm} + \nu_{13}$	8803	$ 20\rangle_{\pm} + 2\nu_2, 2\nu_{15}(c)$
9685	$ 30\rangle_{\pm} + \nu_8$	8873	$ 21\rangle_+$
9756	$ 30\rangle_{\pm} + \nu'_8$	8937	$ 21\rangle_-$
9852	$ 30\rangle_{\pm} + \nu_3, \nu'_{16}$	9294	$ 30\rangle_{\pm} + (\nu_3 - \nu_{17})$
9901	$ 30\rangle_{\pm} + \nu'_8 + \nu'_{10}$	9363	$ 30\rangle_{\pm} + \nu_9$

(1)	(2)	(3)	(4)
11220	$ 40\rangle_{\pm}$	9488	$ 30\rangle_{\pm} + \nu'_9$
13746	$ 50\rangle_{\pm}$	9551	$ 30\rangle_{\pm} + \nu'_{13}$
		9653	$ 30\rangle_{\pm} + \nu'_4, \nu'_4$
		9699	$ 30\rangle_{\pm} + \nu'_8$
		9804	$ 30\rangle_{\pm} + \nu'_8$
		9862	$ 30\rangle_{\pm} + \nu'_3, \nu'_{16}$
		10020	$ 30\rangle_{\pm} + \nu'_2, \nu'_{15}, \nu'_2, \nu'_{15}$
		10162	?
		10288	?
		10616	?
		11223	$ 40\rangle_{\pm}$
		13699	$ 50\rangle_{\pm}$

of 1,2 dihaloethanes the molecular configuration can be regarded as two dynamically independent CH_2X ($\text{X} = \text{Cl}, \text{Br}$) fragments. Such an approach has been adopted for the normal mode analysis of all the dihaloethanes¹⁹. The assumption is again justified by the successful local mode analysis of neopentane³¹ where the CH_3 groups are assumed to be independent. Under this assumption the mode of analyzing the overtone spectra will be the same as in dihalomethanes¹⁵. As already explained in Chapter 1, the C_{2v} model Hamiltonian is used for calculating the spectra. The Hamiltonian is the $N = 2$ version of equation 1.10 i.e.,

$$\begin{aligned}
 H = \omega (V_1 + V_2) - \omega x (V_1^2 + V_2^2 + V_1 + V_2) \\
 + \omega \gamma (a_1^+ - a_1) (a_2^+ - a_2) + \omega \delta (a_1^+ + a_1) (a_2^+ + a_2)
 \end{aligned}
 \tag{5.8}$$

The calculation of overtone energies is performed by neglecting inter-manifold couplings (i.e., the coupling between the states with different values of the total quantum number) and taking into account only the intra-manifold couplings, and under ladder approximation (Chapter 1). The Hamiltonian matrices are given in Chapter 1. In the absence of coupling the Hamiltonian (5.8) reduces to pure local mode Hamiltonian in which case the states $|v_0\rangle$ and $|0v\rangle$ are degenerate. The spectroscopic energies are then given by the Birge-Sponer relation, (eqn.1), which for convenience is now written in the form

$$\Delta E_{v,0} = \omega [v - x(v^2 + v)]
 \tag{5.9}$$

In the presence of coupling the states become the symmetric and antisymmetric types $|v_0\rangle_{\pm} = \frac{1}{\sqrt{2}} (|v_0\rangle \pm |0v\rangle)$, where the degeneracy between $|v_0\rangle$ and $|0v\rangle$ is lifted.

From the Birge-Sponer plot of $\frac{\Delta E_{v,0}}{v}$ versus v , where $\Delta E_{v,0}$ is the average of $\Delta E_{(v,0)+}$ and $\Delta E_{(v,0)-}$ transition energies, the local mode parameters ω and x are obtained. The least square local mode parameters obtained are given in table 5.3. It is known that at room temperature about 80% of 1,2 dichloro- and dibromo-ethanes exist in the trans conformation³² (Fig.5.14). Overtone spectroscopy when used for conformational analysis¹⁴ shows that the peak positions for trans conformers obtained by deconvolution of the spectra deviate very little from the observed peak positions. Thus we take the average of trans A_g and trans B_u CH stretch fundamental frequencies as the value of the transition energy for $\Delta E_{(1,0)+}$ and the average of trans A_u and trans B_g CH stretch fundamental frequencies as the value of the transition energy for $\Delta E_{(1,0)-}$. The fundamental CH stretching frequencies of 1,2 dichloroethane and 1,2 dibromoethane are taken from the work of Nakagawa et al³³ and Tanabe et al²⁰ respectively. This gives $\Delta E_{(1,0)+} = 2960 \text{ cm}^{-1}$ and $\Delta E_{(1,0)-} = 3005 \text{ cm}^{-1}$ for 1,2 dichloroethane and $\Delta E_{(1,0)+} = 2971 \text{ cm}^{-1}$ and $\Delta E_{(1,0)-} = 3022.5 \text{ cm}^{-1}$ for 1,2 dibromoethane. The splitting

between the $|10\rangle_+$ and $|1,0\rangle_-$ transitions in related to the kinetic and potential coupling parameters through

$$\Delta E_{(1,0)_-} - \Delta E_{(1,0)_+} = 2(\gamma - \phi) \omega \quad (5.10)$$

This gives values of 0.0073 and 0.0082 for $(\gamma - \phi)$ for 1,2 dichloro- and 1,2 dibromo-ethanes respectively. All the parameters necessary for calculating the overtone spectra are now available and the diagonalization of the Hamiltonian matrices (table 1.1) gives the pure local mode overtone and local-local combination structure of the two molecules.

The calculated and observed values of the peak positions of the pure local mode overtones and local-local combinations are given in table 5.3. The calculated values are in good agreement with the observations. It is seen from the spectra that the pure local mode overtones show single peaks instead of two split peaks expected from theory. This is due to the fact that the oscillator coupling constant $(\gamma - \phi)$ is small for 1,2 dihaloethanes compared to dihalomethanes¹⁵. Consequently the calculated spectra also show that the energy separation between symmetric and antisymmetric overtone states are small compared to those in dihalomethanes. A similar situation occurs in the CH_2D_2 overtone spectrum reported by Perry et al³ where the $|60\rangle_+$ band is observed as

Table 5.3

Observed and calculated local mode spectra
of 1,2 dihaloethanes

For 1,2 dichloroethane $\omega = 3067 \pm 4.3 \text{ cm}^{-1}$,
 $x = 0.0172 \pm 0.0007$ with correlation -0.999558 .

For 1,2 dibromoethane $\omega = 3152.7 \pm 4.2 \text{ cm}^{-1}$,
 $x = 0.0219 \pm 0.0005$ with correlation -0.999874 .

State	CH ₂ Cl-CH ₂ Cl		CH ₂ Br-CH ₂ Br	
	Observed (cm ⁻¹)	Calculated (cm ⁻¹)	Observed (cm ⁻¹)	Calculated (cm ⁻¹)
$ 10\rangle_+$	2960	2960	2971	2971
$ 10\rangle_-$	3005	3005	3022.5	3022.5
$ 20\rangle_+$	5814	5801	5893	5874
$ 20\rangle_-$	5814	5818	5893	5891
$ 11\rangle$	--	5939	6028	6046
$ 30\rangle_+$	8574	8559	8628	8621
$ 30\rangle_-$	8574	8562	8628	8621
$ 21\rangle_+$	8734	8743	8873	8863
$ 21\rangle_-$	8818	8829	8937	8963
$ 40\rangle_{\pm}$	11220	11206	11223	11223
$ 31\rangle_+$	--	11495	--	11605
$ 31\rangle_-$	--	11535	--	11650
$ 22\rangle$	--	11676	--	11827
$ 50\rangle_{\pm}$	13746	13746	13699	13686

a single peak. For the combination bands $|21\rangle_+$ and $|21\rangle_-$ of 1,2 dichloroethane, since their separation is large two distinct peaks are observed and these peaks agree well with calculations. The $|11\rangle$ band is not observed for 1,2 dichloroethane and we strongly believe that this band is buried under the strong local-normal combination band observed as a shoulder to the $|20\rangle_+$ band. This is possible since the local-local combination bands have low intensities as observed in the case of $|21\rangle_+$ and $|21\rangle_-$ bands. For dibromoethane, all the bands $|21\rangle_+$, $|21\rangle_-$ and $|11\rangle$ are observed which show with the exception of $|21\rangle_-$ a good agreement with the calculations. The $|31\rangle_+$ and $|31\rangle_-$ bands are not observed for both the molecules due to the change of grating of the spectrophotometer in that region. This problem could not be eliminated by a careful recording since the absorptivities involved are very small and the signal to noise ratio is poor.

5.32b Local-Normal Combinations

The bands denoted by 'C' in the spectra are combinations involving a pure CH local mode and two quanta of CH bending normal modes. Their assignments are given in table 5.2. The numbering of the normal modes is as given by Nakagawa and Mizushima³³. The fundamental normal frequencies of 1,2 dichloroethane and 1,2 dibromoethane are from references 33 and 20 respectively. The bands appearing as shoulders to the $|30\rangle_+$

band of 1,2 dichloroethane are not given in table 5.2 due to the large uncertainty in the peak positions. We believe that they are the counterparts of the bands appearing near the $|20\rangle_{\pm}$ overtone band. In the case of 1,2 dibromoethane, the band appearing in the low energy side of $|20\rangle_{\pm}$ overtone band is a combination band involving two quanta of CH bending normal mode. This band (1712 nm) has larger intensity than the pure overtone $|20\rangle_{\pm}$ band (1697 nm). Such intensity stealing has been observed in many overtone spectra^{13,14}. The corresponding combination band (1166 nm) near the $|30\rangle_{\pm}$ pure overtone band is less intense than the pure overtone band. This is due to the detuning effect, that is a decreased matching on passing from $|20\rangle_{\pm}$ region to $|30\rangle_{\pm}$ region. The combination bands involving two quanta of CH bending modes show deviations from simple additive energy relations between the local and normal modes. This is due to the mechanical coupling between the two motions.

The band structures in between the pure local mode overtone bands (Figs.5.12 and 5.13) mainly contains combinations arising from the excitation of a pure CH overtone along with one quantum of a normal mode. There are also present some combination bands involving two quanta of certain normal modes. The assignment of these bands are also given in table 5.2. Comparison of the combination band structure of the two molecules has

helped the unambiguous assignments of the bands arising from ν_{13} , ν_8 , ν'_8 and $2\nu_5$ normal modes. Other combination bands involving one quantum of a normal mode are given more than one assignment. This is due to the fact that there are several nearly equal normal frequencies for the 1,2 dihaloethane molecules and one cannot assign with certainty which normal mode is involved in a particular combination band. In such cases where more than one assignment is given there can be simultaneous contributions from more than one normal mode also.

For 1,2 dichloroethane the band at 1382.5 nm (7233 cm^{-1}) is not sharp. This is due to the contributions from the combinations involving ν'_2 (gauche A δCH_2) and ν'_{15} (gauche B δCH_2). The band at 1358.8 nm (7360 cm^{-1}) is assigned to the excitation of two normal frequencies ν'_{13} (gauche B ρCH_2) and ν'_{17} (gauche B CCl stretch) along with $\Delta v = 2$; since ν'_{13} and ν'_{17} are coupled³³. Similarly, as there is a coupling between the normal modes ν'_5 and ν'_9 ³³, the band at 1348.8 nm (7414 cm^{-1}) is assigned as the excitation of ν'_5 (gauche A CCl stretch) and ν'_9 (gauche A ρCH_2) along with $\Delta v = 2$. The local-normal combination band structures $\Delta v = 3$ plus one low frequency quantum shows correspondence with its counterpart $\Delta v = 2$ plus one low frequency quantum. Since these combination bands are very weak in intensity the signal to noise ratio is very poor

and the determination of the peak positions becomes difficult. Thus we have assigned only five peaks from this structure and these five peaks have corresponding peaks in the $\Delta v = 2$ plus one low frequency quantum structure. For 1,2 dibromoethane also there are a number of combination bands involving one quantum of low frequency normal modes. An examination of table 5.2 reveals that there are combinations common for both the molecules. Almost all the combination bands involving one normal mode show additive energy relation between local and normal modes.

5.33 Overtone Spectrum of 2-Butanone

The overtone spectrum of 2-butanone in the $\Delta v = 2-5$ regions are shown in Figs.5.15-5.18. The $\Delta v = 2$ region shows a structure corresponding to the A_1 and E components characteristic of a C_{3v} methyl group³¹. The $\Delta v = 3$ region shows a main band having both high and low energy shoulders and an additional high energy peak corresponding to a $|210\rangle$ combination. The $\Delta v = 4$ and 5 overtone bands also have high and low energy shoulders.

2-butanone molecule (Fig.5.19) contains two methyl groups; one directly attached to the carbonyl group and the other separated from the carbonyl group by a methylene group. As already explained in sec.4.12 the methyl group adjacent to

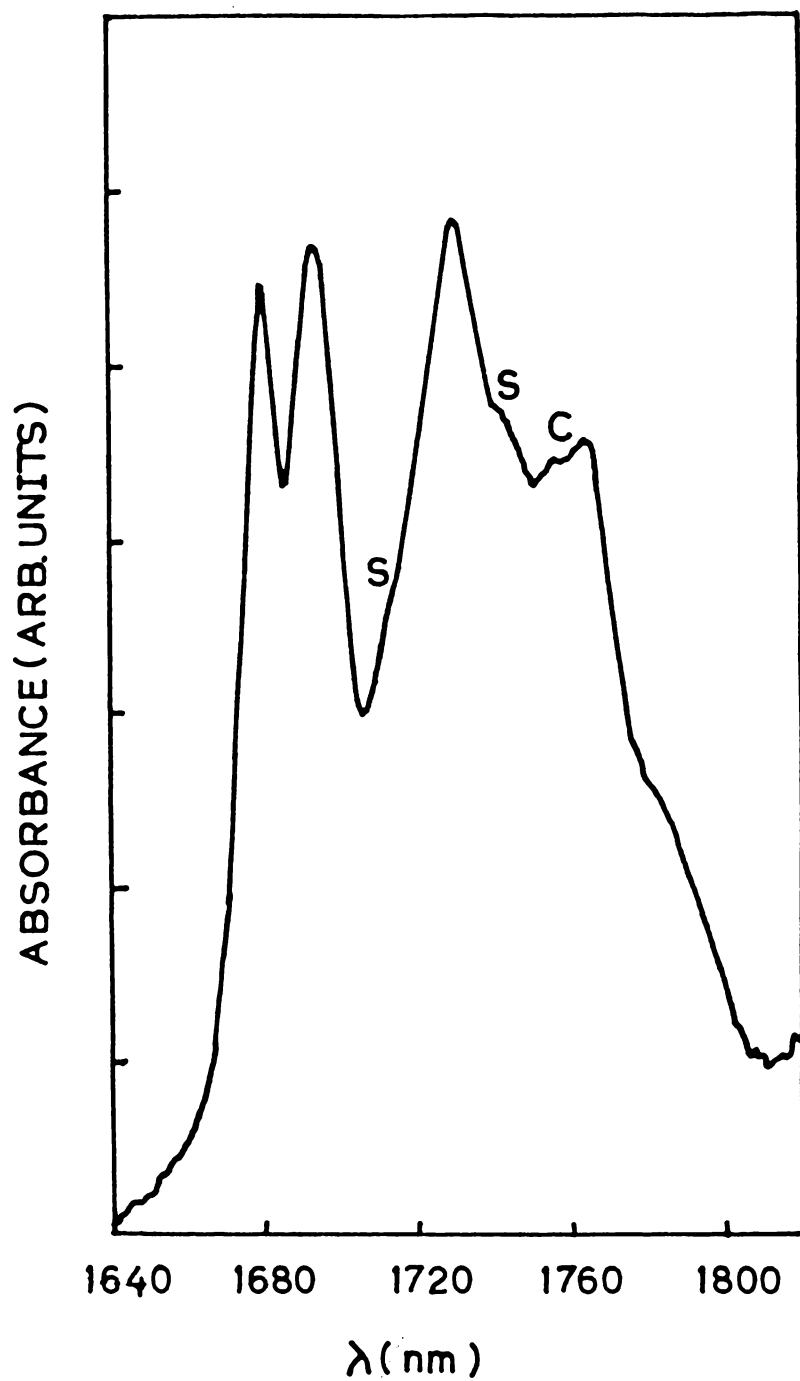


Fig.5.15 Overtone spectrum of 2-butanone in the $\Delta v = 2$ region. Sample dissolved in carbon tetrachloride; Reference - carbon tetrachloride. S - shoulder (see text). C - Local-Normal combination.

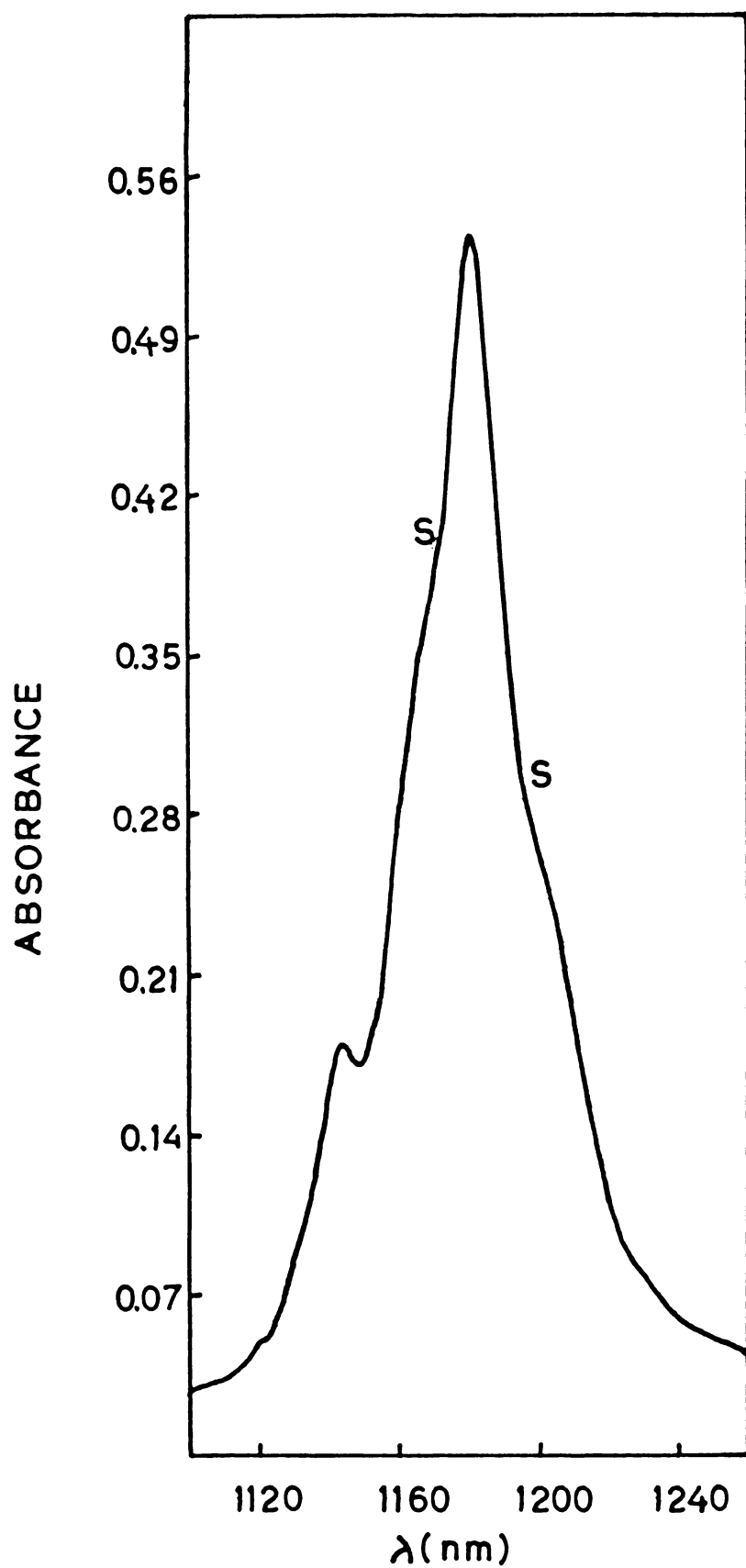


Fig.5.16 Overtone spectrum of 2-butanone in the $\Delta V = 3$ region. Pure liquid; Reference - air. S - shoulder (see text).

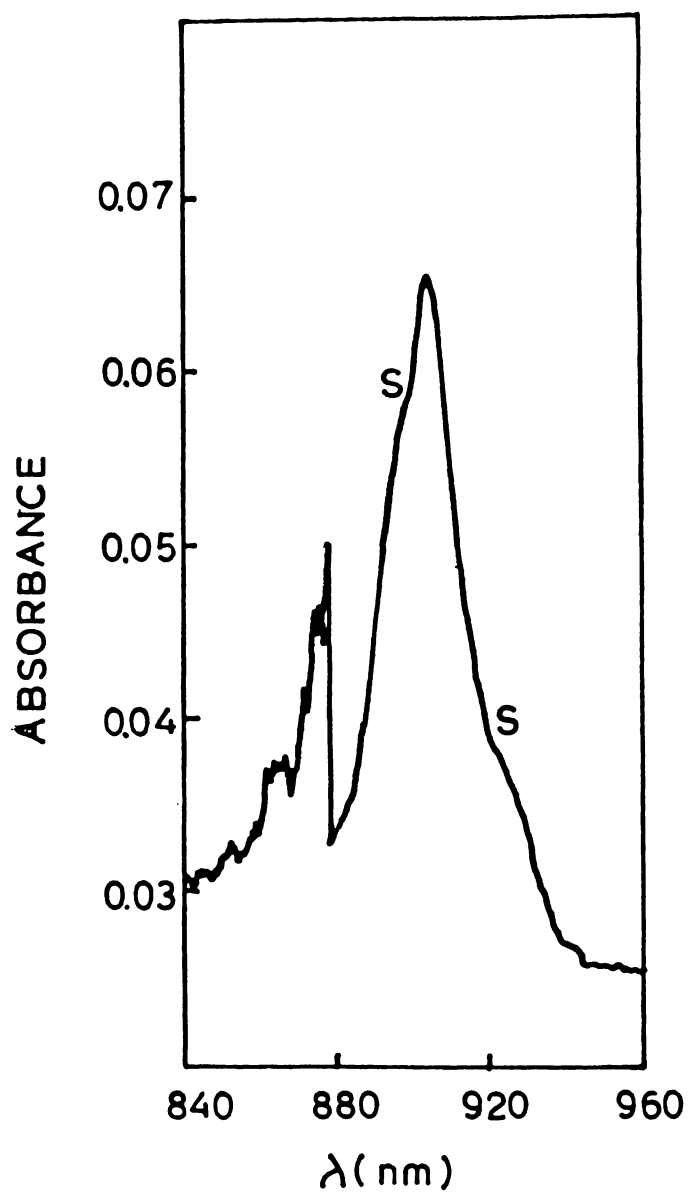


Fig.5.17 Overtone spectrum of 2-butanone in the $\Delta V = 4$ region. Pure liquid; Reference - air. S - shoulder (see text).

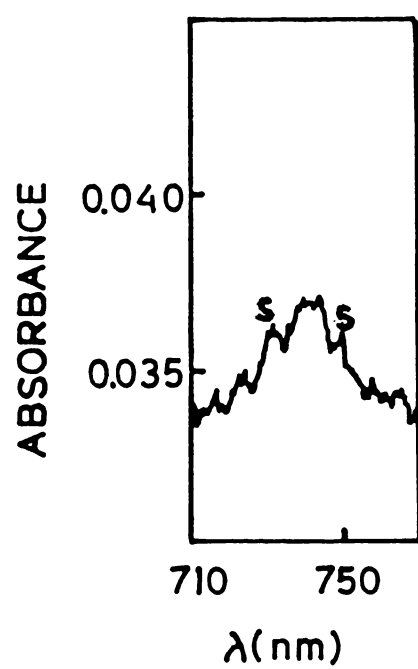


Fig.5.18 Overtone spectrum of 2-butanone in the $\Delta v = 5$ region. Pure liquid; Reference - air. S - shoulder (see text).

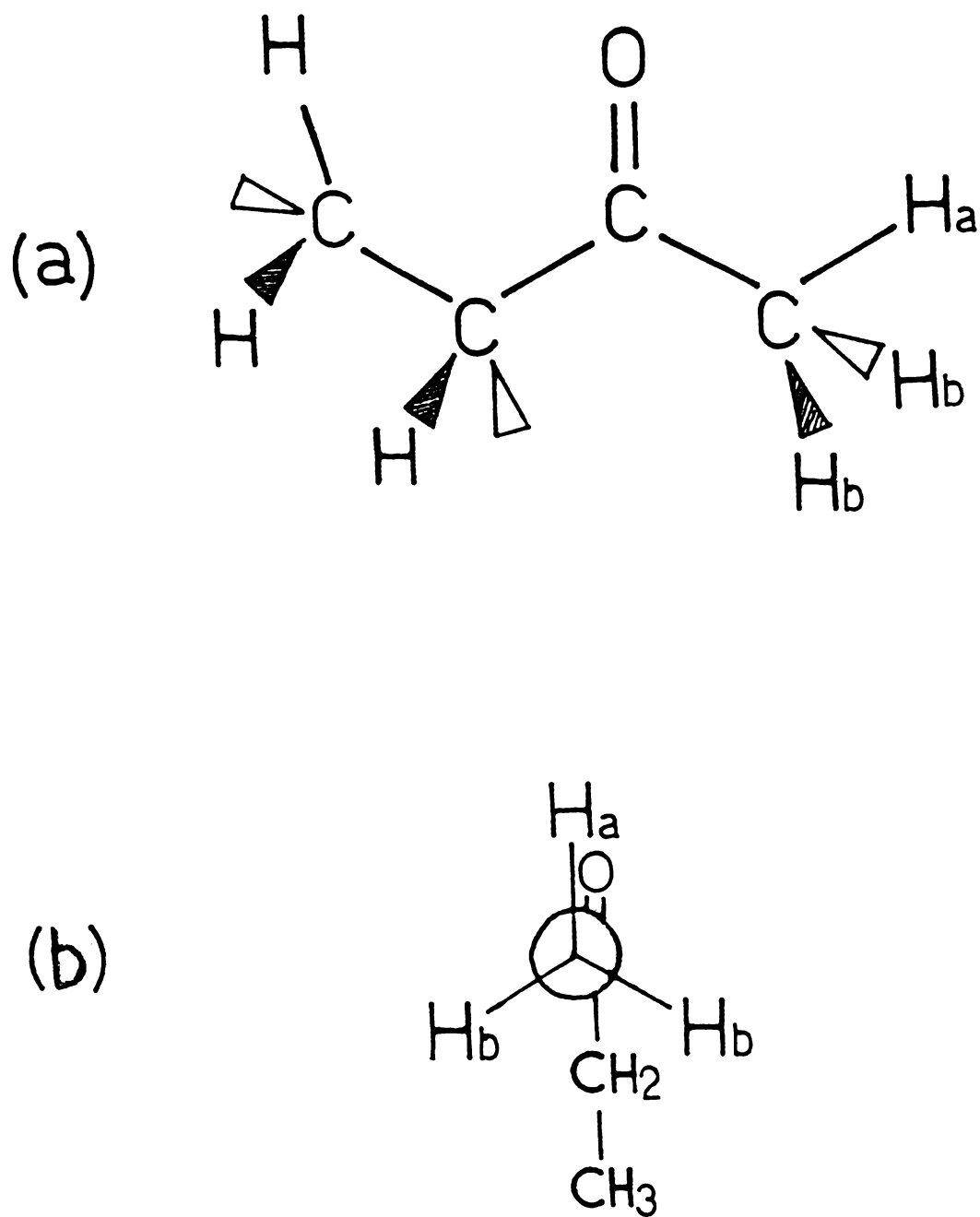


Fig.5.19 (a) Molecular structure of 2-butanone.
(b) The corresponding Newmann projection.

the carbonyl group is affected by the oxygen lone pair and carbonyl π electron interactions, resulting in two types of CH bonds; a stronger in-plane (to the C=O group) and two weaker out-of-planes. Fang et al have compared the $\Delta v = 4$ and 5 overtone patterns of 2-butanone with those of acetone and 3-pentanone²³. In acetone, both methyl groups are affected by the anisotropic environments resulting in two types of CH bonds. The overtone spectrum of acetone shows two bands at each overtone level; the higher energy peak corresponding to the stronger in-plane CH_a bond and the lower energy peak corresponding to the weaker out-of-plane CH_b bonds²³. As one passes from acetone to 2-butanone the higher energy CH_a peak gets suppressed in intensity and another low energy peak appears. The suppression of the higher energy peak is interpreted by Fang et al²³ as due to the loss of bond strengthening mechanism operating on CH_a , since one of the methyl groups is now separated from the carbonyl by a methylene group. The new low energy peak is assigned to be due to the methylene group. On going from 2-butanone to 3-pentanone the high energy peak completely disappears and the new low energy peak grows further in intensity. These observations again confirmed the assignments of Fang et al since in 3-pentanone there is no methyl group directly attached to the carbonyl and the bond strengthening mechanism is no more existing. Also there are two methylene groups in 2-butanone which enhances the intensity of the additional low energy peak.

In all these cases of acetone, 2-butanone and 3-pentanone the CH_b (out-of-plane) peaks show no appreciable energy shift. The intensity changes are also small. This observation led Fang et al to conclude that the normal methyl frequency in a ketone is close to the CH_b frequency of acetone²³.

The near infrared spectrum of 2-butanone reported in the present work clearly demonstrates the arguments of Fang et al that normal methylene frequency in 2-butanone coincides with the CH_b frequency of the methyl group adjacent to the carbonyl. The main peaks observed for all the overtones correspond to the out-of-plane CH_b bonds of the methyl group adjacent to the carbonyl and to the entire methyl group away from the carbonyl, which is not affected by the anisotropic environments. The methyl group away from the carbonyl maintains C_{3v} symmetry and thus gives rise to the symmetrized A and E components in the $\Delta V = 2$ and 3 regions. The high energy shoulders of the main peaks are overtones of the in-plane CH_a bond of the methyl group adjacent to the carbonyl. The low energy shoulders to the main peaks are overtones of the methylene group. However, these high and low energy shoulders are not resolved in the present liquid-phase spectrum and hence a local mode analysis of these overtones are not attempted here. Since the main peaks are also due to the independent methyl group we can apply the local mode theory of C_{3v} molecules³¹ to

calculate the entire peak positions of overtones and local-local combinations. The local mode Hamiltonian is the $N = 3$ version of equation (1.10)

$$\begin{aligned}
 H = & \omega(V_1 + V_2 + V_3) - \omega x (V_1^2 + V_2^2 + V_3^2 + V_1 + V_2 + V_3) \\
 & + \omega\gamma [(a_1^+ - a_1)(a_2^+ - a_2) + (a_2^+ - a_2)(a_3^+ - a_3) + (a_3^+ - a_3)(a_1^+ - a_1)] \\
 & + \omega\phi [(a_1^+ + a_1)(a_2^+ + a_2) + (a_2^+ + a_2)(a_3^+ + a_3) + (a_3^+ + a_3)(a_1^+ + a_1)]
 \end{aligned}
 \tag{5.11}$$

This Hamiltonian is diagonalized under the ladder approximation and neglecting inter manifold couplings, as already discussed earlier. The pure overtone transitions obey the Birge-Sponer equation (5.9). The local mode parameters ω and x obtained by the least square plot of $\frac{\Delta E_{V,0}}{V}$ versus V are given in table 5.4. From the previous discussions these are the local mode parameters of all the CH bonds of the methyl group away from the carbonyl and the two out-of-plane CH_b bonds of the methyl group adjacent to the carbonyl. To calculate the entire spectrum, we further require the parameter $(\gamma - \phi)$ which governs the kinetic and potential energy couplings between the equivalent CH oscillators of the independent methyl group. This parameter is usually obtained empirically from the splitting of the $|100\rangle_{A_1}$ and $|100\rangle_E$ fundamental transitions of the concerned methyl group³¹. The

Table 5.4

Observed and calculated local mode band maxima
of 2-butanone

The local mode parameters are:

$$\omega = 3073 \pm 8 \text{ cm}^{-1}$$

$$x = 0.0202 \pm 0.0005, \text{ with correlation } -0.99947$$

State	Calculated (cm^{-1})	Observed (cm^{-1})
$ 100\rangle_{A_1}$	2920	--
$ 100\rangle_E$	2964	--
$ 200\rangle_{A_1}$	5759	5780
$ 200\rangle_E$	5771	5780
$ 110\rangle_{A_1}$	5885	5903
$ 110\rangle_E$	5916	5952
$ 300\rangle_{A_1}$	8469	8467
$ 300\rangle_E$	8471	8467
$ 210\rangle_{A_1}$	8672	--
$ 210\rangle_E$	8698	--
$ 210\rangle_E$	8754	8740
$ 210\rangle_{A_2}$	8768	--
$ 111\rangle_{A_1}$	8862	--
$ 400\rangle$	11052	11062
$ 500\rangle$	13505	13512

splitting is related to $(\gamma-\phi)$ through

$$\Delta E |100\rangle_E - \Delta E |100\rangle_{A_1} = 3(\gamma-\phi)\omega \quad (5.12)$$

Since the distinct transitions corresponding to the independent methyl group in 2-butanone are not experimentally observed³⁴. We use the fundamental splitting in neopentane³¹ to calculate the overtone spectrum of 2-butanone. The splitting is 44.1 cm^{-1} in neopentane and this gives a value of 0.00478 for $(\gamma-\phi)$ in 2-butanone. The above approximation will not lead to serious errors since the magnitude of the splitting is not expected to vary abruptly among the independent methyl groups of different compounds. Such an approximation was also made by Henry et al³¹ by adopting a common value for $\omega(\gamma-\phi)$ in neopentanes. Thus all the parameters required for calculating the overtone spectrum are obtained and the diagonalization of the C_{3v} local mode Hamiltonian matrices (table 1.2) gives the entire local mode and local-local structures. The calculated and the observed peak positions (table 5.4) of the local mode overtones and the local-local combinations agree within experimental errors.

REFERENCES

1. H.R.Dubal and M.Quack, J.Chem.Phys.81, 3779 (1984) and refs.therein.
2. J.E.Baggot, M.C.Chuang, R.L.Zare, H.R.Dubal and M.Quack, J.Chem.Phys.82, 1186 (1985) and refs.therein.
3. J.W.Perry, D.J.Moll, A.Kuppermann and A.H.Zewail, J.Chem.Phys.82, 1195 (1985).
4. G.A.Voth, R.A.Marcus and A.H.Zewail, J.Chem.Phys.81, 5494 (1984).
5. J.E.Baggot, H.J.Class and I.M.Mills, Spectrochim.Acta.42A(2/3), 319 (1986).
6. T.R.Rizzo, C.C.Hayden and F.F.Crim, J.Chem.Phys.81, 4501 (1984).
7. H.R.Dubal and F.F.Crim, J.Chem.Phys.83, 3863 (1985).
8. T.M.Ticich, T.R.Rizzo, H.R.Dubal and F.F.Crim, J.Chem.Phys.84, 1508 (1986).
9. F.F.Crim, Ann.Rev.Phys.Chem.35, 657 (1984) and refs.therein.
10. M.C.Chuang and R.N.Zare, J.Chem.Phys.82, 4791 (1985) and refs. therein.

11. T.M.A.Rasheed, K.P.B.Moosad, V.P.N.Nampoori and K.Sathianandan, Spectrochim.Acta. (1987), in press.
12. B.R.Henry and I.Fu Hung, Chem.Phys.29, 465 (1978).
13. H.L.Fang and R.L.Swofford, J.Chem.Phys.72, 6382 (1980).
14. B.R.Henry and M.A.Mohammadi, Chem.Phys.55, 385 (1981).
15. O.S.Mortensen, B.R.Henry and M.A.Mohammadi, J.Chem.Phys.75, 4800 (1981).
16. M.K.Ahmed and B.R.Henry, J.Phys.Chem.90, 1081 (1986).
17. M.K.Ahmed and B.R.Henry, J.Phys.Chem.90, 1993 (1986).
18. T.M.A.Rasheed, V.P.N.Nampoori and K.Sathianandan, Chem.Phys.108, 349 (1986).
19. S.Suzuki and A.B.Dempster, J.Mol.Struct.32, 339 (1976).
20. K.Tanabe, J.Hiraishi and T.Tamura, J.Mol.Struct.33, 14 (1976).
21. Margreta Avram, G.H.D.Mateescu, "Infrared Spectroscopy Applications in Organic Chemistry", (Wiley Interscience, New York, 1972), p.234 and refs. therein.
22. M.L.Sage, J.Chem.Phys.80, 2872 (1984); refs.12-16 of Chapter 4.
23. Refs.12 and 15 of Chapter 4.

24. T.M.A.Rasheed, V.P.N.Nampoori and K.Sathianandan, Spectrochim. Acta. (1987), in press.
25. Ta-You Wu, Phys.Rev.46, 465 (1934).
26. J.S.Wong and C.B.Moore, J.Chem.Phys.77, 603 (1982).
27. K.M.Gough and B.R.Henry, J.Phys.Chem.87, 3433 (1983).
28. D.C.Mc Kean, Spectrochim.Acta.31A, 1167 (1975).
29. W.Kaye, Spectrochim.Acta.6, 257 (1954).
30. G.Henzberg, "Infrared and Raman Spectra of Polyatomic Molecules" (Van Nostrand, Princeton, 1945), p.215.
31. B.R.Henry, A.W.Tarr, O.S.Mortensen, W.R.Murphy and D.A.C. Compton, J.Chem.Phys.79, 2583 (1983).
32. L.V.Vilkov, V.S.Mastryukov and N.I.Sadova, "Determination of the Geometrical Structure of Free Molecules", (MIR, Mosco, 1983), p.146.
33. I.Nakagawa and S.Mizushima, J.Chem.Phys.21, 2195 (1953).
34. I.L.Finar, "Organic Chemistry, Vol.I--The Fundamental Principles", (E.L.B.S., 1973), p.208.

Chapter 6

SUMMARY AND CONCLUSIONS

This chapter summarizes the results and conclusions of the present investigations.

The present work has mainly concentrated on the application of overtone spectroscopy for characterizing the CH bonds in some organic molecules. The fifth CH overtone spectra are recorded by using laser induced thermal lens effect. A dual beam thermal lens spectrometer is set up for recording the fifth overtone spectra. The setup uses a commercial CW Rhodamine-6G dye laser as the pump source and a He-Ne laser as the probe source. The modulation produced by the thermal lens in the probe beam is phase sensitively detected and power normalized to get the absorption spectrum of the medium. For successfully carrying out overtone studies using the dual beam technique, various experimental considerations are to be taken into account. The present setup considers all these factors, even though no detailed parametric studies of the thermal lens spectrometer is attempted. The first through the fourth overtones are recorded by conventional method using a commercial UV-VIS-NIR spectrophotometer which uses a tungsten lamp as the source.

The present overtone studies in acetophenone and benzaldehyde in the $\Delta V = 2-6$ regions have shown that, compared with benzene, the aryl CH mechanical frequencies (and hence the force constants) in these compounds are larger than in benzene. The correlation between shift in overtone energy and change in CH bond length has predicted that the aryl CH bonds in acetophenone and benzaldehyde are $\sim 0.001 \text{ \AA}$ smaller than in benzene. The results on acetophenone and benzaldehyde are in agreement with the results of the earlier investigations, that an electron withdrawing substituent causes an increase of the aryl CH force constant. However, the physical picture of this behaviour has not been provided in any of the earlier works. We have proposed that an electron withdrawing group causes an electron deficiency at the ring carbon atoms, which in turn causes a greater attraction of the carbon atoms for the valence electron clouds of the hydrogen atoms resulting in a decreased CH bond length and an increased CH force constant. A reverse effect is expected upon substitution by an electron donating group. We have also discussed in detail the physical mechanism in connection with the earlier studies in halo- and methyl-benzenes.

The present overtone studies have shown that the methyl group in acetophenone contains two types of nonequivalent CH bonds arising from the anisotropic environments created by the oxygen lone pair and carbonyl π electron interactions. This is the first report of the observation of nonequivalent methyl CH

bonds in acetophenone. The mechanical frequency and the anharmonicity of the in-plane CH bond in acetophenone are much larger than those in acetaldehyde and acetone. Quantum mechanical resonance contributions of highly polar structures, which puts large electron densities at the carbonyl oxygen atom, seem to play a key role in this behaviour. The out-of-plane CH bonds show decreased mechanical frequency and anharmonicity with respect to acetone and acetaldehyde. This is attributed to the large C=O bond length in acetophenone which results in a decreased π interaction.

The spectral studies of styrene and polystyrene in the $\Delta V = 3-6$ regions have yielded the result that the aryl CH local mode parameters in these compounds are close to those in benzene. A comparison of the overtone energies of the two compounds with those of benzene has shown that the shifts in the styrene peaks are comparable with experimental uncertainties. Also there is no regularity in the magnitude and sign of the shifts for the various overtone levels. Thus the aryl CH bonds are not much affected by the $-\text{CH}=\text{CH}_2$ group. The polystyrene peaks, on the other hand shows increasing negative shifts with respect to benzene towards higher overtones. Even if the shifts are small, the good least square correlation and the regularity in the magnitude and sign of the shifts indicates that there is a small but detectable effect on the aryl CH bonds. The correlation between shift in overtone energy and change in bond length

predicts the result that the aryl CH bond length in polystyrene is $\sim 0.0005 \overset{\circ}{\text{A}}$ longer than in benzene. Our work on polystyrene presents the first thermal lens overtone spectrum of a solid as well as that of a polymer. In addition to aryl CH overtones the spectrum of polystyrene also shows the overtones of the CH bonds of the side chain. The use of these overtones for probing polymerization has been suggested.

As a typical olefinic molecule containing isolated CH bond, we have studied the overtone spectrum of trichloroethylene in the $\Delta V = 2-6$ regions. Olefinic compounds form a major class of photochemical interest. Moreover, molecules containing isolated CH bonds are potential candidates for observing mode selective rupture of CH bond by overtone excitation. The analysis of the overtone spectrum of trichloroethylene has shown that the CH bond strength in this molecule is much greater than its parent molecule ethylene. This is shown to be due to the electron withdrawing effect of the chlorine atoms. The correlation between CH bond length and fifth overtone energy predicts that the CH bond in trichloroethylene is $\sim 0.002 \overset{\circ}{\text{A}}$ smaller than in ethylene. The overtone spectrum also demonstrates that the pure CH overtone in the $\Delta V = 3$ region is Fermi resonant with a combination involving CH stretching and CH deformation. There are no measurable Fermi interactions in the other overtone quantum levels. The magnitude of the Fermi interaction matrix element is close to

that reported for dichloromethane. Arguments are given to show that the low frequency motion involved in the Fermi interaction is the CH deformation rather than C=C stretch or combination of C=C stretch and CH deformation. The overtone spectral details of trichloroethylene obtained here will be useful in any overtone photochemistry experiments involving this molecule.

The overtone spectra of 1,2 dichloro- and dibromo-ethanes in the $\Delta V = 2-5$ regions show pure local mode overtones, local-local combinations and local-normal combinations. There are two hydrogen atoms each attracted to both the carbon atoms in these molecules. We have shown that the coupled local mode Hamiltonian used for interpreting the overtone spectra of dihalomethanes can be used to interpret the local mode overtones and local-local combinations in the spectra of these larger haloalkanes. Possible assignments of the local-normal combinations are also given. Almost all the local-normal combinations involving one quantum of a low frequency motion show additive relation between local and normal frequencies. The combination bands involving two quanta of CH bending modes show deviations from additive relations due to the mechanical coupling between stretching and bending. However, since the local-normal structures in dihaloethanes are complex one cannot very easily pick out bands arising from different origins.

The analysis of the spectrum of 2-butanone in the $\Delta V = 2-5$ regions has shown that the methyl group away from the carbonyl is not affected by the anisotropic environments and that this methyl group maintains C_{3v} symmetry. The peak positions of the local mode overtones and local-local combinations obtained by diagonalizing a C_{3v} local mode Hamiltonian agrees with the observed values. The overtones of the out-of-plane CH bonds of the adjacent methyl group are coincident with the C_{3v} peaks. While the overtones of the in-plane CH bond appear as a shoulder on the high energy side, those of the methylene group appear as a shoulder on the low energy side.

Extension of the present studies to compounds in the gas phase using the photoacoustic technique can certainly yield more complete information about the spectra. For such experiments one has to use dye lasers which cover the entire near infrared and visible wavelength ranges.

63791